C00-1569-77

THERMAL PHASE FLUCTUATIONS IN A JOSEPHSON JUNCTION
and
PAIR SUSCEPTIBILITY OF A SUPERCONDUCTOR

J. T. Anderson

Solid State and Low Temperature Physics Group

SCHOOL OF PHYSICS AND ASTRONOMY

MARCH 1971

UNIVERSITY OF MINNESOTA
MINNEAPOLIS, MINNESOTA

Work supported in part by the U.S. Atomic Energy Commission

DISCLAIMER

THERMAL PHASE FLUCTUATIONS IN A JOSEPHSON JUNCTION

AND

PAIR SUSCEPTIBILITY OF A SUPERCONDUCTOR

A THESIS

SUBMITTED TO THE FACULTY OF THE GRADUATE SCHOOL

OF THE UNIVERSITY OF MINNESOTA

BY

JOHN THOMAS ANDERSON

IN PARTIAL FULFILLMENT OF THE REQUIREMENTS

FOR THE DEGREE OF

DOCTOR OF PHILOSOPHY

JUNE, 1971

ABSTRACT

THERMAL PHASE FLUCTUATIONS IN A JOSEPHSON JUNCTION

AND

PAIR SUSCEPTIBILITY OF A SUPERCONDUCTOR

Thermal fluctuations play a significant role in determining the properties of a Josephson junction in certain regimes. The characterization of the effects of fluctuations on a Josephson junction provides useful information relating to the basic problem of the nature of the superconducting-normal phase transition. Two experiments have been carried out: one an investigation of the behavior of a Josephson junction when the internal coupling energy is on the order of the thermal energy, the other an investigation of fluctuation induced conductivity in bimetallic Josephson junctions at temperatures between the transition temperatures of the two metal films composing the junction.

The coupling energy of a Josephson junction is reduced to the order of thermal energies in the vicinity of either the transition temperature, or the minima of the zero voltage current versus applied magnetic field curve. The effects of thermal fluctuations can be observed as a rounding of the current-voltage characteristic. Sn-Sn_xO_y-Sn crossed-film Josephson junctions have been used to study this effect. The data is in qualitative agreement with the theory of Ambegaokar and Halperin.

Thermal fluctuations above the transition temperature of a superconductor give rise to electron pairs with a finite lifetime. In a Josephson junction consisting of two metals with

different transition temperatures, fluctuation induced electron pairs result in an enhanced conductivity of the junction at temperatures between the transition temperatures of the individual metals. The enhanced conductivity is manifested by a current in excess of the quasiparticle current which flows in the junction. A phenomenological calculation of the excess current is presented. The excess current has been experimentally investigated using Sn-Sn_xO_y-Pb Josephson junctions masked to eliminate effects resulting from graded flim edges. Details of the variation of the excess current with voltage, magnetic field, and the temperature are in agreement with a calculation by Scalapino in which the excess current-voltage characteristic is a direct measure of the imaginary part of the frequency and wave number dependent pair susceptibility of a superconductor above T_c. Extimates of the pair relaxation frequency in tin based on the data are 50 percent greater than theoretical predictions.

ACKNOWLEDGEMENTS

Professor Allen M. Goldman deserves more than the usual acknowledgement. Both as an advisor and as a friend, his confidence in my approach, his continual support, and his unflagging enthusiasm have been valuable in resolving many of the conceptual and experimental problems which arose in the course of the experiments. Many of the ideas presented later in this thesis were formalized through numerous discussions with Professor Goldman.

The author gratefully acknowledges the theoretical support provided by Professor V. Ambegaokar, Dr. B. I. Halperin and Professor D. J. Scalapino during the progress of the experiments.

The experience of Mr. Peter Kreisman in the preparation of Josephson junctions, and his many helpful suggestions, were essential to the early initiation of these experiments.

The author thanks James C. Solinsky for assistance in the preparation of samples used in the pair susceptibility experiment, and Bette S. Anderson for having drawn many of the figures in this thesis.

Support for this research was provided by the Metallurgy Division of the Atomic Energy Commission through Contract AT(11-1) 1569.

TABLE OF CONTENTS

LIST OF FIGURES

Fig.

LIST OF TABLES

I. INTRODUCTION

In various phase transitions, thermal fluctuations are believed to be responsible for observed precursors of the ordered state which appears below T_c. A correct theoretical description of phase transitions should be able to account for fluctuation induced alterations in the physical properties of systems near T_c. Thus when there are observable effects attributable to fluctuations, a means is provided to test theory. The recent intense interest in thermal fluctuations in superconductors,[1,2] originally thought unobservable,[3] began with the discovery that certain systems, notably metal whiskers[4-6] and amorphous bismuth films,[7] exhibited experimentally detectable changes in electrical resistance[8-11] resulting from fluctuations in the vicinity of T_c. Subsequently, both theoretical and experimental work has been done on other manifestations of the onset of order, among them being the appearance of kinetic inductance[12-14] and diamagnetism[15-19] associated with superconductivity, and a decrease in the density of states at the Fermi level[20] studied by quasiparticle tunneling.[21] Of interest here is fluctuation induced electron pairing above T_c which in a Josephson junction[22-29] produces an excess tunneling current.[30-36]

A different class of fluctuation effects also occurs in Josephson junctions, that associated with a disruption of the coupling in the junction. These fluctuations produce the linewidth of emitted Josephson radiation,[37,38] rounding of microwave induced steps in a driven junction,[39] and rounding of the dc current-voltage characteristic.[38,40-52]

Experiments on the rounding of the dc current-voltage characteristic and the excess tunneling current in Josephson junctions are described in this thesis.

The first experiment described is an investigation of the behavior of a Josephson junction in which the coupling energy has been reduced to the order of $k_B T$. This can be achieved by working near, but below, the transition temperature of the junction, or, since the coupling energy is quasi-periodic in the applied magnetic field, near a minimum of the coupling energy field dependence. In papers by Ambegaokar and Halperin, and by Ivanchenko and Zil'berman, the thermal disruption of the junction coupling has been related to voltages which develop across the junction at currents less than the zero voltage current which would be carried in the absence of fluctuations. We find qualitative agreement with theoretical predictions.

In the second experiment, the onset of order in a superconductor is observed by measurements of an excess current in the dc current-voltage characteristic of a Josephson junction in which one side is the metal of interest, near but above its transition temperature, while the other side is a superconductor well below its transition temperature. Finite lifetime electron pairs, associated with fluctuations, contribute to the junction current through incipient Josephson tunneling. A pair current is able to flow across the junction because in the lower transition temperature superconductor, pair states exist in response to the coupling of the fluctuations to the pairing field of the superconductor with the higher transition temperature.

In the usual second order phase transition, the susceptibility measures the response of the order parameter to a classical field. For example, in a ferromagnetic transition, the magnetization is related to the magnetic field through the magnetic susceptibility. The order parameter of a superconductor is related to the electron pair density, and no classical field can be coupled to it. The appropriate choice of field is the pairing field of a higher temperature superconductor. In analogy to the ferromagnetic transition, the order parameter of the superconductor is related to the pairing field through the pair susceptibility. In the case of a junction with one side superconduc and the other nearly so, the excess tunneling current is proportional to the order parameter of the side undergoing the transition, and since the strength of the pairing field is known, is thus a measure of the pair susceptibility. Scalapino has shown that the frequency and wave-number dependent pair susceptibiltiy can be determined from the temperature, voltage, and magnetic field dependence of the excess current. Using Sn-Sn_xO_y-Pb junctions, we find our data consistent with the theory of Scalapino,[32] but that the pair relaxation rate determined for tin is 50 percent greater than predicted.

Since both experiments depend upon the Josephson effect, an introductory chapter on the Josephson equations is given, along with a section on the electrodynamics of a Josephson tunnel junction. The reader already familiar with the Josephson effect should proceed to Chapter III where a discussion of both the theoretical basis for the two experiments and the associated

experimental work which has been done by other authors is provided. Included is a brief survey of related experiments. Experimental techniques, including junction preparation, temperature measurement and control, and acquisition of current-voltage characteristics, are described in Chapter IV. Chapter V contains the data and its analysis for the two experiments, including a discussion of the difficulties associated with comparison of experiment and theory. In Chapter VI are the conclusions, and suggestions for further experiments.

II. THE JOSEPHSON EFFECT

II.1 Introduction

In the quantum mechanical description of electrons in a metal,[54] the single electron wave functions extend beyond the surface, though decreasing exponentially with distance. If two metals are placed in proximity with a voltage difference between them, the overlap of wave functions will permit current to flow across the gap separating them. This is ordinary electron tunneling, and has been used in the study of semiconductors and superconductors.[55] When the temperature of the metal is dropped below the superconducting transition temperature, some of the electrons condense into the BCS[56] ground state in which a single macroscopic wave function describes the behavior of the electrons in that state. In a manner analogous to that for the single electron wave functions, the wave function for the superconducting state extends beyond the boundaries of the metal. Repeating the tunneling experiment with two superconductors, one again expects that a current will flow, but in this case, one that possesses some of the properties of a current in a true superconductor. The calculation of Josephson[22] predicts just such behavior. Since a reasonable form for the wave function outside the superconductor is an exponential like $e^{-k_F \ell}$, a barrier 10Å thick would reduce the electron concentration by e^{-20}. The fact that the coupling is not very strong led Anderson[23] to describe the Josephson effect as weak superconductivity.

In addition to the supercurrent, Josephson made two other predictions, both consequences of the macroscopic coherence

associated with superconductivity. If a voltage is established across the barrier, the electron pairs, in flowing from the BCS ground state of one superconductor to that of the other, must conserve energy by emitting photons of energy

$$2eV = \hbar\omega \qquad (1)$$

where $\frac{2e}{h} = 483.6$ MHz/μV. This is the ac Josephson effect. As will be shown below, the magnitude of the supercurrent is dependent on the quantum phase difference across the barrier. Josephson predicted that a magnetic field would cause the supercurrent phase to vary over the barrier, with a consequent decrease in the maximum supercurrent as a result of quantum interference. The phase dependence of the Josephson junction has made it the essential element in a number of experiments on long range phase ordering in superconductors.

The first recognized observation of the Josephson supercurrent was that of Anderson and Rowell.[57] Supercurrents on the order of several milliamperes were observed in a tunnel junction consisting of a tin and a lead film separated by an insulating layer of tin oxide grown on the surface of the tin. Previous to the prediction of Josephson, supercurrents in tunnel junctions were thought to be a result of metallic shorts. The significant property of the supercurrent observed by Anderson and Rowell was its sensitivity to an applied magnetic field. Whereas a metallic short would be expected to have a critical field much higher than that of the bulk superconductor, the Josephson current can often be substantially reduced by fields on the order of 1 gauss.

The existence of the ac Josephson effect was first demonstrated by Shapiro[58] who observed constant voltage steps in the dc current-voltage characteristic of a junction in an external microwave field. The steps occurred at voltages satisfying the Josephson voltage frequency relation $n\hbar\omega = 2eV$, and indicate mixing of the applied field with the internally generated rf field. External detection of the Josephson radiation is difficult because of the impedance mismatch between the junction and detector.[25] However, using receivers sensitive to power levels as low as 10^{-14} watts, direct observation of Josephson radiation was achieved by Yanson, Svistunov, and Dmitrenko,[59] and by Langenberg, Scalapino, Taylor, and Eck.[60]

In a discussion of the Josephson effect, it is found that the proper canonically conjugate variables are phase and particle number.[23] This follows from the concept of a superconductor as a macroscopic phase coherent system. From the general principles of quantum mechanics, canonically conjugate variables satisfy an uncertainty relation, which for phase ϕ and number N is[61]

$$\Delta N \Delta \phi > 1 \qquad (2)$$

From the invariance of the physical properties of a superconductor under a translation of phase, there follows a conservation in the total number of particles. Thus, we would not expect to be able to determine anything about the absolute phase. Given two isolated superconductors, the phases of their wave functions are independent. If the separation between the two superconductors is reduced, so that particle exchange by tunneling is allowed, an

uncertainty in the number of particles in each superconductor develops which implies increased knowledge about the phase. Since the total particle number for the system of two superconductors is fixed, the absolute phase of the system is still undetermined. Thus, the only additional knowledge we can learn about the phase is the relative phase of the two superconductors.

The original work of Josephson[22] that led to the prediction of the Josephson effect was a many-body calculation of electron tunneling between superconductors. It is now recognized that tunneling is not a necessary requisite for the Josephson effect, but that it can be exhibited in any system involving weak coupling between superconductors.[23] Commonly used systems are point contacts,[62,63] junctions with metal rather than insulating barriers,[64] and weak link,[65] or Dayem bridges. The first of these consists of a superconducting point pressed into a block of superconductor; presumably, the poor contact provides weak coupling. A Dayem bridge is usually formed by scribing a superconducting film in such a way that a fine neck is the only connection between two sections of the film. If the neck is such that the largest dimensions are no greater than a coherence length, then the condensation energy of the volume of material in the neck will be on the order of $k_B T$. Thermal fluctuations can then destroy the phase coherence across the neck and produce a variation of weak superconductivity that exhibits the Josephson effect.

In the description of the Josephson effect that follows, the objective is to build a basis from which may be drawn details

necessary to the development and execution of the two experiments described. Since current-voltage characteristics play a key role in extraction of data from the experiments, a qualitative review of single particle tunneling, which determines much of the characteristic, is given. Following are two approaches to the Josephson equations, one phenomenological to provide an introduction to the basic results, and the other microscopic to provide the details. The conclusion of the chapter covers the effects of electric and magnetic fields on a Josephson junction as they pertain to the experiments, and is not meant to be totally inclusive.

II.2 Single Particle Tunneling

Before going into the details of the Josephson effect, it will be useful to examine some of the qualitative features of single electron tunneling between metals, either superconducting (SS), normal (NN), or in combination (NS).

The simple structural details of electron tunneling follow from the application of the "Golden Rule", and can be illustrated with the band-like diagrams of Douglass and Falicov[66] (DF). The tunneling current across an insulating barrier can be written[67]

$$I_{12} = \frac{4\pi e}{\hbar}\langle T^2\rangle \int_{-\infty}^{\infty} dE\, N_1(E)N_2(E+eV)[f_1(E)-f_2(E+eV)] \qquad (3)$$

where E is the energy, V the potential difference across the barrier, $\langle T^2\rangle$ the average transition matrix element, $N_1(E)$ and $N_2(E)$ density of state factors for the two metals, and $f_1(E)$ and

$f_2(E)$ the occupancies of the states on each side of the barrier. For small voltages, it is a reasonable assumption that $\langle T^2 \rangle$ is constant and thus it appears outside the integral. It will be convenient to discuss single particle tunneling in terms of dI/dV which is, for very low temperatures, directly proportional to N_1N_2. It has been shown that the transition matrix element contains a factor which cancels the density of states of the normal metal, aside from numerical factors which can be carried along in N.[67] Thus, tunneling is not sensitive to the normal metal density of states.

The DF diagrams plot the density of states as a function of energy. In Fig. 2-1A, the DF diagram for a normal metal is given. As shown, the effective density of states for a normal metal is constant. For a superconductor, the appropriate density of states is[56]

$$N(E) = N(0)_{\text{normal}} \frac{|E|}{(E^2-\Delta^2)^{1/2}} \qquad (4)$$

where Δ is the BCS energy gap. The DF diagram for a superconductor is shown in Fig. 2-1B.

Consider first the case of NN tunneling at T = 0 as shown in Fig. 2-2A and B. When V = 0, the respective Fermi levels of the two are equal. Applying a voltage to the system results in a shift of the Fermi level of one side with respect to the other. Since the effective density of states is approximately independent of E in the normal metal, dI/dV is independent of V and the current-voltage characteristic is linear as is shown in Fig. 2-2C.

If one side of the junction is replaced by a superconductor,

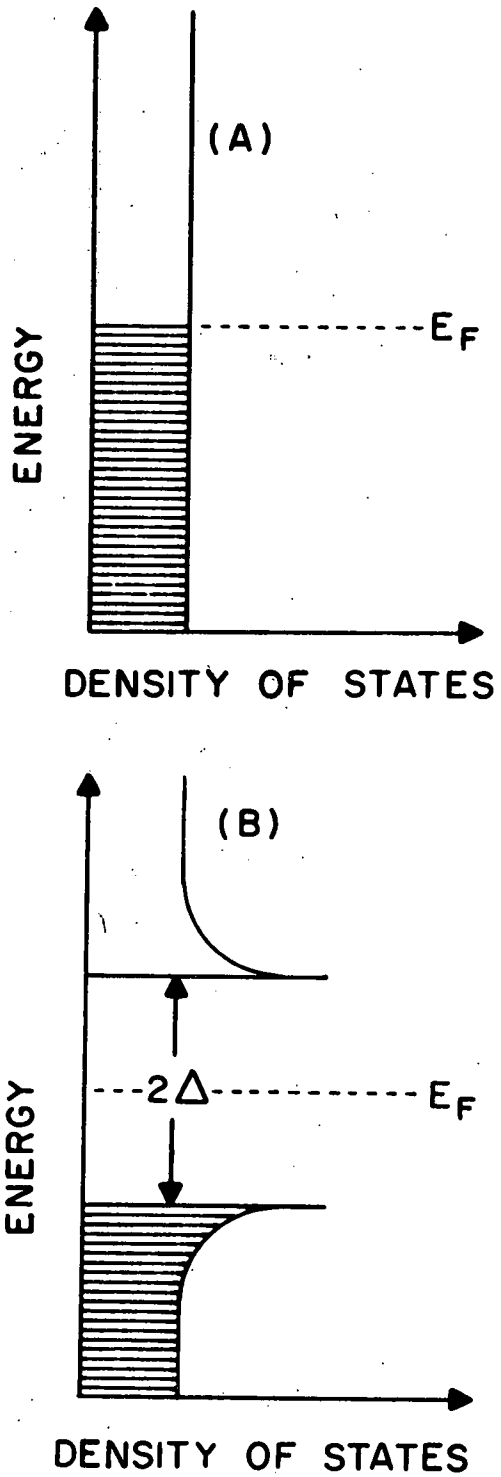

Fig. 2.1 Douglass-Falicov diagrams for a normal metal and a superconductor. The DF diagram for a normal metal is shown in (A) and that for a superconductor in (B). The hatched area represents occupied states.

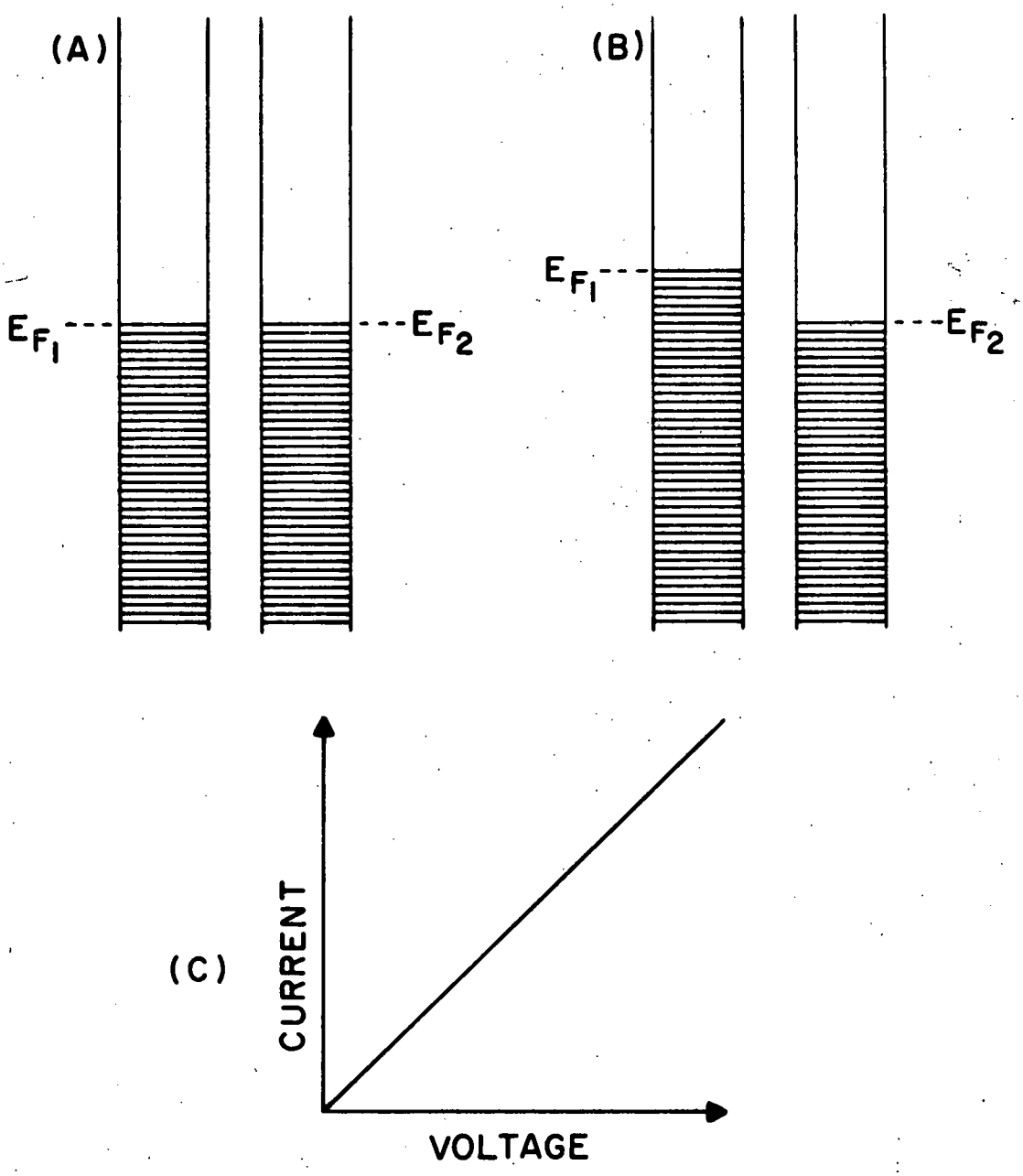

Fig. 2-2 NN tunneling for T = 0. In (A), the applied voltage is zero, and in (B), a voltage $V = E_{F_1} - E_{F_2}$ has been applied. The current-voltage characteristic is shown in (C).

the situation is as shown in Fig. 2-3A and B. With no applied voltage, the Fermi levels again are at the same energy. When a voltage is applied, the gap in the density of states prevents current flow until the voltage reaches $\pm\Delta$. A continued increase in the voltage will cause at first a very rapid rise in the current due to the singularity in the BCS density of states at $E_F+\Delta$, but as the voltage continues to increase, the density of states, and consequently dI/dV, approach a constant value. The appropriate current-voltage characteristic is shown in Fig. 2-3C. For two superconductors, a similar analysis shows that no current will flow until $V = \Delta_1+\Delta_2$, and then proceeds qualitatively the same as for NS tunneling.

For T>0, several alterations occur in the above scheme. The most obvious, since a band picture has been used, is that states above the Fermi level are partially occupied. Second, the BCS energy gap decreases with increasing temperature. Third, because the electrons as quasiparticle excitations have a finite lifetime, the discontinuity in the BCS density of states is no longer sharp,[68] and the singularity at $E_F+\Delta$ disappears. The net effect on the current-voltage characteristic is that for any V>0, current flows, and the discontinuity in the conductance at the energy gap becomes a broadened step. Figures 2-4A, B, and C illustrate NS tunneling for T>0. For SS tunneling, a bump in the conductance at $\Delta_1-\Delta_2$ also occurs. Referring to Fig. 2-5A through D, the initial increase is due to quasiparticles thermally excited above $E_F+\Delta_2$, but that as V continues to increase, those quasiparticles face a lower density of states, and the current

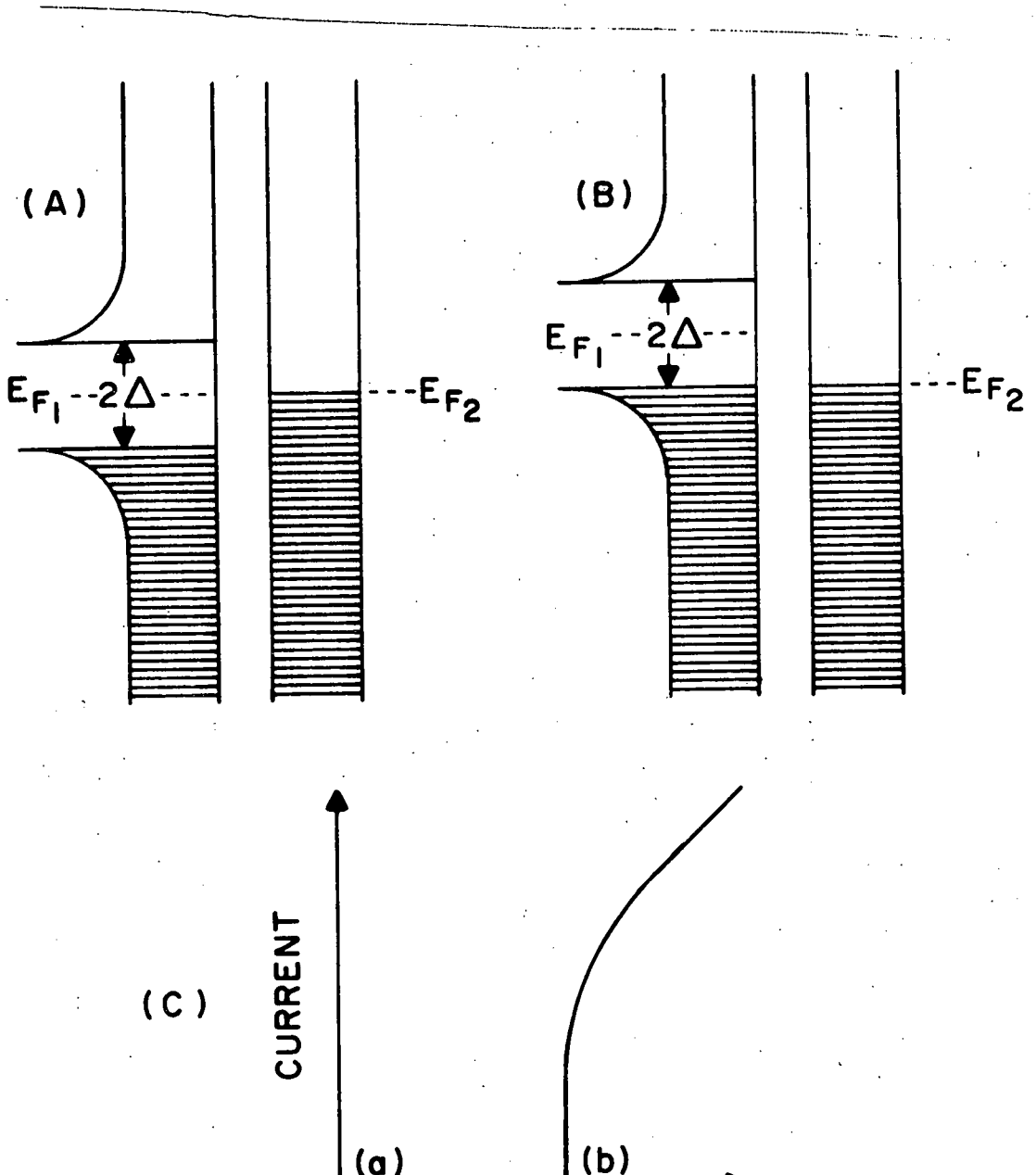

Fig. 2-3 NS tunneling for T = 0. Locations (a) and (b) of (C) show the behaviour of the current-voltage charcteristic corresponding to the situations shown in (A) and (B).

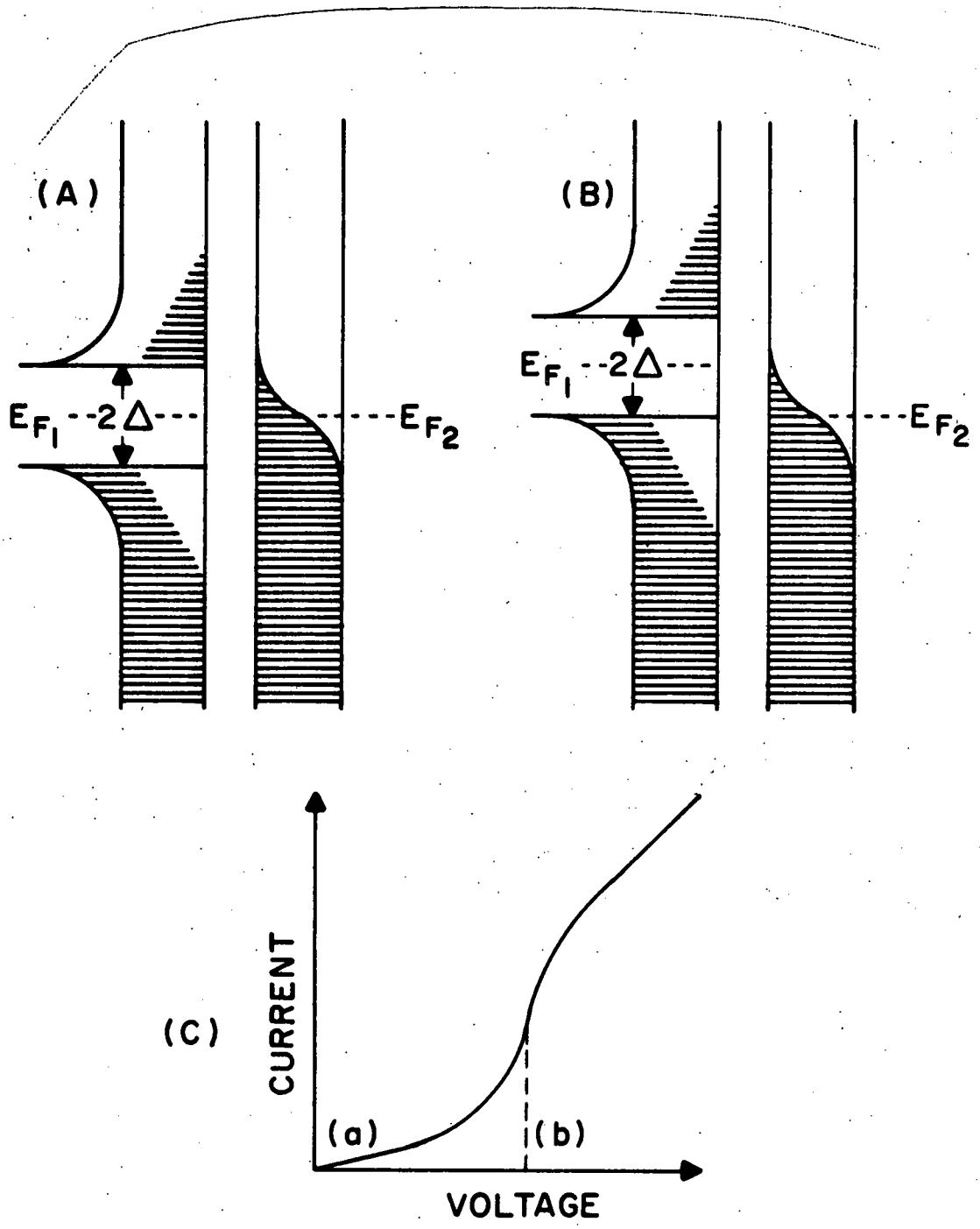

Fig. 2-4 NS tunneling for T > 0.

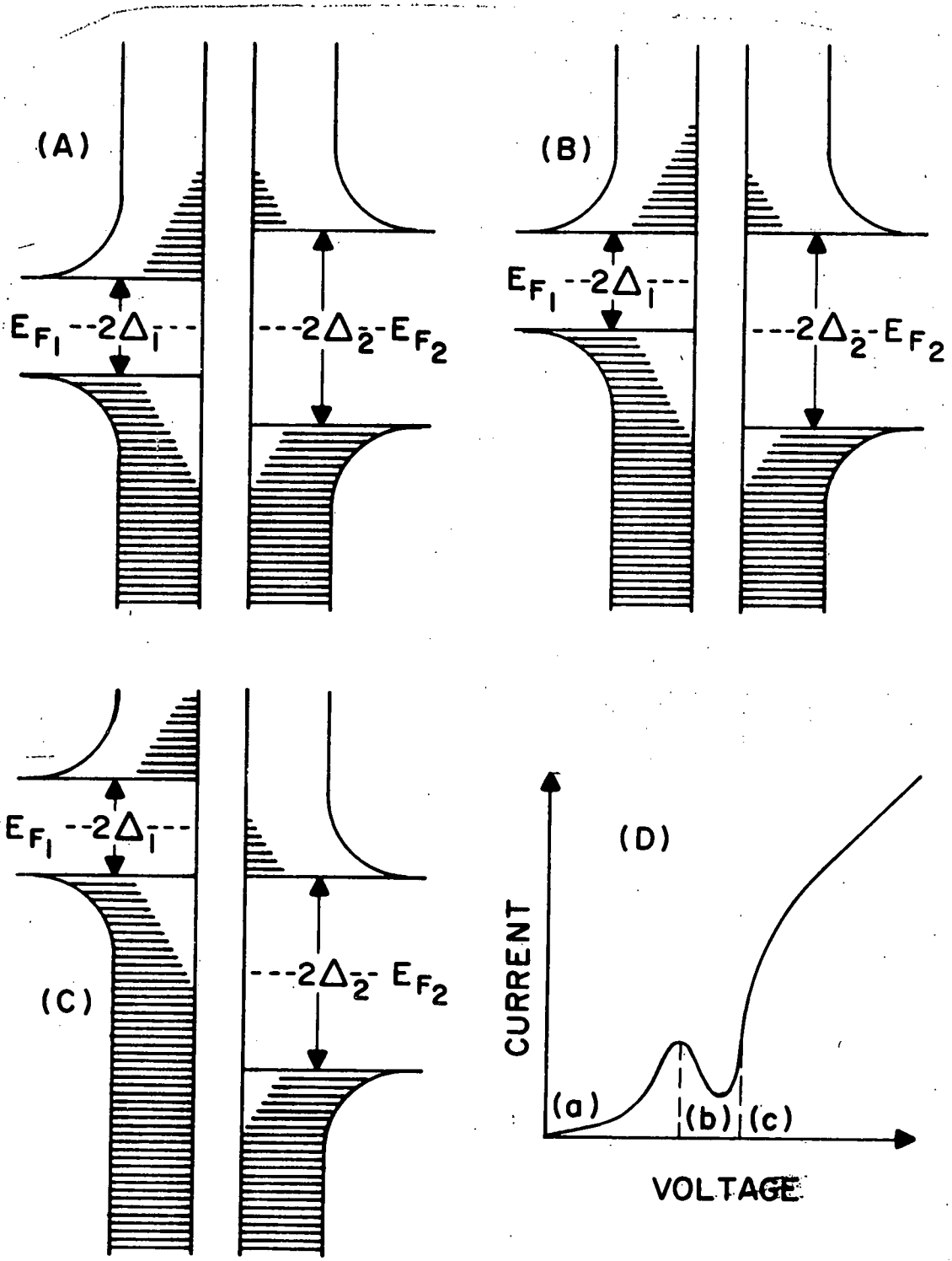

Fig. 2-5 SS tunneling for $T > 0$.

decreases until $V \to \Delta_1 + \Delta_2$.

In the experiments described later, it will be useful to assume that the current-voltage characteristic is linear in the vicinity of the origin at temperatures relatively near either of the transition temperatures for the two superconductors composing the junction. We have observed the linearity experimentally, and it can be justified theoretically from Eq. 2-3. We have not seen the zero-bias anomally[69] in the conductance resulting from spin-flip scattering of electrons in the oxide layer, which is not taken into account in Eq. 2-3, nor have we seen the logarithmic singularity in the resistance at the origin predicted by Larking and Ovchinnikov[70] for junctions made of identical superconductors.

II.3 The Josephson Equations

3.1 The Phenomenological Approach

The Josephson effect depends upon the momentum or phase ordering of the superconductor. Any theory which describes the superconductor by a single, macroscopically occupied quantum states can be used to determine the qualitative features of the Josephson effect. Here we describe the single quantum state by a wave function ψ, and use the Schrödinger equation to calculate the effects of introducing coupling between the two superconductors.

We use a wavefunction suggested by the Ginzburg-Landau phenomenological theory[71] of superconductivity, thus writing

$$\psi = \sqrt{\rho}\, e^{i\phi} \tag{5}$$

where ρ is the charge density, and ϕ is the phase of the wave function. The expression for the current is

$$\vec{J} = i\frac{(2e)\hbar}{2m}(\psi^*\vec{\nabla}\psi - \psi\vec{\nabla}\psi^*) - \frac{(2e)^2}{mc}\vec{A}\psi^*\psi \qquad (6)$$

where $\vec{J}$ is the current density, and $\vec{A}$ the magnetic vector potential. Inserting Eq. 2-5 for ψ into Eq. 2-6 for the current, we have

$$\vec{J} = \frac{(2e)\hbar}{m}\rho(\vec{\nabla}\phi - \frac{(2e)}{\hbar c}\vec{A}). \qquad (7)$$

Equation 2-7 will be useful later in discussing the magnetic field properties of Josephson junctions. From Eq. 2-7, we can find ϕ only to within a constant, which is expected since the absolute value of ϕ has no physical significance. The gradient of the phase is observable as it can be directly related to the current. Flux quantization follows from Eq. 2-7 and the requirement that ψ be single valued.

We are now in a position to obtain some qualitative features of the Josephson effect. Using the Schrödinger equation, and with coupling produced by the overlap of the pair wave functions, we can write[72]

$$i\hbar\frac{\partial\psi_1}{\partial t} = U_1\psi_1 + K\psi_2 \qquad i\hbar\frac{\partial\psi_2}{\partial t} = U_2\psi_2 + K\psi_1 \qquad (8)$$

where U_1 and U_2 are energy terms representing the Hamiltonian, and K is a small coupling constant. The tunneling experiment is shown in Fig. 2-6. An energy difference $U_1 - U_2 = 2eV$ is established between the superconductors. Choosing the zero of energy such that the energies of the respective sides are $\pm eV$, we can write Eq. 2-8 as

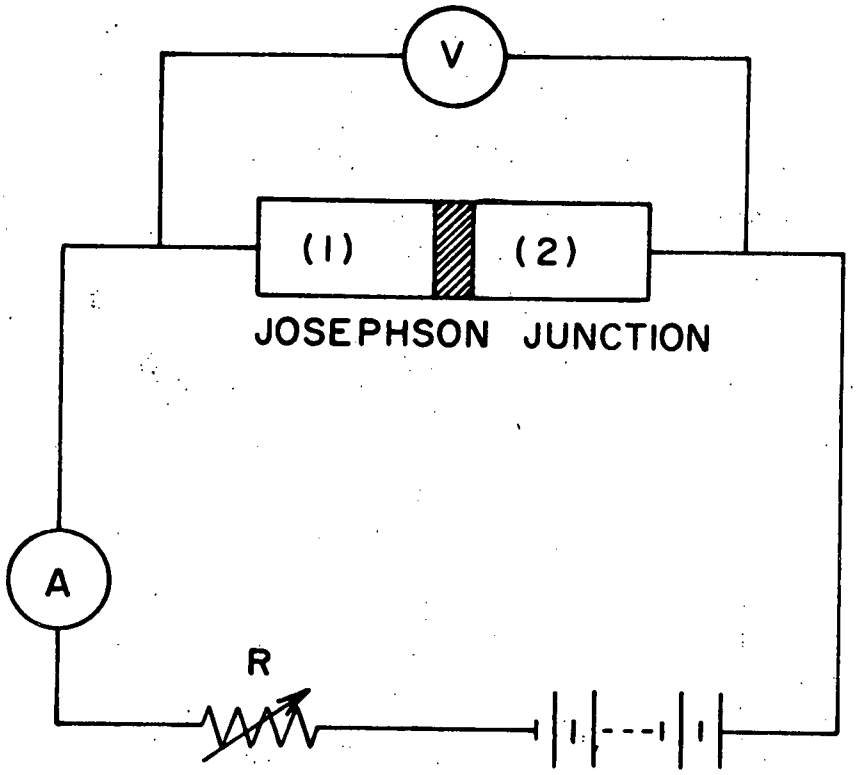

Fig. 2-6 The Josephson tunneling experiment.

$$i\hbar \frac{\partial \psi_1}{\partial t} = eV\psi_1 + K\psi_2 \qquad i\hbar \frac{\partial \psi_2}{\partial t} = -eV\psi_2 + K\psi_1 \tag{9}$$

Introducing $\psi_{1,2} = \sqrt{\rho_{1,2}}\, e^{i\phi_{1,2}}$ and $\phi = \phi_2 - \phi_1$, we find four equations relating ρ_1, ρ_2, ϕ_1, ϕ_2 by separating the real and imaginary parts of Eq. 2-9

$$\dot{\rho}_1 = -\dot{\rho}_2 = \frac{2K}{\hbar}\sqrt{\rho_1\rho_2}\sin\phi \qquad \dot{\phi}_{1,2} = \frac{K}{\hbar}\sqrt{\rho_2/\rho_1}\cos\phi \mp \frac{eV}{\hbar} \tag{10}$$

Since the current from 1 to 2 is $J = \dot{\rho}_1 = -\dot{\rho}_2$, we have the Josephson equations

$$J = \frac{2K}{\hbar}\sqrt{\rho_1\rho_2}\sin\phi = J_{max}\sin\phi \tag{11}$$

$$\dot{\phi} = \frac{2eV}{\hbar} \tag{12}$$

Equations 2-11, 12 contain the essential features of the Josephson effect. The Josephson current depends directly on $\sin\phi$, which for $V = 0$, is constant in time (assuming that a time dependent vector potential is not present). Since $|\sin\phi| < 1$, the supercurrent has an upper bound of J_{max}. When a voltage V is applied, the phase, and consequently the pair current, precesses at a rate $\dot{\phi} = \frac{2eV}{\hbar}$. Unfortunately, the phenomenological theory is unable to provide K, and to determine K, we must resort to the microscopic theory.

3.2 Microscopic Theory

The phenomenological approach to the Josephson effect does not consider the physical details of the coupling between the superconductors, and should not be expected to provide the means of calculating or relating the coupling to other physical

properties such as normal state resistance. The coupling constant K introduced into the phenomenological theory bears no obvious relation to the tunneling properties of the system as determined in the absence of any adjacent superconductor. The microscopic theory connects the single particle tunneling properties of the junction in the normal state to those appearing in the superconducting state.

That there is a relationship in tunneling between normal states and between superconducting states is not difficult to understand. In the tunneling Hamiltonian given below, the transition matrix element T_{kq} is introduced. T_{kq} depends upon the barrier and the momenta, k and q, of the initial and final states, not on the origin of the particle tunneling through the barrier. Electrons originating from the superconducting state are dressed in the sense that they are phase coherent with other superelectrons, however, the condensation energy represented by the phase coherence is far less than the Fermi energy, and has little effect on the tunneling amplitude. Differences in NN, NS, and SS tunnelings can be accounted for by the change in the density of states and quasiparticle excitation spectrum in a superconductor from those of a normal metal. The greater range of barrier thickness over which electron tunneling is observed compared to that of Josephson tunneling is a result of the phase coherence requirement in the latter. The condensation energy required to establish phase coherence must at least be on the order of $k_B T$, and it is not possible to meet that condition for insulating barriers much

greater than 20Å thick.

A microscopic calculation of the Josephson effect can be made using perturbation theory. One uses a certain set of ground state wave functions to describe the two superconductors in the absence of tunneling and an effective Hamiltonian to describe their coupling. The effective Hamiltonian consists of two terms. One is due directly to the tunneling, and the other, a chemical potential term, from the transfer of charge from one side of the junction to the other. Since the coupling is very weak, the perturbation calculation need be carried out only to the lowest non-vanishing order.

In the absence of any tunneling interaction, the two superconductors, (1) and (2), will have a total Hamiltonian given by

$$H = H_1 + H_2 \tag{13}$$

where H_1 and H_2 are the Hamiltonians for the separate superconductors, and contain all energy terms, other than those from tunneling and charge transfer, including the interactions responsible for superconductivity. The eigenfunctions of H_1 and H_2 are given by the BCS wave function[56]

$$\psi(\Delta) = \prod_k (u_k + v_k c_k^* c_{-k}^*)|0\rangle \tag{14}$$

where u_k is real, $|u_k|^2 + |v_k|^2 = 1$, and it is understood that $k \leftrightarrow k\uparrow$, $-k \leftrightarrow -k\downarrow$. The u_k and v_k are chosen such that the expectation value of the number operator is peaked at the true number of particles.[43] We have from BCS theory the usual results:

$$\Delta = \sum_k U c_{-k} c_k \tag{15}$$

$$E_k^2 = \epsilon_k^2 + \Delta^2 \tag{16}$$

$$|u_k|^2 - |v_k|^2 = \frac{\epsilon_k}{E_k} \qquad 2u_k v_k^* = \frac{\Delta_k}{E_k} \tag{17}$$

where Δ is the complex energy gap, U the pair interaction potential, E_k the quasiparticle excitation energy, and ϵ_k the Bloch energy as measured from the Fermi energy. The BCS wave function is a phase coherent superposition of states with differing N. As can be seen from Eq. 2-15, the phase of the term of Eq. 2-14 with N + 1 pairs is ϕ greater than the term with N pairs, where $\phi = \arg(\Delta)$.

In some situations, the number of electron pairs may be well known, and the appropriate wave function can then be composed from a superposition of states having different phases. One can project a state of fixed N from [24]

$$\psi(N) = \frac{1}{2\pi} \int_0^{2\pi} e^{-iN\phi} \psi(\phi)\, d\phi \tag{18}$$

where $\psi(\phi) = \psi(|\Delta| e^{i\phi})$. The inverse relationship is

$$\psi(\phi) = \sum_N e^{iN\phi} \psi(N) \tag{19}$$

From Eq. 2-18 and 2-19, one can infer the following operator equivalences

$$N \leftrightarrow -i \frac{\partial}{\partial \phi} \tag{20}$$

$$\phi \leftrightarrow i \frac{\partial}{\partial N} \tag{21}$$

which also follow from the conjugate nature of N and ϕ. The

operators for N and ϕ will be useful later in determining their time development. It is essential that Δ be treated as complex so that the set of states is sufficiently complete to project a wave function of fixed N. Because the Josephson effect is concerned with particle exchange between superconductors, a basis of fixed ϕ, and not fixed N, should be employed in the calculation.

The coupling between the superconductors is introduced by the tunneling Hamiltonian of Cohen, Falicov, and Phillips[74] which transfers single electrons across the barrier separating the superconductors:

$$H_T = \sum_{k,q} T_{kq} (c_k^* c_q + c_{-q}^* c_{-k}) + H.C. \quad (22)$$

The subscripts k and q are understood to refer to states in superconductors (1) and (2) respectively. It has been shown by Bardeen[75,76] that T_{kq} is a current density matrix element evaluated at the center of the barrier, and taken between single particle states which decay exponentially into the barrier. The tunneling Hamiltonian is time reversal invariant, and spin flip terms have not been included since they have no known significant effect.

Because the wave functions for the superconductors contain only pair states, and H_T transfers single electrons, the lowest non-vanishing order is the second. The binding energy is then

$$\Delta E^{(2)} = \sum_{n \neq 0} \frac{|H_T|^2_{n0}}{E_0 - E_n} \quad (23)$$

where E_0 is the ground state energy, and E_n the energy of the

intermediate states. When T~0, the important intermediate states are those excitations in which a pair is transformed into two quasiparticles, one of which is transferring across the barrier. Using Eq. 2-16 for the quasiparticle energy, we find $E_n - E_0 = E_k + E_q$. Inserting the ground state wave function and the tunneling Hamiltonian into Eq. 2-23, one obtains[23]

$$\Delta E^{(2)} = -\sum_{k,q} |T_{kq}|^2 \frac{1}{E_k+E_q} |u_k v_q + u_q v_k|^2$$

$$\Delta E^{(2)} = -\sum_{k,q} |T_{kq}|^2 \frac{1}{E_k+E_q} [|u_k|^2|v_q|^2 + |u_q|^2|v_k|^2 + 2\mathrm{Re}(u_k^* v_k u_q v_q^*)] \quad (24)$$

The first two terms of Eq. 2-24 are phase independent and are not of interest here. Using Eq. 2-17, and setting $\Delta_k = |\Delta_k| e^{i\phi_k}$, the last term can be written as

$$\Delta E^{(2)} = -N_1 N_2 |\Delta_1||\Delta_2| \langle T^2 \rangle \cos(\phi_1 - \phi_2) \int\int_{-\infty}^{\infty} d\epsilon_1 d\epsilon_2 \frac{1}{E_1 E_2 (E_1+E_2)} \quad (25)$$

where the density of states factors N_1 and N_2 result from the transformation of the sums over momenta into integrals over energy. Anderson has done the relevant integral and finds

$$\Delta E^{(2)} = -N_1 N_2 \langle T^2 \rangle \frac{4\pi |\Delta_1||\Delta_2|}{|\Delta_1|+|\Delta_2|} K\left[\frac{|\Delta_1|-|\Delta_2|}{|\Delta_1|+|\Delta_2|}\right] \cos(\phi_1 - \phi_2) \quad (26)$$

where K is a complete elliptic integral. The density of states factors and the average transition matrix element can be related to the normal state resistance, R_N, allowing Eq. 2-26 to be written

$$\Delta E^{(2)} = -\frac{\hbar}{2e} \frac{1}{R_N} \frac{2|\Delta_1||\Delta_2|}{|\Delta_1|+|\Delta_2|} K\left[\frac{|\Delta_1|-|\Delta_2|}{|\Delta_1|+|\Delta_2|}\right] \cos(\phi_1 - \phi_2) \quad (27)$$

For $0.5 \lesssim \frac{\Delta_1}{\Delta_2} \lesssim 1$, the argument of K varies little and the above reduces to

$$\Delta E^{(2)} = -E_1 \cos \phi = -\frac{\hbar}{2e} \frac{\pi \Delta_1 \Delta_2}{(\Delta_1+\Delta_2)R_N} \cos \phi \qquad (28)$$

where $\phi = \phi_1 - \phi_2$ and $|\Delta| \leftrightarrow \Delta$.

The effective Hamiltonian can be formed by combining the coupling energy of Eq. 2-28 with chemical potential change resulting from charge transfer. Considering the junction as a capacitor,

$$H_\mu = \frac{(2eN)^2}{2C}$$

where C is the capacitance and $N = N_2 - N_1$. The effective Hamiltonian is then given by

$$H_E = \frac{(2eN)^2}{2C} - E_1 \cos \phi. \qquad (29)$$

From the operator equivalences of Eq. 2-20 and 2-21, we can find the Josephson current-phase and voltage-frequency relationships. The current is found from $I = 2e\dot{N}$. Since

$$\dot{N} = \frac{i}{\hbar} \langle [H,N] \rangle = \frac{1}{\hbar} \left\langle \frac{\partial H}{\partial \phi} \right\rangle$$

it follows that

$$I = \frac{2e}{\hbar} E_1 \sin \phi = I_1 \sin \phi \qquad (30)$$

In a corresponding way, we find the time development of ϕ:

$$\dot{\phi} = \frac{1}{\hbar} \left\langle \frac{\partial H}{\partial N} \right\rangle = \frac{2e}{\hbar} \frac{2eN}{C} = \frac{2eV}{\hbar} \qquad (31)$$

The last relationship is also known as the Gor'kov-Josephson equation and has a much wider validity than indicated here.

Equation 2-31 depends neither on a Josephson supercurrent nor on tunneling, but, as originally noted by Gor'kov,[77] is fundamentally related to the time development of Δ in superconductors at different potentials.

It is not immediately clear that the same coherent states can be used when the voltage across the juntion is not zero. P. W. Anderson[24] presents an expression for the phase dependent part of the coupling energy when a voltage exists across the junction, and concludes that I_1 will differ little from its value at $V = 0$ until the voltage is on the order of 2Δ. Riedel[78] has considered the problem, and finds a logarithmic singularity in I_1 at 2Δ, if quasiparticle lifetimes are neglected. When lifetime effects are considered, the singularity is washed out.[79] As the work presented later is in the high temperature regime, the singularity can obviously be neglected.

The temperature dependence of the Josephson current has been calculated, using thermodynamic Green's functions, by Ambegaokar and Baratoff[80] who find

$$I_1(T) = \frac{\pi\Delta_1(T)\Delta_2(T)}{R_N \beta} \sum_{\ell=-\infty}^{\infty} \{[\omega_\ell^2+\Delta_1^2(T)][\omega_\ell^2+\Delta_2^2(T)]\}^{-1/2} \qquad (32)$$

where $\omega_\ell = \pi(2\ell+1)/\beta$ and $\beta = 1/k_B T$. If $\Delta_1 \neq \Delta_2$, it is necessary to resort to a numerical calculation to find $I_1(T)$, but for a symmetrical junction ($\Delta_1=\Delta_2$), the sum may be done analytically leading to

$$I_1(T) = \frac{\pi\Delta(T)}{2R_N} \tanh[\tfrac{1}{2}\beta\Delta(T)] \qquad (33)$$

The temperature dependence of the symmetrical junction differs

qualitatively from that in the asymmetrical junction. In the former, $I_1(T)$ approaches T_c linearly

$$I_1(T) = 2.67\, I_1(0)[1-T/T_c] \tag{34}$$

whereas if $\Delta_1 \neq \Delta_2$, $I_1(T)$ approaches T_c with infinite slope. In Fig. 2-7 is the reduced dc Josephson current versus reduced temperature for two values of Δ_1/Δ_2.

II.4 The Josephson Effect in the Presence of Electric and Magnetic Fields

4.1 Introduction of the Potentials

In the previous sections, it was assumed that the only spatial variation of phase was across the insulating barrier. The last part of this chapter will be devoted to the behavior of a Josephson junction in which the phase is forced to spatially by the presence of a magnetic vector potential, and temporally by the application of a voltage to the junction.

The variation of phase with a vector potential can be shown in an elementary manner by recalling from quantum mechanics the prescription[61]

$$\psi_{A\neq 0} = \psi_{A=0} \exp[i\tfrac{2e}{\hbar c} \int \vec{A}\cdot d\vec{s}], \tag{35}$$

or by carrying out a direct detailed argument based on gauge invariance.[27] It is required that physically observable quantities be invariant under a change in gauge of the electromagnetic potentials

$$\vec{A}' = \vec{A} + \nabla\chi \qquad V' = V - \partial\chi/\partial t \tag{36}$$

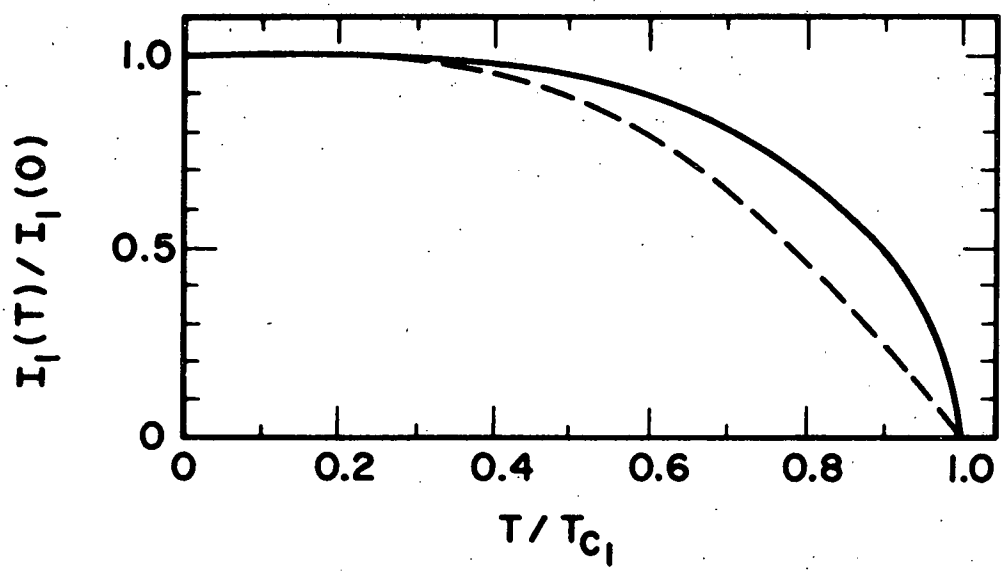

Fig. 2-7 Temperature dependence of the Josephson current. The dashed line is for a symmetrical junction. The solid line is for an asymmetrical junction with $\Delta_1(0)/\Delta_2(0) = 0.5$. (After Ref. 80).

where χ is an arbitrary scalar quantity. In particular, we desire that

$$\vec{J} = \frac{(2e)\hbar}{m}\rho(\vec{\nabla}\phi - \frac{2e}{\hbar c}\vec{A}) = \frac{(2e)\hbar}{m}\rho(\vec{\nabla}\phi' - \frac{2e}{\hbar c}\vec{A}') \qquad (37)$$

and

$$\frac{2eV}{\hbar} = \frac{2e}{\hbar}\int\vec{E}\cdot d\vec{s} = \frac{\partial}{\partial t}(\phi_1-\phi_2) = \frac{\partial}{\partial t}(\phi_1' - \phi_2'). \qquad (38)$$

By direct substitution into Eq. 2.37, it can be verified that the necessary replacement for ϕ is

$$\phi' = \phi + \frac{2e}{\hbar c}\chi \cdot \qquad (39)$$

The phase difference is not gauge invariant and becomes

$$\phi_1' - \phi_2' = \phi_1 - \phi_2 + \frac{2e}{\hbar c}\int\vec{A}\cdot d\vec{s} \cdot \qquad (40)$$

The only requirement that must be met by $\phi_1'-\phi_2'$ is Eq. 2.38 and again it can be verified that Eq. 2-39 provides the correct replacement for ϕ.

The effect of a magnetic field on the junction is to introduce a spacially dependent phase. The total current must be calculated by integrating the phase dependent current density

$$\vec{J} = \vec{J}_1(x,y,z)\sin\phi(x,y,z,t) \qquad (41)$$

over the junction surface. For a uniform junction, $J_1 = I_1/S$, where S is the junction area.

Equations 2-30, 2-31, 2-40, 2-41 and Maxwell's equations are the basis for the electrodynamics of a Josephson junction.

4.2 Junction Behavior in a Static Magnetic Field

We consider the effects of a static magnetic field on a Josephson junction with a geometry shown in Fig. 2-8. The superconducting films are assumed to be thick compared to the London penetration depth λ. Following Scalapino,[28] we would like to develop a relationship between the applied field and the phase gradient by integrating Eq. 2-40 around the boundary shown in Fig. 2-9. The sections of the contours which are parallel to the junction surface are taken several penetration depths into the superconductors so that the contribution of $\vec{J}$ to the phase change along them is zero. Since the dominant part of the current flows parallel to the surface of the barrier, in order to shield the interior of the superconductor from the magnetic field, there is no contribution from J to the phase change along paths normal to the barrier surface. We thus have the following phase differences along the contour:

$$\phi_a(z) - \phi_b(z+dz) = \frac{2e}{\hbar c} \int_{C_1} \vec{A} \cdot d\vec{s}$$

$$\phi_c(z+dz) - \phi_d(z) = \frac{2e}{\hbar c} \int_{C_2} \vec{A} \cdot d\vec{s}$$

Adding the phase changes, including those across the barrier, and replacing the line integral of $\vec{A}$ by the surface integral of $\vec{H}$, we have

$$\phi(z) - \phi(z+dz) = \frac{2e}{\hbar c} (2\lambda+\ell)\, dz\, H(z)$$

or in differential form

$$\nabla\phi = (2ed/\hbar c)\, \vec{H} \times \vec{n} \qquad (42)$$

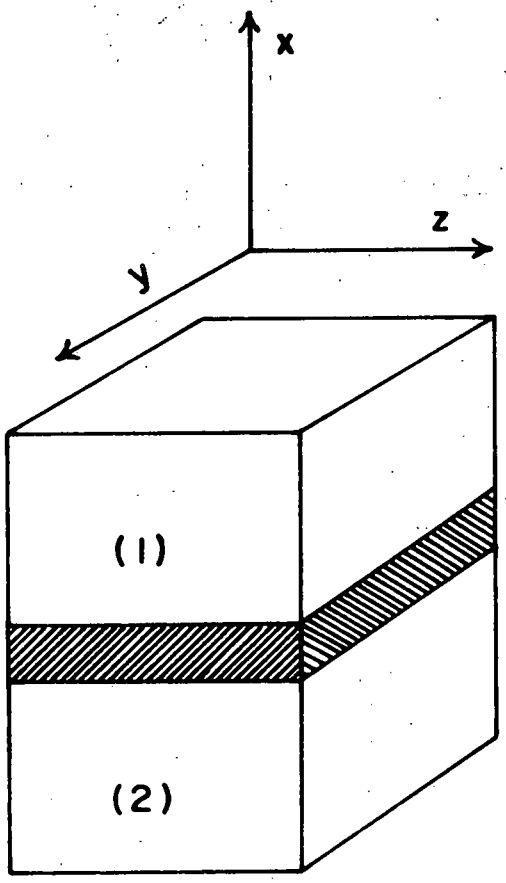

Fig. 2-8 Josephson junction geometry for the magnetic field effects.

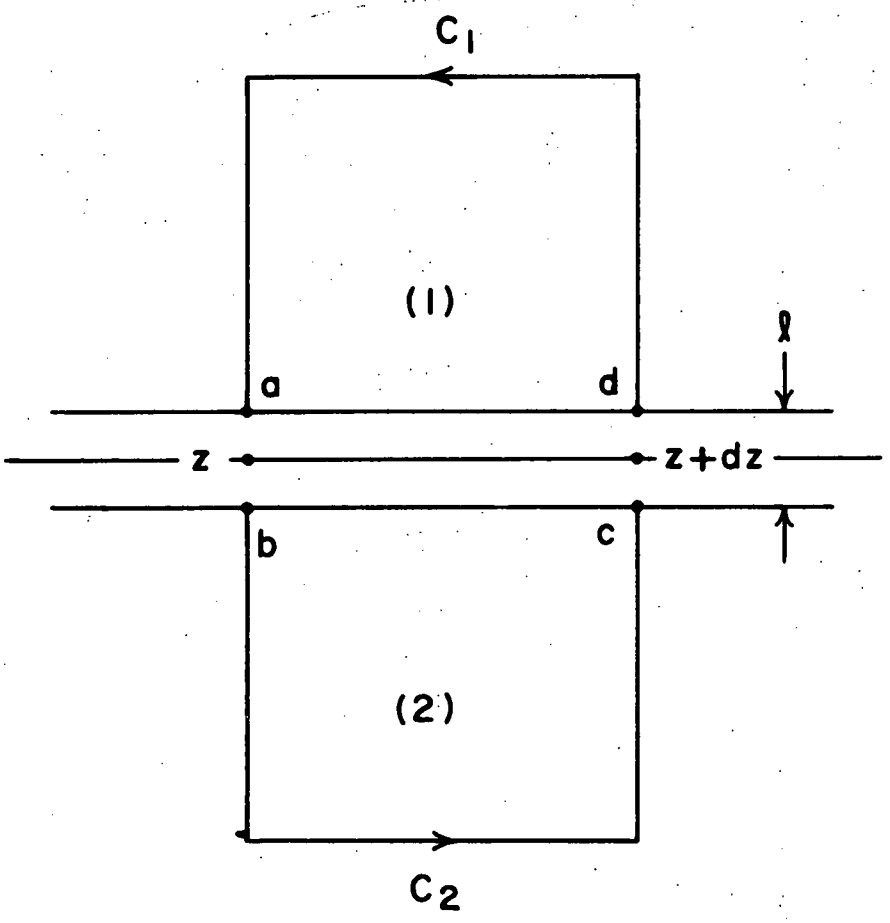

Fig. 2-9 Integration contour for the derivation of Eq. 2-42.

where $\vec{n}$ is a unit vector normal to the barrier directed from (1)→(2), and $d = (2\lambda+\ell)$.

Even when there is no applied field, there will nevertheless be a magnetic field which is associated with the Josephson current. To estimate the significance of the self-generated field, combine Eq. 2-41 with the Maxwell equation

$$\vec{\nabla} \times \vec{H} = \frac{4\pi}{c} \vec{J}$$

where $J = J_1 \sin \phi$. The result is

$$\nabla^2 \phi = \lambda_J^{-2} \sin \phi \qquad \lambda_J^2 = \frac{\hbar c^2}{8\pi e J_1 d} \tag{43}$$

For small ϕ, Eq. 2-43 can be linearized to

$$\nabla^2 \phi = \lambda_J^{-2} \phi \tag{44}$$

which suggests that λ_J plays the role of a penetration depth. A typical value of λ_J, the Josephson penetration depth, is 1 mm. Ferrell and Prange,[81] and Owen and Scalapino,[82] have solved Eq. 2-43 for uniform rectangular junctions and find that for junctions whose length is considerably greater than λ_J, the Josephson current flows only within a few λ_J of the edges. For our work, junctions with dimensions much less than λ_J were used. The qualitative conclusions from the above references in such a case is that the current is uniformly distributed over the surface of the junction, and the self-generated field can be ignored.

For the simple case of a junction small compared to λ_J in a magnetic field applied parallel to the -y axis, Eq. 2-42 can be integrated to give

$$\phi = [\frac{2ed}{\hbar c}]H_e z + \phi_0 \tag{45}$$

with the corresponding current density

$$J = J_1 \sin [(\frac{2ed}{\hbar c})H_e z + \phi_o]. \tag{46}$$

H_e is the external magnetic field since demagnetizing effects need not be considered when the field is parallel to the films. By setting $\phi_0 = -edH_e L/\hbar c$, the current can be maximized. Integrating J(z) along the length, L, of the junction, one finds that the maximum Josephson current varies according to

$$I = I_1 \frac{|\sin[(ed/\hbar c)\ H_e L]|}{(ed/\hbar c)\ H_e L} \tag{47}$$

which is identical to the functional form for single slit Fraunhofer diffraction. Noting that the flux within the junction is $\Phi = dLH_e$, Eq. 2-47 can be written as

$$I = I_1 \frac{|\sin[\pi\Phi/\Phi_o]|}{[\pi\Phi/\Phi_0]} \tag{48}$$

where $\Phi_0 = hc/2e$ is the flux quantum for the Cooper pairs.

For each minim the critical current, the junction contains an integer number of flux quanta. The application of a magnetic field to the junction induces vortex currents to flow, each containing one flux quantum, in a manner similar to that of a Type II superconductor. If J_1 varies spatially, the effects will be analogous to those of a non-uniformly illuminated slit in optics. The magnetic field behavior for a typical junction is shown in Fig. 2-10.

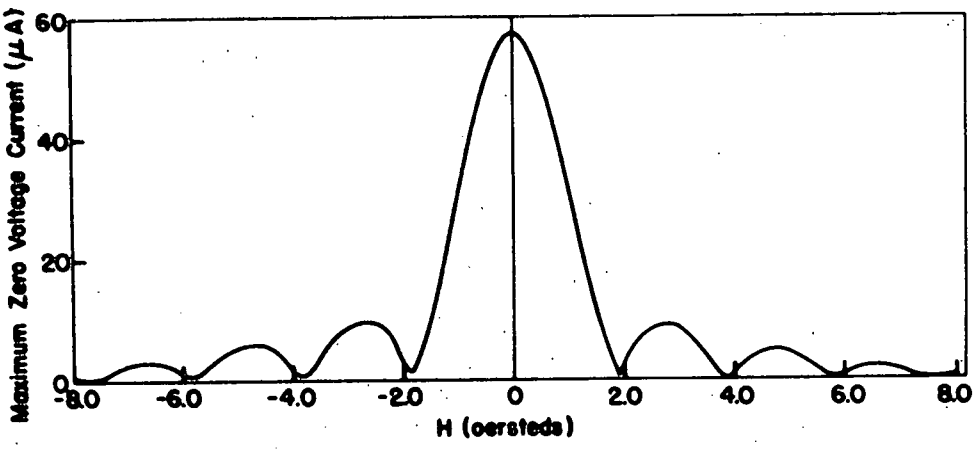

Fig. 2-10 Zero-voltage current versus applied field for a typical Josephson junction. The curve is from sample PS-1 (described in Chapter V) at 3.8 K, and was obtained using the servo system described in IV.4.4.

The quantum mechanical interference effects that occur in the junction are not a property of the junction itself but rather of the macroscopic phase coherence intrinsic to the superconductor. The junction, through the phase dependence of the critical current, serves as an indicator of the phase interference. A number of experiments have been done in which phase interference was observed in superconducting loops interrupted by two Josephson junctions. In this situation, the critical current is that of two junctions in parallel, and the phase gradient necessary for the interference is generated by either the flux enclosed within the loop containing the junctions,[83,84] or be a net current circulating around it.[85,86] The interference observed by the magnetic field dependence of the critical current is analogous to double slit optical interference.

With a derivation like that for the field dependence of the critical current, it can be shown that the coupling energy also varies as[26]

$$E_1(H) = E_1(0) \frac{|\sin[\pi\Phi/\Phi_0]|}{[\pi\Phi/\Phi_0]} \tag{49}$$

Thus, if the junction contains an integer number of flux quanta, the coupling is effectively reduced to zero.

4.3 The Electromagnetic Effects

The simplest example of the ac Josephson effect is the emission of microwave radiation when a dc voltage is applied to the junction. Since the phase precesses at a rate $2eV/\hbar = \dot{\phi}$, the current through the junction oscillates in time according to

$$I = I_1 \sin\left[\left(\frac{2eV}{\hbar}\right)t + \phi_0\right] \tag{50}$$

Because the impedance of the junction is often very low, the rf power coupled out of the junction is considerably smaller than the dc driving power.

The first experimental evidence of the ac Josephson effect[58] was obtained by observing the behavior of the dc current-voltage characteristic of a junction when external radiation was mixed with that generated internally by the application of a dc bias. In this case, the voltage across the junction is given by[25]

$$V = V_0 + V_1 \cos \omega t \tag{51}$$

where V_0 is the dc bias, and V_1 the amplitude of the rf voltage coupled to the junction. For the phase, we have

$$\phi = \left(\frac{2eV_0}{\hbar}\right)t + \left(\frac{2eV_1}{\hbar\omega}\right)\sin \omega t + \phi_0 \tag{52}$$

and for I

$$I = I_1 \sin\left[\left(\frac{2eV_0}{\hbar}\right)t + \left(\frac{2eV_1}{\hbar\omega}\right) \sin \omega t + \phi_0\right] \tag{53}$$

The junction current may be Fourier decomposed in terms of Bessel's functions of order n to give

$$I = I_1 \sum_{n=-\infty}^{\infty} \left[J_n\left(\frac{2eV_1}{\hbar\omega}\right) \sin\left\{\left(n\omega + \frac{2eV_0}{\hbar}\right)t + \phi_0\right\}\right] \tag{54}$$

We see that if the ratio $2eV_0/\hbar\omega$ is the integer n, it is possible for I to have a non-zero mean value given by

$$\bar{I} = I_1(-1)^n J_n\left(\frac{nV_1}{V_0}\right) \sin \phi_0$$

The observed amplitude depends on ϕ_0, V_0, and V_1. Experimentally, one sees constant voltage steps of amplitude $\bar{I}$ in the dc current-voltage characteristic at voltages satisfying $2eV_0/\hbar\omega = n$.

The most general approach to the electrodynamics of the Josephson junction follows from Maxwell's equations and the basic equations for the junction, Eq. 2-30, 2-31, and 2-42. After Scalapino,[28] we form a differential equation for E_x, the x component of the electric field in the junction. We proceed first by integrating the Maxwell equation

$$\vec{\nabla}\times\vec{E} = -\frac{1}{c}\frac{\partial\vec{H}}{\partial t}$$

over the contour shown in Fig. 2-11. The magnetic field integration gives

$$\frac{1}{c}\int\frac{\partial\vec{H}}{\partial t}\cdot d\vec{s} = \frac{1}{c}\frac{\partial H_y}{\partial t}(2\lambda+\ell)\ dz \tag{55}$$

while for the electric field

$$\int\vec{\nabla}\times\vec{E}\cdot d\vec{s} = \ell[E_x(z+dz)-E_x(z)] \tag{56}$$

Combining Eq. 2-55 and 2-56, we have

$$\ell\frac{\partial E_x}{\partial z} = -\frac{2\lambda+\ell}{c}\frac{\partial H_y}{\partial t} \tag{57}$$

In a similar manner, taking the normal of the surface defined by the contour to be parallel to the z axis, we find

$$\ell\frac{\partial E_x}{\partial y} = \frac{2\lambda+\ell}{c}\frac{\partial H_z}{\partial t} \tag{58}$$

From the x component of the Maxwell equation

$$\vec{\nabla}\times\vec{H} = \frac{4\pi}{c}\vec{J} + \frac{\varepsilon}{c}\frac{\partial\vec{E}}{\partial t}$$

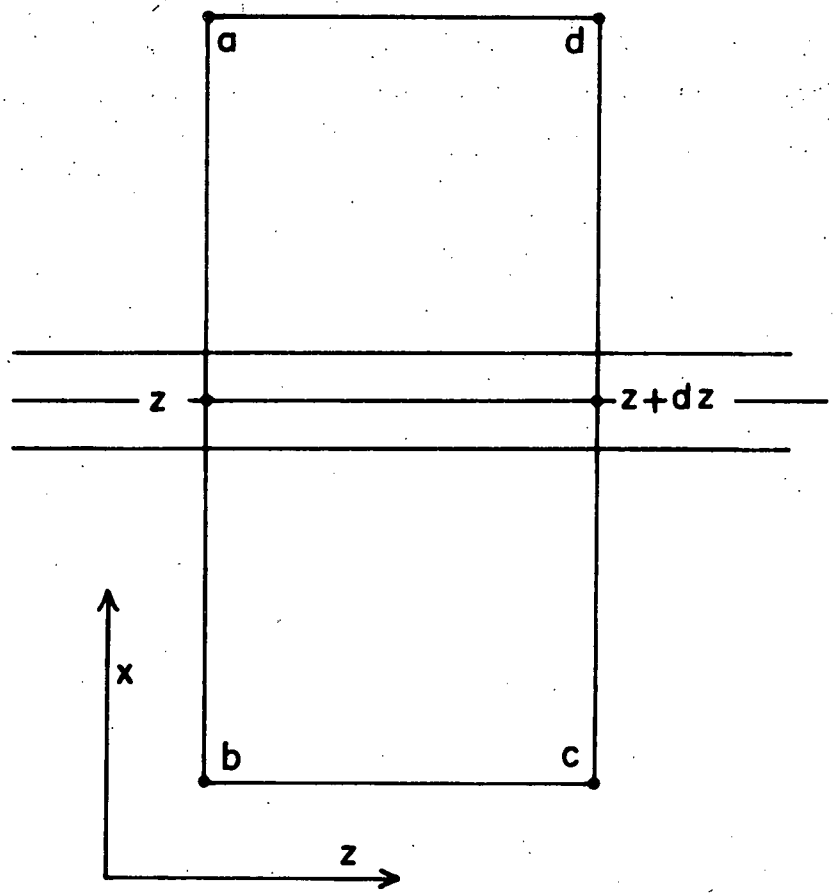

Fig. 2-11 Integration contour for the derivation of Eq. 2-60.

we have

$$\frac{\partial H_z}{\partial y} - \frac{\partial H_y}{\partial z} = \frac{4\pi}{c} J_x + \frac{\varepsilon}{c} \frac{\partial E_x}{\partial t} \tag{59}$$

where ε is the effective dielectric constant for the barrier. Combining Eq. 2-57, 2-58, and 2-59, a wave equation for E_x can be constructed:

$$\left[\nabla^2_{yz} - \frac{1}{\bar{c}^2} \frac{\partial^2}{\partial t^2}\right] E_x = \frac{4\pi}{\varepsilon} \frac{1}{\bar{c}^2} \frac{\partial}{\partial t} J_x \tag{60}$$

where the phase velocity $\bar{c}$ is given by

$$\bar{c} = c\,[\ell/(2\lambda+\ell)\varepsilon]^{1/2} \tag{61}$$

The driving term is the Josephson current density

$$J_x = J_1 \sin \phi.$$

In the absence of the driving term, Eq. 2-60 describes the wave propagation properties of a parallel plate superconducting transmission line.[87] Typically, $\bar{c}$ is on the order of 1/20 c.

Josephson[25] has reduced Eq. 2-60 to an equation in ϕ by substituting

$$\frac{\partial \phi}{\partial t} = \frac{2e}{\hbar} E_x \ell \tag{62}$$

The wave equation for ϕ is

$$\left[\nabla^2_{yz} - \frac{1}{\bar{c}^2} \frac{\partial^2}{\partial t^2}\right] \phi = \lambda_J^{-2} \sin \phi \tag{63}$$

If one assumes that the excitations of the junction are small, as is the case when the excitations are of thermal origin, the wave equation can be linearized by expanding $\sin\phi$ about ϕ_0.

The lowest mode of the junction will be the one in which there is no spatial dependence of ϕ:

$$\frac{\partial^2}{\partial t^2}\phi + \omega_p^2 \phi = 0$$

where

$$\omega_p^2 = \frac{\bar{c}^2}{\lambda_J^2} = \frac{1}{C}\frac{2e}{\hbar} I_1 \tag{64}$$

is the Josephson plasma frequency and C is the junction capacitance. In the absence of applied electric or magnetic fields, the natural frequency of phase oscillations is ω_p, modified by damping as discussed later.

If the junction is excited by a driving voltage, and the phase spatially modulated by the magnetic field, two types of natural junction resonances can be excited. The simplest resonance to visualize is the one in which the k-vector for the spatial variation of phase,

$$k_\phi = \frac{2ed}{\hbar c} H \tag{65}$$

matches the k-vector of the electromagnetic waves with frequency $2eV/\hbar$ and phase velocity $\bar{c}$:

$$k = \frac{\omega}{\bar{c}} = \frac{2eV}{\hbar \bar{c}} = \frac{2ed}{\hbar c} H = k_\phi \tag{66}$$

which provides the condition that a peak in the current-voltage characteristic will occur at a voltage

$$V = \frac{\bar{c}}{c} Hd \tag{67}$$

Such a resonance has been observed by Eck, Scalapino, and Taylor.[88]

The second resonance is a consequence of the transmission line properties of the junction. Considered as an open circuited transmission line, the junction has geometrical resonances determined by

$$n\lambda = 2L \quad \text{or} \quad \frac{n\pi\bar{c}}{\omega} = L \tag{68}$$

The most obvious resonance of this type is the one discussed above. However, because of the highly non-linear nature of Eq. 2-60, many resonances can be excited simultaneously, each corresponding to a different integer ratio of k_ϕ to the electromagnetic wave k-vector. The voltages at which the resonances, called Fiske steps,[89] can occur are fixed by the junction dimensions and $\bar{c}$, but the response is determined by the coupling energy, Q of the junction, and the tuning of the resonance by the applied magnetic field. As is the case of an external applied electromagnetic field, the resonances appear as steps in the dc current-voltage characteristic.

The usefulness of the Fiske steps for our work is that they provide the means of determining the junction capacitance.[90] Since a Josephson junction often has a resistance in the range of a few ohms, it is not convenient to make a direct measurement of the capacitance. Since the junction is considered to be a parallel plate capacitor, the capacitance is

$$C = \frac{1}{4\pi}\frac{\varepsilon}{\ell} Lw \tag{69}$$

where w is the width of the junction. L and w are known for the junction, but (ε/ℓ) is not. The phase velocity can be deter-

mined from the dimensions of the junction and the voltages for which the resonances occur. From the phase velocity, we have

$$\frac{\varepsilon}{\ell} = (c/\bar{c})^2/(2\lambda) \qquad (70)$$

The capacitance is then found by substituting (ε/ℓ) from Eq. 2-70 into the formula for the capacitance of a parallel plate capacitor given above.

III. THEORY

III.1 Phase Fluctuations in Josephson Junctions

1.1 Introduction

In Chapter I, it was stated that phase fluctuations in a Josephson junction could cause dc voltages to appear at currents less than the maximum critical current in the absence of fluctuations. The purpose of the first section of Chapter III is to provide the background and physical basis for the theoretical results of other authors which will be presented later.

From the Gor'kov-Josephson equation, the voltage and phase precession are related by

$$2eV/\hbar = \dot{\phi}. \tag{2-12}$$

If there is no applied voltage, as is the case when the junction is driven from a current source, any voltage appearing across the junction must result from internal conditions which make phase precession energetically possible. We will develop first an expression for the free energy of a junction carrying current, and then its equation of motion. It will be found that without fluctuations, the current carrying states are metastable, and the phase adjusts itself so that the free energy is a local minimum, but that with fluctuations, thermal activation out of a metastable state, accompanied by a phase change, is possible. The phase change will occur preferentially in the direction of the current, and result in a non-zero average voltage across the junction.

Because the driving force for the phase fluctuations is

thermal noise, the equations of motion for the junction can not be solved directly, but most be treated using statistical techniques. The problem will be shown to be analogous to Brownian motion of a particle in a potential, for which there already exists extensive literature. The approach is to find the equation of motion, called the Fokker-Planck[91,92] equation, for the probability distribution of the system, the solution of which enables the various averages, such as $\dot{\phi}$ and consequently the voltage, to be calculated. In practice, one usually finds approximate solutions to the Fokker-Planck equation in different limits, and certain cases will be discussed.

To compliment the work presented in this thesis, a review will be given of other recent experiments on phase fluctuations in Josephson junctions.

1.2 Free Energy of a Junction Carrying Current

The free energy of a junction carrying current must include both the coupling energy and the energy added to the junction by the external source of current.[23] The contribution to the free energy per unit area, f_{ext}, by the current is

$$f_{ext} = \int_0^t J_{ext} V dt' \qquad (1)$$

where J_{ext} is the local current density in the junction due to the external current which is assumed to be turned on at t = 0. The instantaneous value of the voltage across the junction, V, is given by

$$V = (\hbar/2e)\,\dot{\phi} \,. \qquad (2\text{-}12)$$

Inserting Eq. 2-12 into Eq. 3-1 and integrating, the contribution from the external source is

$$f_{ext} = (\hbar/2e)\, J_{ext}\, \phi \qquad (2)$$

Thus the total free energy per unit area is

$$f = -e_1 \cos \phi - (\hbar/2e)\, J_{ext}\, \phi \qquad (3)$$

where e_1 is the coupling energy per unit area. The free energy of the junction as a function of ϕ is shown in Fig. 3-1 for two values of current.

For a given value of current, equilibrium occurs when

$$\frac{\partial f}{\partial \phi} = 0 \qquad \text{and} \qquad \frac{\partial^2 f}{\partial \phi^2} > 0 \qquad (4),$$

which leads to the result

$$J_{ext} = (2e/\hbar) e_1 \sin \phi \qquad (4)$$

obtained earlier. From Fig. 3-1, it can be seen that the system resides in potential wells which become shallower as the external current is increased. Since there is no absolute minimum in the free energy, all possible states are metastable.

For wells sufficiently shallow, there is a reasonable probability that transitions to adjacent states will occur. The predominant process will be thermal activation over the potential barriers. The probability for quantum mechanical tunneling through the potential barrier is quite small, and not likely to be observed except in weakly coupled junctions at extremely low temperatures where thermal processes would be insignificant.[44,93]

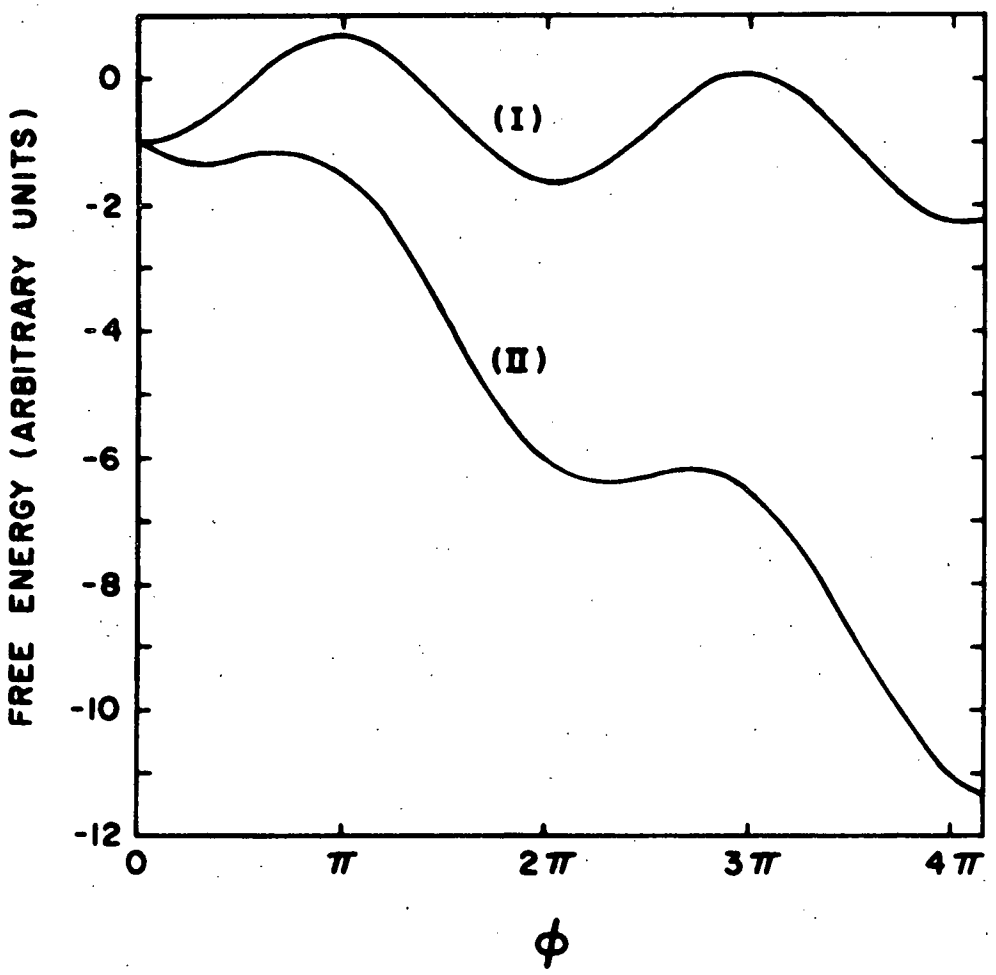

Fig. 3-1 Phase dependence of the free energy of a Josephson junction. The currents for the two curves are:

(I) $J = 0.1\ (2e/\hbar)e_1$

(II) $J = 0.8\ (2e/\hbar)e_1$

We can also neglect any quantization of states in the wells because the level spacing, $\hbar\omega_p$, is small compared to k_BT, and the levels are broadened by the random phase fluctuations. Since it is energetically favorable to decrease the potential, downward transitions will occur with greater frequency than upward transitions, and $\dot{\phi}$ will assume a non-zero average value in the direction of the current.

The activation model was used by Tilley and Clark[94] as the basis of an approximate calculation of the temperature dependence of the resistance of an array of Josephson junctions made by pressing together a number of tin balls. Assuming that the transition probability is proportional to the Boltzmann factor $\exp(-\Delta E/k_BT)$, where ΔE is the barrier height, they folded in the temperature dependence of the coupling energy to obtain an expression for the temperature dependence of the resistance which agreed with experiment over a limited range of temperature.

An early calculation of Ivanchenko and Zil'berman[42] uses a simple kinetic model to estimate the effect of fluctuations on the current-voltage characteristic. The system is assumed to oscillate in one of the minima of the potential at ω_p with a probability of making a transition to an adjacent minima proportional to the product of the attempt frequency ω_p and the Boltzmann factor $\exp(-\Delta E/k_BT)$. Using the mean value for $\dot{\phi}$, they then find a finite, current dependent voltage for $I<I_1$. The theory is only qualitatively correct since it does not either provide the transition probabilities, consider transitions to other than adjacent minima, or take into account the damping of motion in a

real junction. However, it does provide an initial theoretical basis for the observed voltage across the junction at less than the critical current.

1.3 Equations of Motion

The equations of motion are quite simply obtained from the Gor'kov-Josephson equation and conservation of charge at the junction. They are

$$\dot{\phi} = 2eV/\hbar \tag{2-12}$$

$$I = I_1(T) \sin \phi + \frac{V}{R} + C\frac{dV}{dt} - \tilde{L}(t) \tag{5}$$

The contributions on the rhs of Eq. 3-5 are respectively the Josephson current, the quasiparticle current through the barrier resistance which is approximated by the normal state resistance, the displacement current, and a fluctuating noise current. An equation of motion containing a randomly fluctuating term is called a Langevin equation. For $eV < k_B T$, which is in the region of interest, the noise is thermal[93,95] with

$$\tilde{L}(t+\tau)\,\tilde{L}(t) = [2k_B T/R]\,\delta(\tau) \tag{6}$$

The Brownian motion analogy is illuminated by making the following change of variables:[45]

$$\begin{aligned} p &= (\hbar/2e)\,CV & M &= (\hbar/2e)^2 C & x &= \frac{I}{I_1} \\ \gamma &= 2(\hbar/2e)\,I_1/k_B T & \eta &= (RC)^{-1} & & \\ L &= (\hbar/2e)\,\tilde{L} & U(\phi) &= -\frac{1}{2}\gamma k_B T\,(x\phi + \cos\phi) & & \\ \Omega &= RC\,[(2e/\hbar)\,I_1/C]^{1/2} = \eta\omega_p & & & & \end{aligned} \tag{7}$$

We can now write the equations of motion as

$$\dot{\phi} = p/M \tag{8}$$

$$\dot{p} = dU/d\phi - \eta p - L(t) \tag{9}$$

It is clear that the problem is completely equivalent to the Brownian motion of a particle of mass M in a potential U.

The parameter γ is the height of the potential barrier compared to $k_B T$ at I = 0. The parameters η and Ω characterize the damping which originates from the resistive losses in the barrier. Though the Josephson plasma oscillations are intrinsicly lossless, the variations in the phase inherent in the oscillations result in a voltage across the barrier which couples to the dissipative quasiparticle conductivity.

To visualize the effects of damping, we shall pursue the analogy of Brownian motion in a potential. Since a Josephson junction is a single macroscopic quantum system, we need consider only a single particle of mass M in the potential U. Initially assuming no losses, the frequency of small oscillations in a well is ω_p. A particle placed in a well would reside there metastably. Once activated over the barrier, it would gain energy and slide continuously along the potential. If the particle is surrounded by a viscous medium, all motion would undergo damping. The effects of damping on the oscillatory mode are to reduce the amplitude response to an excitation of the system, and to lower the frequency of the damped oscillations relative to those undamped. In particular, a value of $\Omega = 1/2$ signifies the transition from underdamped to overdamped motion in the solution of the

damped harmonic oscillator problem. The damping also provides a means of absorbing energy gained by the particle in sliding down the potential. For very heavy damping, which is the situation most easily solved, the oscillations do not substantially affect the motion, and the problem becomes one of the particle diffusing along the potential.

It is of interest to study the effects of the damping term in Eq. 3-5 in the absence of noise, a problem considered by McCumber.[96]

Introducing the dimensionless voltage

$$\alpha = \frac{V}{I_1 R}, \tag{10}$$

the dimensionless time

$$\tau = (2e/\hbar)\, I_1 R t, \tag{11}$$

and setting $\vec{L}(t) = 0$, we obtain

$$x = \Omega^2 \frac{d^2\phi}{d\tau^2} + \frac{d\phi}{d\tau} + \sin\phi \tag{12}$$

A computer solution to Eq. 3-12 results in the following conclusion. For any value of $\Omega>0$, there is a range of currents $x_c<x<1$ for which Eq. 3-12 has two possible solutions. One solution is $\alpha = 0$, which is expected in the steady state case for $x<1$. A second solution yields a value of $\alpha>0$, where α must be obtained from the numerical solution of Eq. 3-12. The value of x_c and the expected current-voltage characteristics for different values of Ω are shown in Fig. 3-2 and Fig. 3-3 respectively, both after McCumber. A junction with large Ω exhibits hysteretic behavior

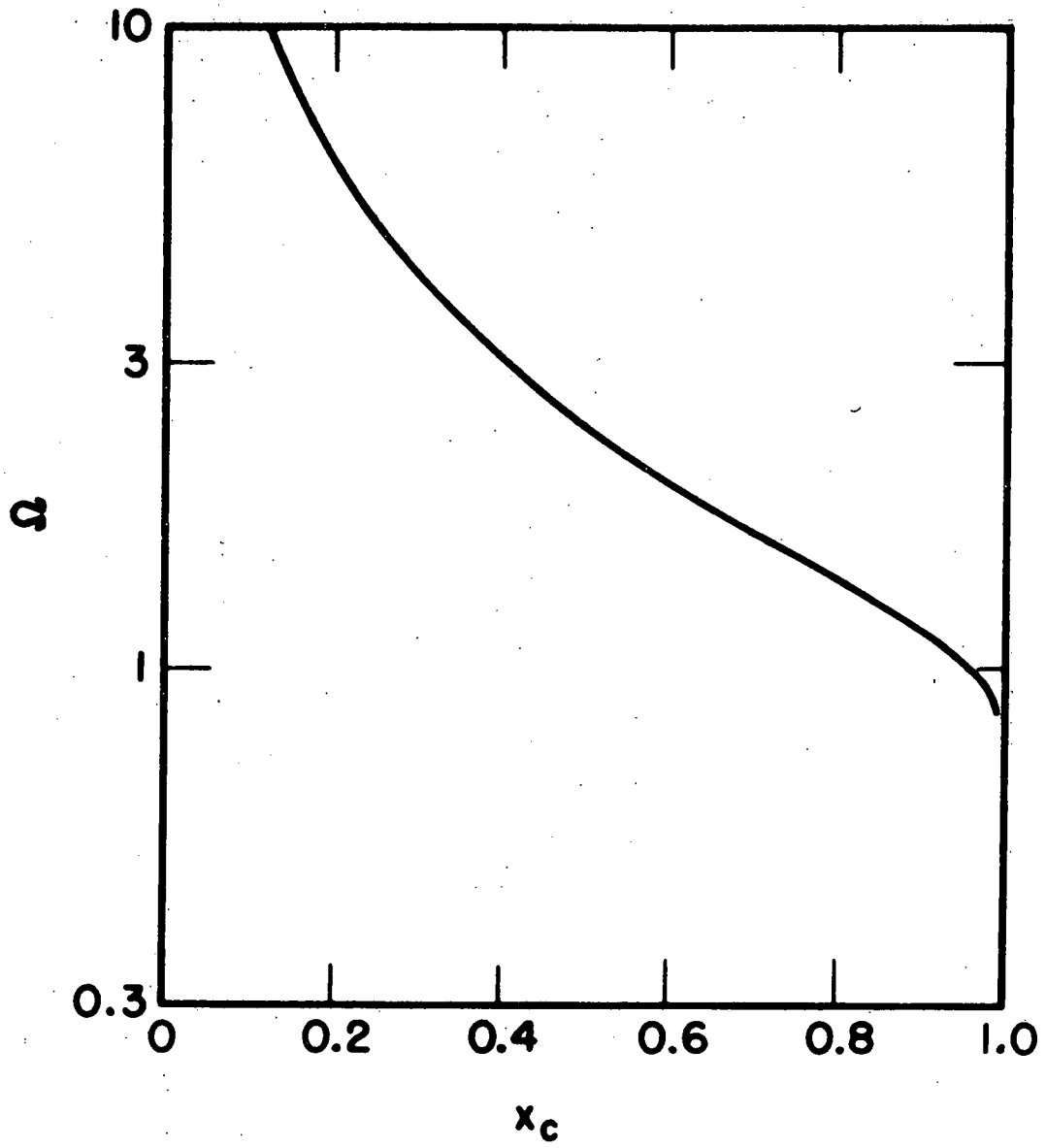

Fig. 3-2 The cut-off current x_c as a function of Ω. (After Ref. 96).

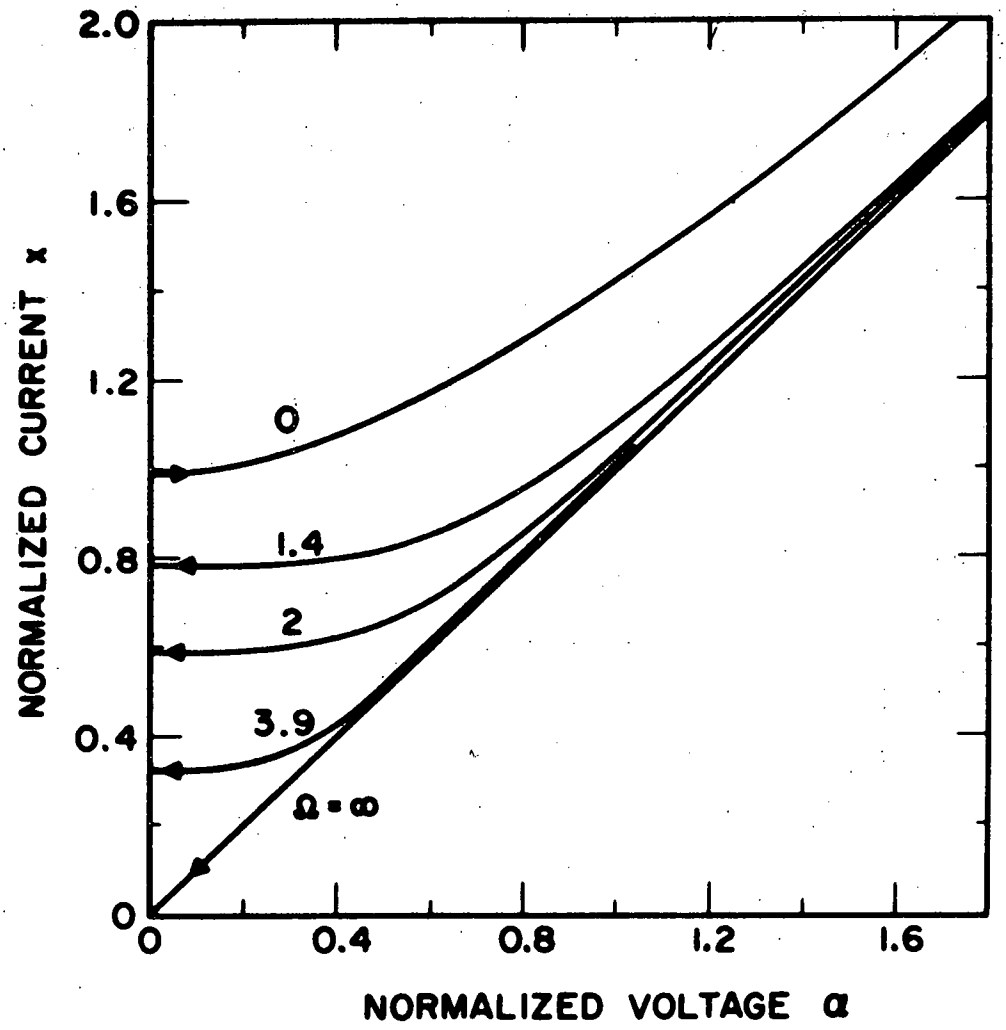

Fig. 3-3 Expected current-voltage characteristics for different values of Ω in the noise free case. (After Ref. 96).

suggested by Fig. 3-3. With increasing current, no voltage appears until $x>1$, but when the current is subsequently decreased (at rates at least comparable to audio frequencies), the voltage does not return to zero until $x<x_c$. To aid later interpretation of the data, we note two consequences of Fig. 3-3. First, with hysteresis, the voltage for $x>x_c$ is always greater than the case with $\Omega = 0$. Second, the effects of hysteresis are only significant for $\Omega \gtrsim 1$. Thus if $\Omega \lesssim 1$, the effects of junction capacitance are minimal.

1.4 Fokker-Planck and Smoluchowski Equations

As indicated previously, the Langevin equations can only be solved using statistical techniques. The final motion of the system is determined from ensemble averages of the variables obtained using a probability distribution function which is a solution to the Fokker-Planck equation.

The validity of the statistical approach is based on the assumption that the noise impulses are completely random, that is, they are totally uncorrelated. In practice, this usually means that the correlation time for the noise must be very short compared to the time resolution of the system being considered. For a Josephson junction, that time scale is set by $1/\omega_p$, which is on the order of 10^{-9} seconds. Since the mean collision time between electrons in a metal is in the range of 10^{-11} to 10^{-14} seconds, the assumption that the noise is uncorrelated is valid.

The probability distributions used to describe Brownian motion have the property that the probability of reaching a given

point in phase space at time t depends only upon the location of the system at t-Δt, where Δt is short compared to the time over which substantial changes in the coordinates take place. The probability distribution is independent of the past history of the system. A stochastic process having the above property is defined as a Markoff process, and the derivation of the Fokker-Planck equation is fundamentally related to the Markoff process.[97]

Recognizing the analogy between phase fluctuations in a Josephson junction and Brownian motion in a potential, the Fokker-Planck equation will be developed in terms of Brownian motion. Following Chandrasekhar,[98] we wish to find a differential equation for the probability distribution P(q,v,t) which is defined as

$P(q,v,t)dqdv$ = probability of finding q in the range q,q+dq and v in the range v,v+dv at time t

where $v = \dot{q}$ and q is the appropriate space coordinate. In addition, we need a transition probability $F(q,v|\Delta q,\Delta v)$ defined as

$F(q,v|\Delta q,\Delta v)d(\Delta q)d(\Delta v)$ = probability that given q and v, Δq will be in the range Δq,Δq+d(Δq) and Δv will be in the range Δv, Δv+d(Δv).

where Δq, Δv are the changes in q and v respectively occuring over a time Δt.

From the definition for a Markoff process, for P and for F, the fundamental equation to be satisfied by P is

$$P(q,v,t) = \iint P(q-\Delta q,v-\Delta v,t-\Delta t)\, F(q-\Delta q,\, v-\Delta v|\Delta q,\Delta v) \times d(\Delta q)d(\Delta v). \quad (13)$$

Incremental changes in q and v are related by

$$\Delta q = v\Delta t \qquad \Delta v = -(\beta v - K)\Delta t + v_f(\Delta t) \tag{14}$$

where K is the acceleration resulting from the presence of a force field, β is a damping constant, and $v_f(\Delta t)$ is the net acceleration from the random forces acting over a time Δt. From Eq. 3-14, we can thus reduce the transition probability to

$$F(q,v|\Delta q,\Delta v) = F'(q,v|\Delta v)\delta(\Delta q - v\Delta t). \tag{15}$$

With this form for F, we can immediately perform the integration over Δq in Eq. 3-13 to obtain

$$P(q,v,t) = \int P(q-v\Delta t, v-\Delta v, t-\Delta t)F'(q-v\Delta t, v-\Delta v|\Delta v)d(\Delta v). \tag{16}$$

For convenience in the calculation below, we write Eq. 3-16 as

$$P(q+v\Delta t, v, t+\Delta t) = \int P(q, v-\Delta v, t)F'(q, v-\Delta v|\Delta v)d(\Delta v). \tag{17}$$

To obtain the Fokker-Planck equation, we first expand each side of Eq. 3-17 in a Taylor series, retaining only terms up to $(\Delta v)^2$:

$$P(q,v,t) + \{\frac{\partial P}{\partial t} + v\frac{\partial P}{\partial q}\}\Delta t + O(\Delta t^2) = \tag{18}$$

$$\int\{P(q,v,t) + \frac{\partial P}{\partial v}(-\Delta v) + \frac{1}{2}\frac{\partial^2 P}{\partial v^2}(-\Delta v)^2 + \ldots\} \times$$

$$\{F'(q,v|\Delta v) + \frac{\partial F'}{\partial v}(-\Delta v) + \frac{1}{2}\frac{\partial^2 F'}{\partial v^2}(-\Delta v)^2 + \ldots\}\, d(\Delta v).$$

Eq. 3-18 can be considerably simplified by introducing the quantities

$$M_1(v) = \lim_{\Delta t \to 0} \frac{\langle \Delta v \rangle_{av}}{\Delta t} \tag{19}$$

and

$$M_2(v) = \lim_{\Delta t \to 0} \frac{\langle \Delta v^2 \rangle_{av}}{\Delta t} \tag{20}$$

where the indicated averages are defined as

$$\langle \Delta v \rangle_{av} = \int P \Delta v \, d(\Delta v) \tag{21}$$

and

$$\langle \Delta v^2 \rangle_{av} = \int P (\Delta v)^2 \, d(\Delta v). \tag{22}$$

With the quantities $M_1(v)$ and $M_2(v)$, Eq. 3-18 becomes

$$P + \{\frac{\partial P}{\partial t} + v\frac{\partial P}{\partial q}\}\Delta t = P - \frac{\partial}{\partial v}[M_1(v)P]\Delta t + \frac{1}{2}\frac{\partial^2}{\partial v^2}[M_2(v)P]\Delta t \tag{23}$$

which leads immediately to the Fokker-Planck equation

$$\frac{\partial P}{\partial t} + v\frac{\partial P}{\partial q} = -\frac{\partial}{\partial v}[M_1 P] + \frac{1}{2}\frac{\partial^2}{\partial v^2}[M_2 P]. \tag{24}$$

M_1 and M_2 can be found by direct integration of the Langevin equation, which for our problem has the form

$$\dot{v} = K - \beta v + A(t) \tag{25}$$

where A(t) is a random acceleration. A(t) has the properties

$$\langle A(t) \rangle_{av} = 0$$

and (26)

$$\langle A(t+\tau)\, A(t) \rangle_{av} = 2D\, \delta(\tau)$$

where D is a "diffusion" constant. Integrating Eq. 3-25, we find

$$\langle \Delta v \rangle_{av} = -(\beta v - K)\Delta t + \int_t^{t+\Delta t} A(t')dt' = -(\beta v - K)\Delta t \tag{27}$$

Therefore, by Eq. 3-19

$$M_1 = -(\beta v - K). \tag{28}$$

Similarly for $\langle \Delta v^2 \rangle_{av}$, we have

$$\begin{aligned} \langle \Delta v^2 \rangle_{av} &= (\beta v - K)^2 (\Delta t)^2 - 2(\beta v - K)\Delta t \int_t^{t+\Delta t} A(t')dt' \\ &\quad + \iint_t^{t+\Delta t} \langle A(t')\, A(t'') \rangle_{av}\, dt'dt'' \\ &= (\beta v - K)^2 (\Delta t)^2 + 2D\Delta t. \end{aligned} \tag{29}$$

Therefore, by Eq. 3-20

$$M_2 = 2D. \tag{30}$$

Using the above values for M_1 and M_2, the Fokker-Planck equation can now be written as

$$\frac{\partial P}{\partial t} = -K \frac{\partial P}{\partial v} - v \frac{\partial P}{\partial q} + \beta \frac{\partial}{\partial v} \left[vP + \frac{D}{\beta} \frac{\partial P}{\partial v} \right]. \tag{31}$$

With the potential U given by Eq. 3-7 and the Langevin Eq. 3-9, an analytic solution for the Fokker-Planck equation has been found only for the case of heavy damping.[45] Heavy damping is taken to mean that the damping forces are much greater than those due to the potential U. With heavy damping, the Fokker-Planck equation reduces to a diffusion equation. To show this,[99] we first write Eq. 3-31 as

$$\begin{aligned} \frac{\partial P}{\partial t} &= \beta \left(\frac{\partial}{\partial v} - \frac{1}{\beta} \frac{\partial}{\partial q} \right) \left(vP + \frac{D}{\beta} \frac{\partial P}{\partial v} - \frac{K}{\beta} P + \frac{D}{\beta^2} \frac{\partial P}{\partial q} \right) \\ &\quad - \frac{\partial}{\partial q} \left(\frac{K}{\beta} P - \frac{D}{\beta^2} \frac{\partial P}{\partial q} \right) \end{aligned} \tag{32}$$

and integrate along the straight line $q+v/\beta = q_0$ over the range

$-\infty \leq v \leq \infty$:

$$\frac{\partial}{\partial t}\int_{q+\frac{v}{\beta}=q_0} P dv = \int_{q+\frac{v}{\beta}=q_0} \frac{\partial}{\partial q}\left(\frac{D}{\beta^2}\frac{\partial P}{\partial q} - \frac{K}{\beta}P\right) dv. \qquad (33)$$

We shall assume that the scale of variation of K(q) and P(q,v,t) is less than the mean free path $\ell = (D/\beta^3)^{1/2}$, and that $|v|<v_d = (D/\beta)^{1/2}$, the thermal drift velocity. For heavy damping, we expect that an arbitrary initial distribution P(q,v,0) will pass to a Maxwellian distribution for $t >> 1/\beta$. Thus

$$P(q,v,t) \simeq \left(\frac{m}{2\pi k_B T}\right)^{1/2} \sigma(q,t)\, \exp[-mv^2/2k_B T] \qquad (34)$$

where m is the particle mass. Using P(q,v,t) given by Eq. 3-34, Eq. 3-33 becomes

$$\frac{\partial\sigma(q_0)}{\partial t} \simeq \frac{\partial}{\partial q_0}\left(\frac{D}{\beta^2}\frac{\partial\sigma(q_0)}{\partial q_0} - \frac{K(q_0)}{\beta}\sigma(q_0)\right). \qquad (35)$$

With the assumptions above on the scale of variation of K and σ, and the magnitude of v, Eq. 3-35 can be generalized to

$$\frac{\partial\sigma}{\partial t} = \frac{\partial}{\partial q}\left[\frac{D}{\beta^2}\frac{\partial\sigma}{\partial q} - \frac{K}{\beta}\sigma\right] = -\frac{\partial w}{\partial q} \qquad (36)$$

which is called the Smoluchowski equation. if σ is normalized to unity, then w represents a probability current giving the rate of motion of the particle along the potential.

The type of stochastic equation for the distribution function is determined by the number of variables required to define the Markoff process.[100] In Eq. 3-13, the starting point for the derivation of the Fokker-Planck equation, it was assumed that q and v were sufficient to describe the Markoff process. If only q were necessary, we would then have arrived at the

Smoluchowski equation. Higher order equations than the Fokker-Planck equation are possible, but are not of physical interest here. In general, one decides the number of variables on the basis of the order of the Langevin equation. In particular, the Smoluchowski equation for $\sigma(q,t)$ is appropriate for a Langevin equation which is a first order differential equation, and the Fokker-Planck equation for $P(q,v,t)$ is appropriate when the Langevin equation is second order. As an example, consider the differential equation of McCumber with a noise term $\tilde{\tilde{L}} = \tilde{L}/I_1$ added to produce a Langevin equation:

$$x = \Omega^2 \frac{d^2\phi}{d\tau^2} + \frac{d\phi}{d\tau} + \sin\phi - \tilde{\tilde{L}} . \tag{37}$$

The solution of Eq. 3-37 entails the use of the full Fokker-Planck equation. In the limit $\Omega \to 0$, the condition for heavy damping, Eq. 3-37 reduces to

$$x = \frac{d\phi}{d\tau} + \sin\phi - \tilde{\tilde{L}} \tag{38}$$

which can be solved using the Smoluchowski equation.

1.5 Solutions of the Stochastic Equations

The proper variables for the Fokker-Planck and Smoluchowski equations in the case of a Josephson junction are

$$v = \frac{p}{M} \qquad K = -\frac{\partial U}{\partial \phi} \qquad \beta = \eta \qquad \frac{D}{\beta} = Mk_BT . \tag{39}$$

The Fokker-Planck equation thus becomes

$$\frac{\partial P}{\partial t} = \frac{\partial U}{\partial \phi}\frac{\partial P}{\partial p} - \frac{p}{M}\frac{\partial P}{\partial \phi} + \eta\frac{\partial}{\partial p}\left[pP + Mk_BT\frac{\partial P}{\partial p}\right] \tag{40}$$

and the Smoluchowski equation, appropriate for $\Omega<1$, is

$$\frac{\partial \sigma}{\partial t} = \frac{1}{\eta M} \frac{\partial}{\partial \phi} \left[\left(\frac{\partial U}{\partial \phi} \right) \sigma + k_B T \frac{\partial \sigma}{\partial \phi} \right]. \tag{41}$$

We will consider first the solution of the Smoluchowski equation, as an exact solution to it has been found by Ambegaokar and Halperin.[45] For the potential U, the phase ϕ need only be considered modulo 2π, $0 \leq \phi \leq 2\pi$, and Eq. 3-41 is solved with periodic boundary conditions.

For a steady state solution, $\frac{\partial \sigma}{\partial t} = 0$, and w must be constant. With σ normalized to unity, w^{-1} is the average time required for the phase to diffuse one periodicity length of 2π. Thus the mean voltage is given by

$$V = (\hbar/2e)\, 2\pi w. \tag{42}$$

The Green's function found for Eq. 3-41 by Ambegaokar and Halperin is

$$\sigma(\phi) = \frac{w \eta M}{k_B T} \frac{f(\phi)}{f(2\pi) - f(0)} \left[f(0) \int_0^{\phi} \frac{d\phi'}{f(\phi')} + f(2\pi) \int_{\phi}^{2\pi} \frac{d\phi'}{f(\phi')} \right] \tag{43}$$

where $f(\phi) = \exp(-U/k_B T)$. The mean voltage is then

$$V = I_1 R \frac{4\pi}{\gamma} \left\{ (e^{\pi \gamma x} - 1)^{-1} \left[\int_0^{2\pi} d\phi f(\phi) \right] \left[\int_0^{2\pi} \frac{d\phi}{f(\phi)} \right] + \int_0^{2\pi} d\phi \int_{\phi}^{2\pi} d\phi' \frac{f(\phi)}{f(\phi')} \right\}^{-1} \tag{44}$$

A more compact form, obtained by Biswas and Jha, is

$$V = I_1 R \frac{8\pi}{\gamma} \sinh \left(\frac{\pi \gamma x}{2} \right) \left[\int_{-\pi}^{\pi} d\phi \int_{-\pi}^{\pi} d\phi' \, f(\phi) \, f(\phi' - \phi) \right]^{-1} \tag{45}$$

Results similar to these have been obtained by Ivanchenko and Zil'berman.[38,44] Current-voltage characteristics calculated from Eq. 3-44 are shown in Fig. 3-4.

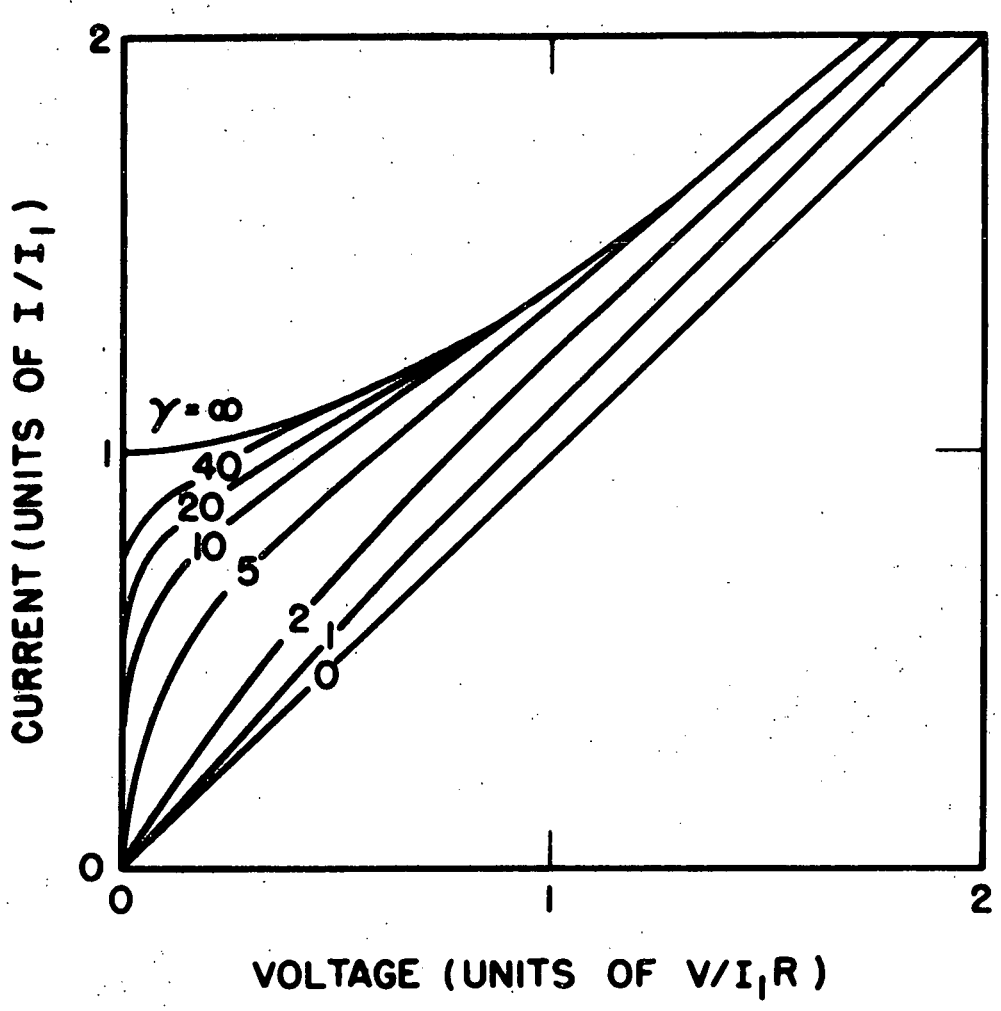

Fig. 3-4 Predicted current-voltage characteristics in the presence of noise with $\Omega = 0$. (After Ref. 45).

In the derivation of the Smoluchowski equation, conditions were placed on the maximum drift velocity v_d, and the mean free path $\bar{\ell}$. For the Josephson junction problem, the conditions of applicability are that

$$V < V_m = (k_B T/C)^{1/2} \tag{46}$$

and that the spatial variation of U and σ be slow compared to

$$\bar{\ell} = (2e/\hbar)\, V_m RC. \tag{47}$$

For a heavily damped junction, the voltage range of experimental interest is usually such that these conditions are met.

Analytic forms of Eq. 3-44 can be found in several limits:[45]

$$V = IR, \quad \gamma \to 0 \tag{48}$$

$$= I_1 R\,(x^2-1)^{1/2}, \quad \gamma \to \infty, \quad x>1 \tag{49}$$

$$= 0, \quad \gamma \to \infty, \quad x<1$$

$$= 2(1-x^2)^{1/2} \exp\{-\gamma[(1-x^2)^{1/2} + x \arcsin x]\} \sinh \frac{\pi\gamma x}{2}, \tag{50}$$

γ large, $x<1$.

Equation 3-49 corresponds to the case of no noise, and was obtained earlier by McCumber. As a means of experimentally determining γ, a useful limit is[45]

$$\lim_{I \to 0} \frac{V}{IR} = [I_0(\tfrac{\gamma}{2})]^{-2} \tag{51}$$

where I_0 is the modified Bessel function. In practice, Eq. 3-51 is only useful for small values of γ.

No analytic solutions are currently available for cases of intermediate or light damping, for which the full Fokker-Planck

equation must be solved. Assuming that the shape of the maxima of the potential can be approximated by the harmonic oscillator potential, and that transitions can occur only between adjacent wells, Halperin[101] provides the following correction formula for $\Omega>1$, $\gamma>>1$, and $x<<x_c$ obtained from Fig. 3-2.

$$V = I_1 R \frac{[\{1 + 4\Omega^2(1-X^2)^{1/2}\}^{1/2} - 1]}{2\Omega^2(1-x^2)^{1/2}} V_{\Omega=0} \qquad (52)$$

This result was also obtained by Biswas and Jha,[48] and agrees with the earlier work of Ivanchenko and Zil'berman.[42]

Using computer techniques, Ambegaokar and Kurkijärvi[49] have performed numerical calculations of the current-voltage characteristic valid in all regimes by integrating the Langevin equation directly, supplying noise pulses distributed in amplitude and time corresponding to collisions with an ideal gas of light particles. In addition to being able to provide current-voltage characteristics for any set of (Ω,γ), Ambegaokar and Kurkijärvi have verified the previous observation that for a given γ, curves having a larger Ω have a larger voltage for a given current than those with smaller Ω. Further, for a given Ω, curves including noise cross the hysteretic curves of no noise, and approach them from above. Exact comparison of theory to experiment awaits data with values of γ and Ω confidently known.

As an interesting historical note, the Langevin of Eq. 3-38 was first solved for a system entirely unrelated to the Josephson

effect. Tikhonov[102] in 1947 considered the problem of the effects of noise on the frequency synchronization of two oscillators using a phase feedback technique. The operation of the system is as follows. For two oscillators at the same frequency, the phase difference in constant. Any shift in frequency results in a phase change which is detected by a phase sensitive detector, and the output used to adjust the frequency of one of the oscillators. Tikhonov has shown that the coupling of the oscillators varies with ϕ identically the same as shown in Fig. 3-1 for the coupling of a Josephson junction. The variables corresponding to I and V of the junction are Δ_0 and δf, the oscillator detuning and relative frequency respectively. The effect of noise is to temporarily unlock the phase correlation, and allow the phase to jump by 2π. The rate of phase jump is simply δf.

The method for solving the Fokker-Planck equation used by Ivanchenko and Zil'berman is the same as that used by Tikhonov, but they were apparently unaware of his work. Figure 3 of Tikhonov is identical in appearance to the current-voltage characteristics of Fig. 3-4. A frequency locking scheme such as this might be a useful analog means to obtain the theoretical I-V characteristics.

1.6 Survey of Experimental Work

The earliest evidence of phase fluctuation rounding of the current-voltage characteristic is that of Shigi et al.,[40] who observed qualitatively the rounding but did not recognize its significance. Further, there is insufficient information pre-

sented to properly characterize the data. Following the first paper of Ivanchenko and Zil'berman on phase fluctuations, Galkin et al.[43] observed rounding of the current-voltage characteristics in high resistance Josephson junctions subjected to a magnetic field. Again, the difficulty of properly characterizing the data existed, and no attempt was made to treat the data according to the theory of Ivanchenko and Zil'berman. In addition, there is evidence that the noise sources are very strong, inducing a finite voltage at currents on the order of 0.1 mA, too large to be assumed thermal in the absence of a thermal noise generator.

In order to eliminate the ambiguities associated with the noise environment, Anderson and Goldman,[46,47] employed a shielded room and equipment designed to provide as little extraneous noise to the sample as feasible. Josephson tunnel junctions with characteristics close to ideal were used to minimize the possibility that effects peculiar to the particular junction would not make interpretation of the data difficult. Despite the precautions taken, it was necessary to make multiparameter fits to the data, using T and I_1 as the fitted parameters, in order to achieve agreement with the theory of Ambegaokar and Halperin. Details will be provided later in this thesis.

Since the tunnel junction structure is a capacitor, the junctions produced have $\Omega>0$. To reduce Ω, Parker and Simmonds[50] used weak link bridges, resulting in an upper limit of 0.1 for Ω. With only the critical current as a fitted parameter, they obtained good agreement with the theory of Ambegaokar and Halperin. At the time, the current-phase relationship for a weak link was

not known, and attempts were made to eliminate the remaining discrepancy by adjusting the form of the current-phase relationship. Though it was found that a sawtooth rather than a sinusoidal form was marginally better, an experiment by Fulton and Dynes[103] showed that the correct form, at least in the vicinity of T_c, is the usual Josephson current-phase relation.

Rather than adjust γ by varying the temperature or magnetic field, alternately, one can vary the amount of noise to which the junction is subjected. Kanter and Vernon[51] have used a gas-discharge noise tube, which has a thermal noise output up to at least 60 GHz., to illuminate a Nb-Nb point contact kept at 4.2 K. Because the coupling from the radiation field to the junction could not be determined, the absolute value of γ was not know, but for a constant current of 0.8 I_1 through the junction, the change in junction voltage with the input noise power follows the predicted dependence. In a related experiment,[53] they have shown that low frequency noise, that is noise with $f_{max} < \omega_p$, produces a qualitatively similar current-voltage characteristic for low values of γ. The implication is that experiments which make use of an effective noise temperature may in fact be adjusting the temperature to account for unidentified low frequency or discrete noise sources. With the exception of the experiment of Parker and Simmonds, this covers all experiments which have attempted quantitative agreement.

A further experiment using external noise is that of Buckner et al.[52] The experiment was performed with extremely small junction, on the order of 10^{-6} cm^2, so that geometric rf reso-

nances would not be excited until V reached several millivolts. This specifically meets the conditions for one aspect of the theory of Ivanchenko and Zil'berman[44] to which the experiment was compared. Reasonably good agreement was found except that a high internal noise temperature of 800 K was indicated from the manner in which they estimated the thermal noise in the junction. By the criterion of Kanter and Vernon, the noise source used in the experiment of Buckner et al., was in the low frequency regime. Since comparison of the theory to experiment was at low values of γ, no difference is expected in the current-voltage characteristic from what would appear had broadband noise been used.

III.2 Pair Susceptibility of a Superconductor

2.1 Introduction

In the remaining sections of Chapter III, we shall consider the contribution to junction conductivity associated with electron pairs produced by fluctuations above the transition temperature. The Josephson junctions used in these experiments are asymmetrical, one side being the superconductor of interest with a relatively low transition temperature and the other side being the reference, a superconductor with a high transition temperature. For convenience, we use the subscripts (1) and (2) to refer to the superconductors with the lower and higher transition temperatures respectively.

As the theoretical treatment of Scalapino,[32] using microscopic electron tunneling theory, is beyond the scope of this

thesis, we introduce a phenomenological calculation which gives most of the results of the complete theory. In this calculation, we solve for the pair current I_1 by equating the power dissipated in the pair tunneling channel I_1V to the rate of change of the internal energy in the normal metal produced by a perturbation which is the effective Hamiltonian coupling the order parameter in the superconductor with the order fluctuations in the normal metal. Because of the simultaneous presence of the usual quasiparticle tunneling current, we call the pair current an excess current. The procedure works because it is possible to experimentally and theoretically distinguish between the pair and quasiparticle tunneling channels and the dissipation associated with each.

In a very crude way, one could consider the excess current as arising from an ephemeral Josephson junction, the reference superconductor well below T_{c_2} serving as one side of the junction and the superconductor of interest just above T_{c_1} as the other. Even though one side is not superconducting, local fluctuations produce short lived regions in which the superelectron density is not zero. These regions, coupled through the barrier to the reference superconductor, act as small Josephson junctions, and as such, contribute a pair current to the total tunneling current. One can develop a heuristic model of the excess current using these ideas, and with certain assumptions, obtain the temperature, voltage, and magnetic field dependence of the excess current. However, such a calculation misses the physics inherent in the concept of pair susceptibility used to calculate the excess

current.

Because our phenomenological calculation requires explicit use of the Ginzburg-Landau theory, we begin with a brief discussion of Ginzburg-Landau theory. Since linear response theory is also employed, a brief introduction to certain aspects of that theory is presented. A definition of the generalized susceptibility is given in the framework of linear response theory. After showing that the dissipative response of a system is related to the imaginary part of the susceptibility, we calculate the imaginary part of the susceptibility using the Fluctuation-Dissipation theorem[104] introduced in III.2.3. The specific form of the time rate of change of the internal energy applicable to a Josephson junction is derived in III.2.5, and in section III.2.6, the phenomenological calculation of the excess current and its temperature, voltage, and magnetic field dependence is presented.

To conclude the last half of Chapter III, a brief survey of other pertinent theoretical and experimental work will be given.

2.2 Ginzburg-Landau Theory

In the simple theory of the excess current presented in the next section, the Ginzburg-Landau (GL) theory of superconductivity[71,105] will be used. At this point, we will consider some basic results from that theory.

In the Landau theory[106] of phase transitions, a phase transition occurs as a result of the development of a minimum in the free energy at the transition temperature. In second-

order phase transitions, of which the superconducting transition is an example, a power series expansion of the free energy, valid near T_c, is made in terms of an order parameter which has a non-zero average value only below T_c. For a superconductor, the order parameter is ψ, normalized such that $|\psi|^2 = n_s$, the superelectron density.

The general expansion for the Helmholtz free energy density near T_c is considered to be

$$f = f_N + a_1\psi + a_2|\psi|^2 + a_3|\psi|^2\psi + a_4|\psi|^4 \qquad (53)$$

where f is the free energy density, f_N the free energy density of the normal state at T_c, and the a_i are expansion coefficients which may be functions of other parameters of the system. Because of the assumption that $\psi = 0$ above T_c, symmetry conditions require that coefficients of the odd powers of ψ be zero. For a superconductor, the free energy will be written as

$$f = f_N + \alpha|\psi|^2 + \frac{\beta}{2}|\psi|^4. \qquad (54)$$

Note that the theory is equally valid both above and below T_c.

For small values of the order parameter, $\alpha|\psi|^2$ determines the initial behavior of the free energy, and thus the simplest manner to achieve a minimum in the free energy is to have $\alpha<0$. The conditions for a minimum in the free energy are

$$\frac{\partial f}{\partial \psi} = 0 \qquad \text{and} \qquad \frac{\partial^2 f}{\partial \psi^2} > 0 \qquad (55)$$

from which we find

$$|\psi|^2 = -\frac{\alpha}{\beta}.$$

For $T>T_c$, the minimum occurs at $|\psi|^2 = 0$. In the vicinity of T_c, one assumes that α varies linearly with T:

$$\alpha(T) = (T_c - T)\left(\frac{d\alpha}{dT}\right)_{T=T_c} \tag{56}$$

and that β is approximately a constant. Below T_c,

$$f_N - f = \frac{H_c^2(T)}{8\pi}, \tag{57}$$

where $H_c(T)$ is the bulk critical field, the relationship

$$H_c^2(T) = 8\pi\frac{\alpha^2}{\beta} = 4\pi(T_c - T)^2 \frac{1}{\beta}\left(\frac{d\alpha}{dT}\right)^2_{T=T_c} \tag{58}$$

follows. Equation 3-58 provides an experimental means of determining α and β.

To further generalize GL theory, terms allowing for a spatial variation of ψ and the presence of a magnetic field must be added. The spatial variation of ψ is taken to be $\frac{1}{2m}|-i\hbar\nabla\psi|^2$, a kinetic energy-like term. The magnetic field H adds an energy per unit volume of $H^2/8\pi$. To maintain gauge invariance, we make the usual change in the definition of the momentum:

$$\frac{1}{2m}|-i\hbar\nabla\psi|^2 \rightarrow \frac{1}{2m}\left|(-i\hbar\nabla - \frac{2e\vec{A}}{c})\psi\right|^2. \tag{59}$$

The complete expression for the free energy becomes

$$f = f_N + \alpha|\psi|^2 + \frac{\beta}{2}|\psi|^4 + \frac{1}{2m}\left|(-i\hbar\nabla - \frac{2e\vec{A}}{c})\psi\right|^2 + \frac{H^2}{8\pi}. \tag{60}$$

By minimizing f with respect to both ψ and $\vec{A}$, we obtain the Ginzburg-Landau equations:

$$\alpha\psi + \beta|\psi|^2\psi + \frac{1}{2m}(-ih\nabla - \frac{2e\vec{A}}{c})^2\psi = 0 \tag{61}$$

and

$$J = -\frac{e\hbar}{im}(\psi^*\nabla\psi - \psi\nabla\psi^*) - \frac{4e^2}{mc}\psi^*\psi\vec{A} \tag{62}$$

the latter of which was originally introduced in Eq. 2-7.

At this point, we will make a large jump in the development of GL theory. The original GL theory was simply another application of the earlier work of Landau on phase transitions. Following the development of BCS theory, Gor'kov[77] derived the GL equations from microscopic theory, in the vicinity of T_c, and calculated the constants α and β:

$$\alpha = \alpha_0\varepsilon \qquad \text{and} \qquad \beta = \frac{\alpha_0^2}{N(0)(3.2k_BT_c)^2} \tag{63}$$

where

$$\varepsilon = \frac{T-T_c}{T_c}$$

Limiting forms for the constant α_0 are:

$$\alpha_0 = \frac{24\pi^2(k_BT_c)^2}{7m\zeta(3)\,v_F^2} \quad \text{(long mean free path)} \tag{64}$$

and

$$\alpha_0 = \frac{12\hbar k_BT_c}{\pi m v_F \ell} \quad \text{(short mean free path)} \tag{65}$$

where ζ is the Riemann zeta function, v_F the Fermi velocity, and ℓ the conduction electron mean free path. The conditions for long or short mean free path can be stated in terms of the BCS coherence length

$$\xi_0 = \frac{2\hbar\, v_F}{3.5\pi\, k_BT_c}\,. \tag{66}$$

The condition $\ell >> \xi_0$ corresponds to the long mean free path or clean limit and $\ell << \xi_0$ to the short mean free part or dirty limit. For some purposes, it is more convenient to work with the temperature dependent coherence length defined from α by

$$\xi^2(T) = \frac{\hbar^2}{2m} \frac{1}{|\alpha|} = \frac{\hbar^2}{2m} \frac{1}{\alpha_0} |\varepsilon^{-1}| \tag{67}$$

which on combining with Eq. 3-66 and inserting explicitly the numerical constants gives

$$\xi(T) = 0.74\ \xi_0 |\varepsilon|^{-1/2} \qquad \text{clean limit}$$

$$\xi(T) = 0.85\ (\xi_0 \ell)^{1/2} |\varepsilon|^{-1/2} \qquad \text{dirty limit}$$

or

$$\xi(T) = \xi_0' |\varepsilon|^{-1/2} \tag{68}$$

where ξ_0' is taken in the appropriate limit. The temperature dependent coherence length represents the natural length for variations in ψ, as changes in ψ may not occur over lengths short in comparison to ξ.

The GL theory as introduced above does not consider time variations of ψ in other than a quasi-static sense. Thus time independent GL equations can not be used to describe non-equilibrium situations such as flux flow in Type II superconductors, electrical resistance in the vicinity of T_c, and the problem to be considered shortly, that of the excess current in a Josephson junction above T_{c_1}. If ψ is disturbed from its equilibrium value, what is desired is the simplest equation for ψ which will allow it to relax to its equilibrium value. The time dependent GL equation[107,108] is based on the assumption that the functional derivative of the GL free

energy is a generalized force which will act to restore ψ to its equilibrium value, and the consequent motion is damped through a term proportional to $\frac{d\psi}{dt}$, giving

$$\gamma \hbar \frac{\partial \psi}{\partial t} = - \frac{\delta F}{\delta \psi}. \tag{69}$$

From microscopic theory,

$$\gamma = \frac{\alpha}{\hbar \Gamma_0} \tag{70}$$

where Γ_0 is the relaxation frequency for ψ and has the value

$$\Gamma_0 = \frac{8}{\pi} \frac{k_B T_c}{\hbar} \varepsilon. \tag{71}$$

In its final form, the time dependent GL equation in the absence of a magnetic field is

$$\{\frac{\partial}{\partial t} + \frac{\Gamma_0}{\alpha} [\alpha + \frac{1}{2m} (-i\hbar\nabla)^2 + \beta|\psi|^2]\}\psi = 0. \tag{72}$$

In many situations, as in the pair susceptibility calculation of Scalapino, the pair potential $\Delta(r)$ is taken as the order parameter. The relationship between Δ and ψ is

$$\psi(r) = [N(0)/\alpha_0]^{1/2} \Delta(r). \tag{73}$$

2.3 Linear Response Theory

Linear response theory[109,110] provides several basic relationships with which one can calculate the excess current in a straightforward manner. Below we outline those basic results applicable to the phenomenological calculation of the excess current presented in III.2.6.

In linear response theory, one is interested in the change of expectation value of various operators when the system to which they are related is subjected to a small perturbation of

the form

$$H_I(r,t) = -\int d^3r\, F(r,t)\, A(r) \tag{74}$$

where H_I is the interaction portion of the total Hamiltonian for the system. F is in some sense a force, and A an appropriate Hermitian operator. The expectation value of an operator B is found from

$$\langle B(r)\rangle_0 = Tr(\rho_0 B) \tag{75}$$

where ρ_0 is the equilibrium density matrix defined as

$$\rho_0 = \frac{\exp(-\beta H_0)}{Tr\{\exp(-\beta H_0)\}} \tag{76}$$

In equilibrium, ρ_0 is constant in time, and

$$i\hbar \frac{\partial \rho_0}{\partial t} = [H_0,\rho_0] = 0. \tag{77}$$

Under the influence of the perturbation

$$i\hbar \frac{\partial \rho}{\partial t} = [H,\rho] \neq 0 \tag{78}$$

and the density matrix evolves in time. Consequently, <B> also evolves in time. Since the perturbation is weak, the time development of ρ can be found using a first order correction to ρ_0 giving

$$\rho(t) = \rho_0 + \Delta\rho(t) = \rho_0 + \frac{i}{\hbar} \int_{-\infty}^{t} dt' \int d^3r\, F(r,t')\, [A(r,t'),\, \rho_0]. \tag{79}$$

Correspondingly, the expectation value of B becomes

$$\langle B(r,t)\rangle = \langle B(r)\rangle_0 + \frac{i}{\hbar}\int_{-\infty}^{t} dt' \int d^3r' \, F(r',t') \langle [B(r,t), A(r',t')]\rangle_0 . \tag{80}$$

In terms of the response function

$$R_{BA}(r,t;r',t') \equiv \frac{i}{\hbar}\langle [B(r,t), A(r',t')]\rangle_0 \, \theta(t-t'), \tag{81}$$

the change in the expectation value is

$$\delta\langle B(r,t)\rangle = \langle B(r,t)\rangle - \langle B(r)\rangle_0 = \int_{-\infty}^{t} dt' \int d^3r' F(r',t') \, R_{BA}(r,t;r',t') \tag{82}$$

The response function is the kernel of an integral operator relating the change of a given operator to the perturbing force.

By taking the Fourier transform of Eq. 3-82, we obtain, assuming translation invariance, the simple relation

$$\delta\langle B(k,\omega)\rangle = \chi_{BA}(k,\omega) \, F(k,\omega) \tag{83}$$

where

$$\chi_{BA}(k,\omega) = \int_{-\infty}^{\infty} dt \int d^3r \, R_{BA}(r,t) \, e^{-i(\vec{k}\cdot\vec{r}-\omega t)} \tag{84}$$

is called the generalized susceptibility. It possesses the property that

$$\chi_{BA}(k,\omega) = \chi^{*}_{BA}(-k, -\omega) \tag{85}$$

Thus the Fourier components of the change in the operator B are directly related through the generalized susceptibility to the Fourier components of the force.

In relating the excess current to the pair susceptibility,

it is necessary to realize that the power dissipated by a perturbing force is the time rate of change of the internal energy which is proportional to the imaginary part of the generalized susceptibility. Formally, this is shown by computing

$$\frac{dE}{dt} = Tr\ \{H \frac{d\rho}{dt}\} \tag{86}$$

which, from Eq. 3-79 for ρ, is

$$\frac{dE}{dt} = \int d^3r\ F(r,t)\ \frac{\partial}{\partial t} \langle A(r,t)\rangle_0 \tag{87}$$

For a real force F, we can write

$$F(r,t) = \frac{1}{2} F_A \{e^{i(\vec{k}\cdot\vec{r}-\omega t)} + e^{-i(\vec{k}\cdot\vec{r}-\omega t)} \tag{88}$$

which gives for $\delta\langle A(r,t)\rangle$

$$\delta\langle A(r,t)\rangle = \frac{1}{2} F_A\{\chi'_{AA} \cos(\vec{k}\cdot\vec{r}-\omega t) - \chi''_{AA} \sin(\vec{k}\cdot\vec{r}-\omega t)\} \tag{89}$$

where

$$\chi_{AA} = \chi'_{AA} + i\chi''_{AA} \tag{90}$$

By substitution of Eq. 3-88 and 3-89 into Eq. 3-87 and averaging over one period, the power dissipated is

$$\frac{dE}{dt} = \frac{1}{2}\omega \int F_A^2\ \chi''_{AA}(k,\omega)\ d^3r \tag{91}$$

which is the desired result. Since the coupling Hamiltonian for a Josephson junction involves complex fields, Eq. 3-91 can not be used as it is. The appropriate modification will be made in III.2.5.

To obtain the imaginary part of the pair susceptibility

using Ginsburg-Landau theory, we need an additional relation from linear response theory, the Fluctuation-Dissipation theorem.[104] If the commutator of the response function in Eq. 3-81 is expanded,

$$R_{BA}(r,t) = \frac{i}{\hbar}\{\langle B(r,t)\,A(0,0)\rangle - \langle A(0,0)\,B(r,t)\rangle\}\theta(t) \quad (92)$$

each term has the form of a correlation function. If we define

$$G_{BA}(r,t) = \langle A(0,0)\,B(r,t)\rangle \quad (93)$$

and its Fourier transform,

$$G_{BA}(q,\omega) = \int dr \int_{-\infty}^{\infty} dt\; e^{-i(\vec{q}\cdot\vec{r}-\omega t)} G_{BA} \quad (94)$$

it can be shown that

$$\chi''_{BA}(q,\omega) = \frac{1-e^{-\hbar\omega/k_B T}}{2\hbar} G_{BA}(q,\omega) \quad (95)$$

which is known as the Fluctuation-Dissipation theorem. For $\hbar\omega<<\beta$, a condition easily met by the frequencies used to probe the pair susceptibility,

$$\chi''_{BA}(q,\omega) = \frac{1}{2}\frac{\omega}{k_B T} G_{BA}(q,\omega). \quad (96)$$

2.4 Calculation of the Imaginary Part of the Pair Susceptibility

Usually, the generalized susceptibility measures the response of the order parameter to a classical field. In a superconductor there is no classical field that can be coupled to the order parameter. In the tunneling junction geometry, the quantum

mechanical pairing field of superconductor (2) is coupled to the fluctuating pair field amplitude (order parameter) in superconductor (1) by means of the tunnel interaction. The measure of the response to the coupling is the pair susceptibility. In this section, we will calculate the imaginary part of the pair susecptibility from GL theory and the Fluctuation-Dissipation theorem.

Initially, two approximations will be made. We will assume that the thickness of the film exhibiting fluctuation superconductivity is much less than $\xi(T)$, a situation easily realized in the experiment. Thus variations in ψ in a direction perpendicular to the plane of the junction can be neglected. The fluctuations are thus considered only in two dimensions. Since the temperatures of interest are greater than T_c, we can assume that the fluctuations are small and that the free energy expansion may be terminated at $|\psi|^2$. We use a quasi-classical approximation in which the effects of a magnetic field appear only in the phase of ψ.

Taking into account the assumptions above, the total free energy is

$$F = F_N + d\int d^2r \frac{\hbar^2}{2m}\left[\frac{1}{\xi^2}|\psi|^2 + |(-i\nabla)\psi|^2\right] \tag{97}$$

where d is the thickness of the film of interest. It is necessary to first decompose F into its Fourier components:

$$F = \frac{\hbar^2}{2m} Sd \sum_k \left\{\frac{1}{\xi^2} + k^2\right\}|\psi_k|^2 \tag{98}$$

where S is the normalization area,

$$\psi_k = \frac{1}{S}\int d^2r\, e^{i\vec{k}\cdot\vec{r}}\, \psi(\vec{r})$$

and (99)

$$\psi(\vec{r}) = \sum_k e^{-i\vec{k}\cdot\vec{r}}\, \psi_k .$$

The thermal averages of time independent quantities such as ψ_k and $|\psi_k|^2$ can be found by weighting the fluctuations according to the free energy which is associated with them.[111] In this way, we find that

$$\langle\psi_k\rangle = \frac{\int \exp(-F/k_BT_c)\, \psi_k d\psi_k d\psi_k^*}{\int \exp(-F/k_BT_c)\, d\psi_k d\psi_k^*} = 0, \tag{100}$$

$$\langle\psi_k, \psi_k\rangle = \langle\psi_k^*, \psi_k^*\rangle = 0, \tag{101}$$

and similarly

$$\langle\psi_k^*, \psi_k\rangle = \delta_{k'k} \frac{k_BT_c}{Sd} \frac{2m}{\hbar^2} \left\{\frac{1}{\xi^2} + k^2\right\}^{-1} \tag{102}$$

where, since T is very close to T_c, we have set $T = T_c$. Thus, above T_c, $\langle\psi\rangle = 0$ as had been previously assumed in the GL free energy. However, $\langle|\psi_k|^2\rangle \neq 0$, and since $n_s = |\psi|^2$, superelectrons may exist above T_c.

The lifetimes of the fluctuations can be obtained from the time dependent GL equation

$$\left\{\frac{\partial}{\partial t} + \Gamma_0 \left[1 + \xi^2(-i\nabla)^2\right]\right\}\psi = 0. \tag{103}$$

It can be written in terms of the Fourier components of ψ as

$$[i\omega + \Gamma_k]\psi_{k,\omega} = 0 \tag{104}$$

with

$$\psi(\vec{r},t) = \sum_{k,\omega} \psi_{k,\omega}\, e^{-i(\vec{k}\cdot\vec{r}-\omega t)}$$
$$\psi_{k,\omega} = \frac{1}{S}\int d^2r\, dt\, e^{i(\vec{k}\cdot\vec{r}-\omega t)}\, \psi(\vec{r},t) \qquad (105)$$

and where Γ_k is the wave vector dependent pair relaxation frequency

$$\Gamma_k = \Gamma_0(1 + \xi^2 k^2). \qquad (106)$$

For a fluctuation with wave vector k, Eq. 3-104 implies that the temporal correlation of ψ is exponentially decaying:

$$\langle \psi^*(\vec{r},0)\, \psi(\vec{r},t)\rangle = \langle |\psi(\vec{r})|^2\rangle\, e^{-\Gamma_k |t|}. \qquad (107)$$

To find $G_{\psi^*\psi}(k,\omega)$, and subsequently $\chi''_{\psi^*\psi}$, we note that

$$G_{\psi^*\psi}(k,\omega) = \int d^2r \int dt\, e^{-i(\vec{k}\cdot\vec{r}-\omega t)} \langle \psi^*(0,0)\, \psi(\vec{r},t)\rangle \qquad (108)$$

which upon using Eq. 3-107 becomes

$$G_{\psi^*\psi}(k,\omega) = \int d^2r\, e^{-i\vec{k}\cdot\vec{r}}\, \langle \psi^*(0)\, \psi(\vec{r})\rangle \int dt\, e^{i\omega t} e^{-i\Gamma_k |t|}. \qquad (109)$$

The integration over time can be carried out to give

$$G_{\psi^*\psi}(k,\omega) = \frac{2\Gamma}{\Gamma^2 + \omega^2} \int d^2r\, e^{-i\vec{k}\cdot\vec{r}}\, \langle \psi^*(0)\, \psi(\vec{r})\rangle \qquad (110)$$

The remaining integral can be found by relating $\langle |\psi_k|^2\rangle$ to the spatial correlation function:

$$\langle |\psi_k|^2\rangle = \frac{1}{S^2} \int d^2r\, d^2r' \langle \psi^*(\vec{r}')\, \psi(\vec{r})\rangle\, e^{i\vec{k}\cdot(\vec{r}-\vec{r}')} \qquad (111)$$

$$= \frac{1}{S}\int d^2r \, \langle\psi^*(0)\,\psi(\vec{r})\rangle \, e^{i\vec{k}\cdot\vec{r}} \tag{112}$$

since $\langle\psi^*(\vec{r}')\,\psi(\vec{r})\rangle$ depends only on $\vec{r}-\vec{r}'$. Using Eq. 3-102, we have

$$\int d^2r \, \langle\psi^*(0)\,\psi(\vec{r})\rangle \, e^{i\vec{k}\cdot\vec{r}} = \frac{k_B T_c}{d}\frac{2m}{\hbar^2}\left\{\frac{1}{\xi^2} + k^2\right\}^{-1} \tag{113}$$

Thus for $G_{\psi^*\psi}(k,\omega)$ we have

$$G_{\psi^*\psi}(k,\omega) = \frac{k_B T_c}{d}\frac{2m}{\hbar^2}\left\{\frac{1}{\xi^2} + k^2\right\}^{-1}\frac{2\Gamma_k}{\Gamma_k^2 + \omega^2} \tag{114}$$

Using Eq. 3-96 and 3-106, the imaginary part of the pair susceptibility is found to be

$$\chi''_{\psi^*\psi} = \frac{\xi^2}{d}\frac{2m}{\hbar^2}\frac{\omega/\Gamma_0}{(1+\xi^2k^2)^2 + (\omega/\Gamma_0)^2}\,. \tag{115}$$

2.5 Coupling Hamiltonian and Power Dissipation Formula for a Josephson Junction above T_{c_1}

In this section we present the effective Hamiltonian derived by Scalapino[32] to describe the coupling due to the fluctuating pair field, and the correct form for dE/dt, the power dissipation formula appropriate to this Hamiltonian.

From the low temperature coupling energy given by Eq. 2-28, in the limit $\Delta_2 >> \Delta_1$, Scalapino obtains for the coupling energy per unit area the expression

$$E_1/A = C|\Delta_1|\, e^{i\phi_1} + \text{c.c.} \tag{116}$$

where A is the junction area,

$$C = (R_N A)^{-1} \ln |4\Delta_2/\Delta_1| \, e^{-i\phi_2} \tag{117}$$

is a measure of the strength of the pairing field, and R_N is the reduced junction resistance defined such that

$$I_{NN} = e^2 V/(\hbar R_N). \tag{118}$$

Below T_{c_2}, Δ_2 has a well defined average value and negligible fluctuations (here the energy gap Δ is taken to be the order parameter) and hence can be used as a reference against which to measure the fluctuations of Δ_1 in the temperature range $T_{c_1}<T<T_{c_2}$.

Scalapino writes the effective coupling Hamiltonian as

$$H_I = \int d^2r \, \bar{C} \, \Delta_1(r) + \text{h.c.} \tag{119}$$

where $\bar{C}$ differs from C by the replacement

$$\ln |4\Delta_2/\Delta_1| \rightarrow \ln |4T_{c_2}/T_{c_1}| \tag{120}$$

In the presence of a dc bias voltage V and a static magnetic field H parallel to the plane of the junction, $\bar{C}$ is modulated in space and time according to

$$\bar{C} \rightarrow \bar{C} \, e^{i(\vec{q}\cdot\vec{r}-\omega t)} \tag{121}$$

where the frequency is determined by the Josephson condition

$$\omega = \frac{2eV}{\hbar} \tag{2-12}$$

and the wave vector q is selected by

$$q = \frac{2e}{\hbar c} H(\lambda_2 + \frac{d}{2}). \tag{122}$$

The wave vector in this case differs slightly from that of Eq. 2-65 since now the magnetic field is assumed to uniformly penetrate the film in the fluctuating state.

In terms of $\bar{C}$ and ψ, the Hamiltonian is written as

$$H_I = \int d^2r\, \bar{C}[N(0)/\alpha_0]^{-1/2} \psi(r) + h.c. \tag{123}$$

Since it is immaterial whether the factor of $[N(0)/\alpha_0]^{-1/2}$ is carried with ψ or $\bar{C}$, we define the effective force as

$$F = \bar{C}\,[N(0)/\alpha_0]^{-1/2} \tag{124}$$

and finally write for the effective Hamiltonian

$$H_I = \int d^2r\, F\psi + h.c. \tag{125}$$

The power dissipation formula[112] can now be calculated in a manner analogous to that used to derive Eq. 3-91. First write

$$\frac{dE}{dt} = \int d^2r \left\{F \frac{\partial}{\partial t} \langle\psi\rangle + F^* \frac{\partial}{\partial t} \langle\psi^*\rangle\right\} \tag{126}$$

From Eq. 3-82, one can show that

$$\delta\langle\psi(k,\omega)\rangle = F^*(k,\omega)\, \chi_{\psi^*\psi}(-k,-\omega) = F^*(k,\omega)\, \chi^*_{\psi^*\psi}(k,\omega)$$

and (127)

$$\delta\langle\psi^*(k,\omega)\rangle = F(k,\omega)\, \psi_{\psi^*\psi}(k,\omega)$$

which upon insertion into Eq. 3-127 gives

$$\frac{dE}{dt} = \int d^2r \left\{FF^* (-i\omega)\, \chi^* + F^*F\, (i\omega)\chi\right\} \tag{128}$$

$$= \int d^2r\ |F|^2 \left\{i\omega\, [\chi' + i\chi''] - i\omega[\chi' - i\chi'']\right\} \tag{129}$$

$$= -2A\ |F|^2\ \omega\chi''. \tag{130}$$

This is the desired modification of Eq. 3-91.

2.6 Calculation of the Excess Current

With the ground work having been laid in the previous sections, the excess current can now be calculated by equating the power dissipated by the excess current to the time rate of change of the internal energy in the normal metal calculated from the effective Hamiltonian, Eq. 3-125. The latter is the unique source of power dissipation in the pair channel.

Using Eq. 3-130,

$$\frac{dE}{dt} = 2A\,|F|^2\,\omega\chi'' = I_1 V = I_1 \frac{\hbar}{2e}\,\omega \tag{131}$$

or

$$I_1 = \frac{4e\,|F|^2\,A}{\hbar}\,\chi'' \tag{132}$$

Using Eq. 3-114 for the imaginary part of the susceptibility, the excess current as a function of temperature, voltage, and magnetic field is

$$I_1 = \frac{4e|\bar{C}|^2\,A}{\hbar\, d\, N(0)}\,\frac{1}{\varepsilon}\,\frac{\omega/\Gamma_0}{(1+\xi^2q^2)^2 + (\omega/\Gamma_0)^2}\,. \tag{133}$$

If the excess current is normalized to I_{NN}, the ratio is

$$\frac{I_1}{I_{NN}} = \frac{\ell n^2\,|4T_{c2}/T_{c1}|}{\ell n|\,4\Delta_2/\Delta_1|}\,\frac{E_1(0)}{U\varepsilon^2}\left|(1+\xi^2q^2)^2 + (\omega/\Gamma_0)^2\right|^{-1} \tag{134}$$

where U is the condensation energy of a volume Ad of superconductor (1) and is given by

$$U = \frac{1}{2}N(0)\,\Delta_1^2\,Sd = \frac{H_c^2(0)}{8\pi}\,Sd\,. \tag{135}$$

The coupling energy E_1 can be found from $I_1(0)$ or calculated from Eq. 2-28. For small junctions, $I_1(0)$ is probably the best measure of the effective junction coupling since any factor tending to decrease $I_1(0)$ from the theoretical value (other than self limiting) would be likely to affect the excess current in the same manner.

We now note the experimentally interesting features of the theory. Maximizing the current given by Eq. 3-133 with respect to ω, the peak current, I_p, occurs when the resonance condition

$$\omega = \Gamma_0 \tag{136}$$

is met. Since V_p, the voltage at which the peak current occurs, is proportional to Γ_0, a graph of V_p versus ε is a direct measure of the temperature dependence of the relaxation rate. The peak voltage as a function of ε is

$$V_p = \bar{V}\varepsilon \tag{137}$$

where the slope $\bar{V}$ is

$$\bar{V} = \frac{4}{\pi}\frac{k_B T_c}{e} . \tag{138}$$

Shown in Fig. 3-5 is the excess current as a function of voltage. In a magnetic field, the dependence of the relaxation rate on wave vector changes the resonance condition to

$$\omega = \Gamma_q . \tag{139}$$

The peak voltage as function of magnetic field and temperature is

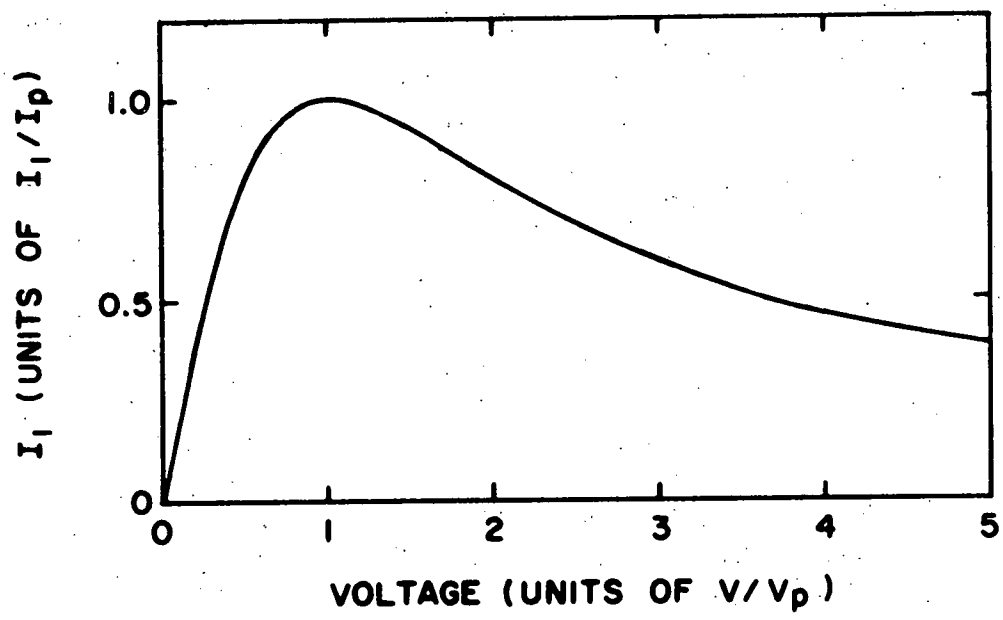

Fig. 3-5 Theoretical dependence of the excess current on voltage.

$$V_p = \bar{V}\epsilon_H \tag{140}$$

where

$$\epsilon_H = \epsilon + [(\frac{2e}{\hbar})(\lambda_2 + \frac{1}{2} d)\, \xi_0']^2 H^2. \tag{141}$$

Thus a graph of V_p versus H^2 should be a straight line with slope

$$\frac{dV_p}{d(H^2)} = \bar{V}[\frac{2e}{\hbar}(\lambda_2 + \frac{1}{2} d)\, \xi_0']^2. \tag{142}$$

Aside from the small temperature variation of λ_2 (within the temperature range of interest), this slope is temperature independent.

From Eq. 3-134, we can show that the peak current as a function of H and ϵ is

$$I_p = \frac{\bar{V}}{2R_N} \frac{\ell n^2 \,|4T_{c2}/T_{c1}|}{\ell n\,|4\Delta_2/\Delta_1|} \frac{E_1(0)}{U}\, \epsilon_H^{-1} \tag{143}$$

where R_N is now measured in ohms. A graph of I_p^{-1} versus ϵ_H should be a straight line. One further experimentally interesting quantity is

$$(\frac{dI_1}{dV})_{V=0} = \sigma(0) \tag{144}$$

the static conductivity at the origin, given by

$$\sigma(0) = \frac{1}{R_N} \frac{\ell n^2 \,|4T_{c2}/T_{c1}|}{\ell n\,|4\Delta_2/\Delta_1|} \frac{E_1(0)}{U}\, \epsilon_H^{-2}. \tag{145}$$

The restrictions placed on the theory are mainly concerned with the fact that in a magnetic field, χ is modified from its field free form. We have made the same semiclassical approxi-

mation as did Scalapino, that is, χ is calculated from the zero field form of the free energy and the effect of a magnetic field is contained in the phase factor $\exp(i\vec{q}\cdot\vec{r})$ of the pair field of the reference superconductor. The semiclassical approximation is strictly correct in the reference superconductor which is far below T_{c_2}. For it to be valid in the normal metal, it is sufficient that

$$1/q>\xi(T)>d \tag{146}$$

where q is given by Eq. 3-122. These are the conditions for the magnetic field not introducing spatial variations in ψ.

There is an experimental difficulty associated with the negative resistance feature of the excess current-voltage characteristic for $V>V_p$. In parallel with the excess current is an approximately ohmic quasiparticle current. The equivalent dynamic resistance is

$$R_T = \left[\frac{1}{R_Q} + \frac{1}{R_1}\right]^{-1} \tag{147}$$

where R_T is the equivalent resistance, R_Q the resistance of the quasiparticle channel, and R_1 the dynamic resistance of the excess current channel. When the junction is driven from a current source, which is done in the experiments described later, upon reaching the region where $R_T<0$, it will switch to a region, at higher voltage, where R_T is again positive. The switching section will appear as a horizontal line on the current-voltage characteristic. For R_T to be positive,

$$\varepsilon_H > \left[\frac{R_Q}{8R_N} \frac{\ln^2 |4T_{c2}/T_{c1}|}{\ln |4\Delta_2/\Delta_1|} \frac{E_1(0)}{U}\right]^{1/2} \quad (148)$$

If lead impedances are kept low enough to prevent oscillation in the negative resistance region, it may be possible to investigate that region of tightly coupled junctions by driving them from a voltage source. For the junctions used in the experiments described later, the minimum ε_H at which to avoid this difficulty is about 5×10^{-4}, which is approximately the smallest ε_H used. We can not conclusively say that we have seen the negative resistance region.

The discussion of the excess current has not considered the effects of phase fluctuations described in III.1. During the lifetime of a fluctuation, the stochastic noise currents associated with the quasiparticle current channel should weaken the ephemeral coupling existing between superconductor (2) and the fluctuation in superconductor (1). The very obvious effect would be to reduce the excess current, but in some yet undetermined manner. The extent to which the resonance $\omega = \Gamma_q$ is shifted is quite critical to the interpretation of the data since the temperature dependence of Γ_q is one of the primary objectives of the experiment on pair susceptibility. The effect of phase fluctuations on the excess current must be determined if absolutely definitive conclusions are to be obtained.

2.7 Survey of Additional Theoretical and Related Experimental Work

The theory of Scalapino and the measurements presented in

this thesis will offer a clear indication that dc tunneling measurments are a direct probe of the frequency and wave number dependent susceptibility. Earlier studies of dc and rf electrical conductivity, magnetic susceptibility, and quasiparticle tunneling involved convolutions of the pair susceptibility and are thus indirect. Of these, only quasiparticle tunneling and rf conductivity[113,114] are able to provide, though indirectly, an experimental value for the pair relaxation frequency. Below will be discussed only those experiments and theories which are concerned either with the pair lifetime or the fluctuation induced junction conductivity.

The first measurements of the relaxation rate in a superconductor above T_c came from the work of Cohen, Abeles, and Fuselier[21] on structure in the density of states, determined by quasiparticle tunneling, of a superconductor above T_c. Using a simple phenomenological argument, they were able to show that one can read directly from the density of states curve a value for Γ_0. Experimentally, the data for Γ_0 has large scatter, but does include some points with approximately the theoretical value. Once can not with certainty detect the expected linear dependence of Γ_0 on ϵ.

The original suggestion that an excess conductivity might exist in a Josephson junction above T_{c_1} is due to Ferrell.[30] In loose analogy with the diverging paramagnetic susceptibility of a ferromagnet above the Curie point, the divergent conductance was termed "paraconductivity". The original physical idea was much the same as that discussed in III.2.1, that is, an

ensemble of ephemeral Josephson junctions contributing to the junction conductivity. Ferrell used a form of the Fluctuation-Dissipation theorem which relates the frequency dependent conductivity of the junction to the temporal correlation of the current:

$$\sigma'(\omega) = \frac{1}{2k_B T} \int d^2 r \int_{-\infty}^{\infty} dt\, e^{i\omega t} \langle J(r,t)\, J(0,0) \rangle \tag{149}$$

where $\sigma'(\omega)$ is the real part of the conductivity. The primary result of Ferrell's calculation is that the conductivity is

$$\sigma'(\omega) = \frac{4C^2\, \Gamma_0}{a(\Gamma_0^2 + \omega^2)} \,. \tag{150}$$

C is a coupling constant for the junction which, within a numerical factor close to 1, is

$$C \simeq \sigma_{NN} \tag{151}$$

and a/2 is the coefficient of the $|\psi|^2$ term in the GL expansion for the free energy:

$$a = dN(0)\varepsilon \,. \tag{152}$$

One can consequently write the ratio of the static conductivity ($\omega = 0$) to the normal state conductivity as

$$\sigma'(0)/\sigma_{NN} = K\, \varepsilon^{-2} \tag{153}$$

where

$$K = \frac{\hbar\, \sigma_{NN}}{dN(0)\, k_B T\, e^2} \,. \tag{154}$$

Ferrell suggested that an experiment at a sufficiently high

frequency (which would be in the neighborhood of 1 GHz) could be used to confirm the temperature dependence of Γ_0 through Eq. 3-150.

The first experimental evidence of fluctuation conductivity in a Josephson junction was observed by Lipson et al.[36] in a Clark type junction. The experiment was qualitative, and difficult to properly characterize due to the uncertain structure of a Clark type junction. A more convincing experiment is that of Yoshihiro and Kajimura[35] who measured the resistance of a lead-aluminum thin film Josephson junction as a function of temperature. Though they were able to confirm the ε^{-2} behavior of the resistance, the value of K obtained experimentally was a factor of 1/40 of the theoretical value. An experiment of this type is very susceptible to peculiarities of the sample, and it is not clear that the samples used were free of edge effects and filamentary shorts which could drastically alter the results of the experiment.

The experiment of Anderson and Goldman[33] was performed using lead-tin cross film Josephson junctions in which care had been taken to eliminate the possibility of shorts and edge effects. The data was analysed in accordance with the theory of Scalapino discussed in the previous sections. Since details are presented later in this thesis, it is sufficient to say that the data are consistent in detail with the theories of Scalapino a nd Ferrell.

The microscopic approach to fluctuation tunneling, using the theory of Aslamasov and Larkin,[8] has been done by Takayama[34] who

obtained results essentially equivalent to those of Ferrell and Scalapino. Whereas tunneling calculations are usually carried out assuming specular reflection at the barrier surface, Takayama also calculated the fluctuation tunneling in the case of diffuse scattering and showed that the excess current behaves qualitatively differently from the case of specular scattering. The normalized current for the specular and diffuse cases is given by

$$\frac{I_1}{I_{NN}} = \frac{2BC_1^2(x)\sigma_{NN}}{dN_1(0)} \{\epsilon_H^2 + (2eVB)^2\}^{-1} \quad \text{specular} \tag{155}$$

$$\frac{I_1}{I_{NN}} = 16\pi^3 C_1^2 A \frac{a_0 M^4 N_2^2(0) N_1(0)}{Ad} X$$

$$\{\tan^{-1}\left(\frac{2eVB}{\epsilon_H}\right) - \tan^{-1}\left(\frac{2eVB}{\epsilon_H + Ak_c^2}\right)\} \text{ diffuse} \tag{156}$$

where $C_1(x)$ is

$$C_1(x) = \sum_{n>0} \frac{x}{(n+\frac{1}{2})\{(n+\frac{1}{2})^2 + x^2\}^{1/2}}$$

$$x = \Delta_2(T)/2\pi k_B T \tag{157}$$

M is a tunneling matrix element, and a_0 a constant describing the diffuseness of the transmission. A/ϵ and B/c are the coefficients of the q^2 and $i\omega$ terms of the pair susceptiiility, which in the mean field form are

$$A = (\xi_0')^2 \quad \text{and} \quad B = \frac{\epsilon}{\Gamma_0} = \frac{\pi\hbar}{8k_B T_{c_1}} . \tag{158}$$

The cutoff wave vector k_c is expected to be on the order of $\xi^{-1}(T)$ for clean materials and $(\xi(T)\ell)^{-1}$ for dirty materials.

The reduced termperature ε_H given by Takayama is

$$\varepsilon_H = \varepsilon + \frac{[(2e/\hbar)\,\xi_0 d]^2\, H^2}{24} \tag{159}$$

which differs slightly from that of Eq. 3-141. Takayama also provides expressions for the peak voltage which are

$$V_p = \left(\frac{2eB}{\hbar}\right)^{-1} \varepsilon_H \qquad \text{specular} \tag{160}$$

$$V_p = \left(\frac{2eB}{\hbar}\right)^{-1} [\varepsilon_H(\varepsilon_H + Ak_c^2)]^{1/2} \qquad \text{diffuse} \tag{161}$$

Equation 3-160 is the same as Eq. 3-140 when the difference between the reduced temperatures is taken into account.

Kulik[31,115] has calculated the average amplitude of the Josephson current in symmetrical junctions in the normal-normal state, a situation physically different from the present experiments so that no comparison of the work presented here is possible.

IV. Experimental Techniques

IV.1 Introduction

In Chapter IV are described the techniques used to perform the experiments on phase fluctuations and pair susceptibility. As is the case of many solid state experiments, sample preparation was a crucial problem, and it required the most time to solve. A second problem of almost equal difficulty was that of electromagnetic shielding, and grounding. Because of the radiation sensitivity of a Josephson junction, a small amount of electromagnetic radiation can drastically alter the observed current-voltage characteristic from the intrinsic characteristic to which the theories have been addressed. In addition to sample preparation and electronics, thermometry, temperature stabilization, and data acquisition are discussed.

IV.2 Sample Preparation

The basic structure of a Josephson junction consists of two superconductors separated by an insulating barrier on the order of 10-20 angstroms thick. The sample preparation problem can be reduced to finding a means of preparing the insulating layer in a selected region of the sample so as to produce a junction of known dimensions and structure. The usual technique is to form the junction from two evaporated films of superconductor separated by a layer of oxide grown on one of the metals in an intermediate step. We use this basic technique.[116]

For the phase fluctuation experiments, tin was employed as the superconducting metal. Its transition temperature of 3.72 K

is particularly convenient since it is easily obtained by moderate pumping on a liquid helium bath. For the experiment on pair susceptibility, it is necessary to use two superconductors with different transition temperatures, and for this purpose lead, with a transition temperature of 7.19 K, was chosen as the second superconductor. Both metals were obtained from Johnson, Matthey & Company, and had impurity levels lower than 5 parts in 10^5.

The junctions were prepared in a thin film evaporating system designed by Mr. Peter Kreisman. The system is of three sections, the vacuum system, the evaporating and collimating section, and the sample holder and masking section. The vacuum system consists of a mechanical roughing pump, a titanium sublimator pump, and an ion pump. To prevent backstreaming and consequent oil contamination of the high vacuum chamber in which the evaporations are made, the roughing pump was separated from the rest of the vacuum system by a molecular sieve trap which was periodically baked to maintain its effecacy.

Since thin film evaporation techniques[117] are well known, we will provide only an outline of the evaporation and masking system. What is desired is a means of depositing a thin film of material of required thickness in the correct location on a flat substrate. To do this, the material is evaporated in the direction of a mask which defines the region on the substrate where the material is to be deposited. A well defined pattern on the substrate requires that the "beam" of evaporated material be collimated, and this is accomplished by placing the mask and

substrate approximately 25 cm from a source which is about 1 cm in diameter. The materials are evaporated by direct contact with electrically heated refractory metal boats.

The films were evaporated onto 1" x 1" glazed alumina substrates obtained from the American Lava Company. The masks and substrate holder were each contained on rotatable disks so that the substrate could be positioned over any of six available sources and masked by any of twelve masks on the mask changer. The precision with which the mask changer was built allowed mask registration to within 0.001".

The thicknesses of the various films deposited ranged from 1000 Å to 10,000 Å, and were measured by a Sloan crystal thickness monitor. The principle of this instrument is rather simple. The sensing element is the resonant crystal of a quartz crystal oscillator. When placed so as to receive a fraction of the evaporant, the mass increase due to the deposited material alters the resonant frequency. By noting the change in frequency and comparing it to a calibration obtained by measuring the film thickness directly with an interference microscope, one can infer the film thickness.

All the junctions made were of the crossed-film variety, that is, the two films constituting the superconducting portions of the junction were prependicular. As shown in Fig. 4-1, the area of the junctions used in the phase fluctuation experiment was defined by the overlap of the two crossed films, each 3000 Å thick. It was not possible to utilize this simple configuration for the junctions used in the pair susceptibility experiment

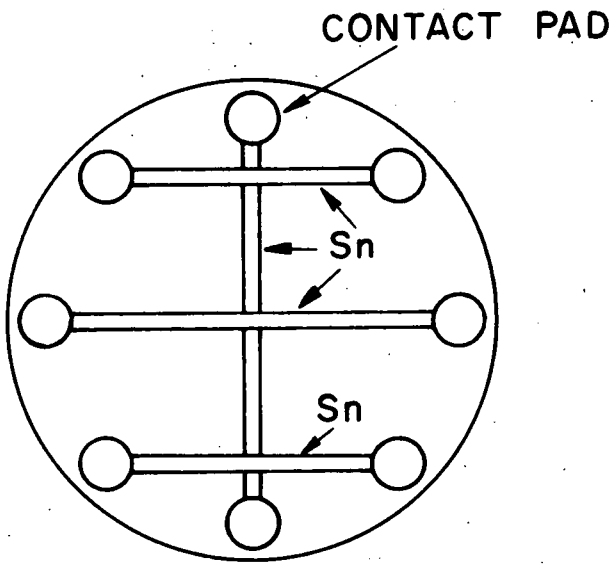

Fig. 4-1 Junction structure for the phase fluctuations experiment.

because the edges of thin superconducting films generally have a higher transition temperature then the thicker central area of the film. Consequently, the transition appears broadened and there is no unique transition temperature. Josephson currents can be observed between the lead and the tin film edges at temperatures substantially higher than the bulk transition temperature for tin. Fig. 4-2 shows the Josephson tunneling current for a lead-tin junction made by overlapping a tin and a lead film. Since in the pair susceptibility experiment one is trying to see a Josephson tunneling current above T_{c_1}, an obvious confusion can result from edge effects. To eliminate the effects of edges, they were covered with a layer of bismuth oxide,[118] Bi_2O_3, a minimum of 1000 Å thick so that only a region .004" x .004" in the middle of the tin film was available for tunneling currents. This junction structure is shown in Fig. 4-3. The thicknesses of the tin and the lead films are 1500 Å and 3000 Å respectively. The only unique aspect of the bismuth oxide evaporation was that it was necessary to use a platinum source in order that the decomposition of the bismuth oxide did not occur. A slow evaporation rate of 100 Å/min had to be used to prevent the vacuum system pressure from rising above 10^{-5} torr. Silicon monoxide was tried as the masking material but no samples made with it were successful. It was also thought necessary that the masking be done after the oxidation in order that the oxide layer be free of defects at the edge of the masked area.

The substrates were first scrubbed with reagent grade

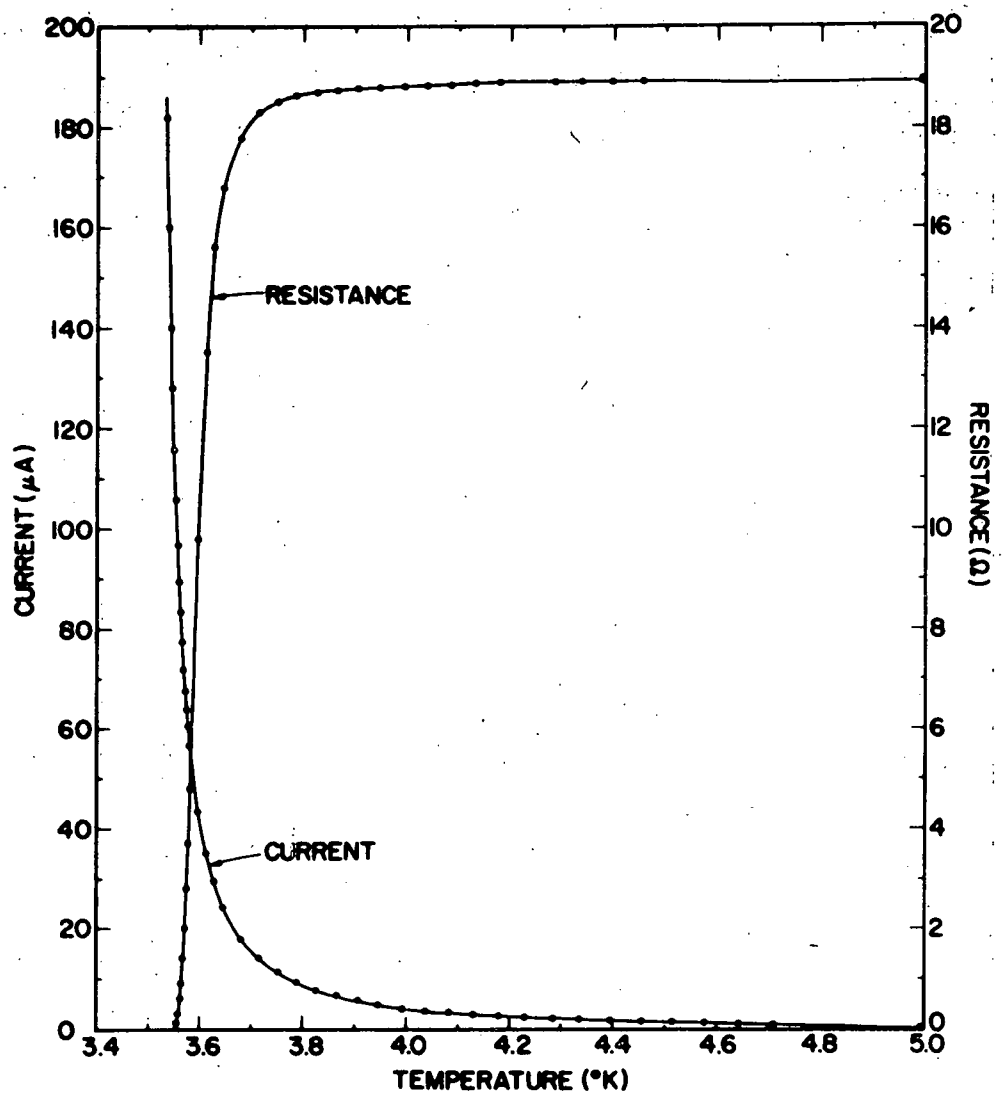

Fig. 4-2 Zero-voltage currents observed in an unmasked Sn - Pb Josephson junction. The resistance curve shown is that of a 0.1" section of the 0.002" wide Sn film forming one side of the junction.

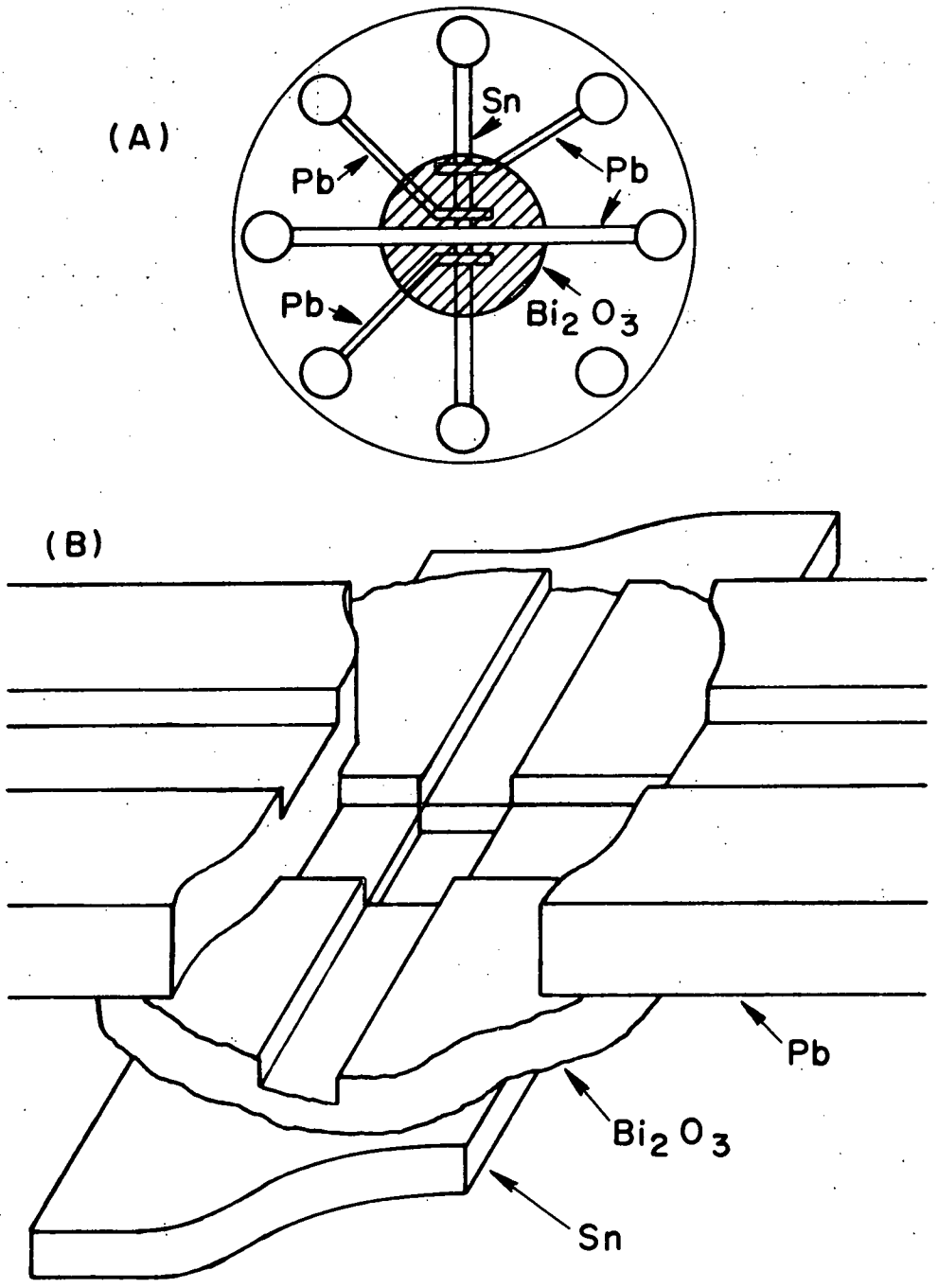

Fig. 4-3 Junction structure for the pair susceptibility experiment. The general structure is shown in (A), and in (B) is shown the detail of the junction region. The lead film has been broken to reveal the bismuth oxide masking formed by two successive evaporations through separate perpendicular wire shadow masks.

acetone to remove most oils, finger prints, and other surface contaminants. The final cleaning is done in a Freon[119] vapor degreaser which both removes the remainder of the contaminants and warms the substrate. In transferring the substrate from the degreaser to the evaporator, the warmth of the substrate creates a convective air layer to prevent the attachment of dust to the substrate[120] until the evaporator can be evacuated, which usually follows in less than a minute after the substrate is placed in the evaporator. The evaporations are not made until the pressure is less than 3×10^{-6} torr.

The oxidation step was the most difficult to perform in a uniform manner since many factors other than oxidation time seem to affect the thickness of the oxide barrier. For example, a junction produced on a day having high humidity was likely to have thicker barrier than one produced on a dry day. Initially, the usual manner to oxidize the tin was to vent ordinary bottled oxygen at 1 atm into the evaporator after the first tin film was deposited. The tin was allowed to oxidize for approximately 10 to 12 hours after which time the evaporator was again evacuated and the remaining evaporations completed. The resulting junctions had conductivities which were in the range of $(0.4\text{-}7) \times 10^{5}$ mhos/cm^2. A drastic change in the oxidation technique became necessary when bismuth oxide evaporations began, apparently due to an increase in the background contaminants. Oxidation times became typically 20 minutes at 100μ for junction conductivities comparable to those above. It was also found that reproducibility improved if after the oxidation a two hour pumpout followed. It is suspected

that this removed some of the adsorbed oxygen and allowed the remainder to diffuse uniformly into the upper surface of the tin.

Electrical contact was made to the sample by eight spring-loaded berylium-copper contacts which were soldered to the sample using a eutectic solder[121] that was liquid at room temperature. Connection was made to eight evaporated contact pads on the substrate. Since the eutectic solder would rapidly dissolve either lead or tin, aluminum was used for the contact pads. As the eutectic did not adhere well to the aluminum, a smaller lead pad was placed in the center of the aluminum pad. Contacts made this way proved to be very reliable. Thicknesses of the metal layers were not critical and several thousand angstroms of each was convenient.

At room temperature, the lifetime of a junction is on the order of half a day. Presumably, this results from diffusion of the oxygen in the barrier into the films. Also, even with the aluminum layer on the electrical contact pads, the eutectic solder will eventually dissolve the aluminum and subsequently the lead and tin as well. Destruction of the junction follows. To prevent junction deterioration, as soon as the cryostat was sealed, usually within an hour of the final evaporation, the lower end was immersed in liquid nitrogen to immediately cool the sample to 77 K and thus freeze the solder. At this temperature, junction properties were very stable. On junction was kept for over nine months, cycling between LHe and LN_2, without any substantial change in its properties. No electrical tests, other than continuity of the films, were attempted until the sample was

at 77 K.

IV.3 Thermometry and Temperature Stabilization

3.1 Thermometry

Temperatures were determined by measuring the resistance of a germanium resistance thermometer,[122] the calibration of which is based on the National Bureau of Standards 1958 He vapor pressure scale.[123] The absolute accuracy of the temperatures determined from the resistance thermometer can be within 2 mK, however the resistance bridge used was designed primarily to have high resolution rather than high absolute accuracy and the temperatures quoted in later sections should be considered accurate only to within 1/2%. This is not of much concern in the final results as the predictions of the theories are much more dependent on relative temperatures than on absolute temperatures.

To interpolate between the calibration points supplied with the germanium resistor, a computer program was written to convert the measured resistance to a temperature. Germanium resistors used as thermometers are highly doped to obtain a sufficiently low resistance at LHe temperatures for convenient use. At present, there is no completely satisfactory expression for the temperature dependence of the resistance of such thermometers, and one usually uses a least-squares fit to a polynomial[124] of some function of R, T, or both. The polynomial used here is

$$\log_{10}(T) = \sum_{i=0}^{N} A_i \log_{10}(R)^i \qquad (1)$$

and was suggested by the fact that a graph of log(T) versus log(R) for the germanium resistor is nearly a straight line over the temperature range of interest. A total of 9 terms were used in the polynomial to fit the resistance over a temperature range from 1.5 K to 4.24 K with an average error from the calibration of 0.5 mK. Though the number of terms seems quite large, the first and second derivatives were both smoothly varying, indicating that the fit had not been carried to too many terms. From the calibration and the polynomial which had been fit to it, a table of R versus T was generated, and the temperatures were then obtained from the table.

3.2 Temperature Stabilization

As discussed in II.3.2, the temperature dependence of the Josephson current can be very strong in the vicinity of T_c, in particular, in either symmetrical junctions with large $I_1(0)$ or asymmetrical junctions. Since a small temperature change while recording a current-voltage characteristic would then be expected to significantly alter the shape of the current-voltage characteristic, care was taken to maintain the temperature constant. To do so, two different systems were used. Coarse temperature stabilization was obtained by holding the vapor pressure of the LHe bath constant. Additional stabilization was obtained by a servo feedback loop which sensed a change in the resistance of the germanium resistor and used the resulting error signal to control the amount of current to a 100Ω Manganin heater mounted on the sample block.

The vapor pressure of the He bath was held constant by a mechanical manostat referenced to a pressure ballast tank. Short term stability was on the order of 0.2 mK. Long term stability depends on the temperature stability of the reference, being on the order of 3 mK/K of ambient temperature change at 3.7 K. We found that the long term stability was better than 2 mK since the shielded room in which the experiment was conducted provided some isolation for the reference from such local rapid temperature changes as opening and closing of windows and doors, and cycling of the heating system. Pressure in the reference could be controled by two needle valves which allowed small amounts of gas to be either withdrawn from, or added to, the reference for fine temperature changes.

The electronic temperature measuring and stabilization system is shown in block form in Fig. 4-4 with the bridge circuit[125] given in Appendix A. The heater control sums the error signal from the resistance bridge with a bias level which in the absence of any error signal provides a quiescent power level of approximately 0.1 mW to the heater. By adjustment of the gain and bandwidth of the lock-in amplifier, the servo loop can be stabilized against oscillations. Within the 5 mK operating range of the servo loop, dc temperature variations at the germanium resistor were reduced by a factor of 300 over any drift in the bath temperature. The actual temperature stability at the sample was not this good. The heater produced a thermal gradient on the order of 1 mK between the sample and the germanium resistor, and modulation of this gradient by changes in the heater power in

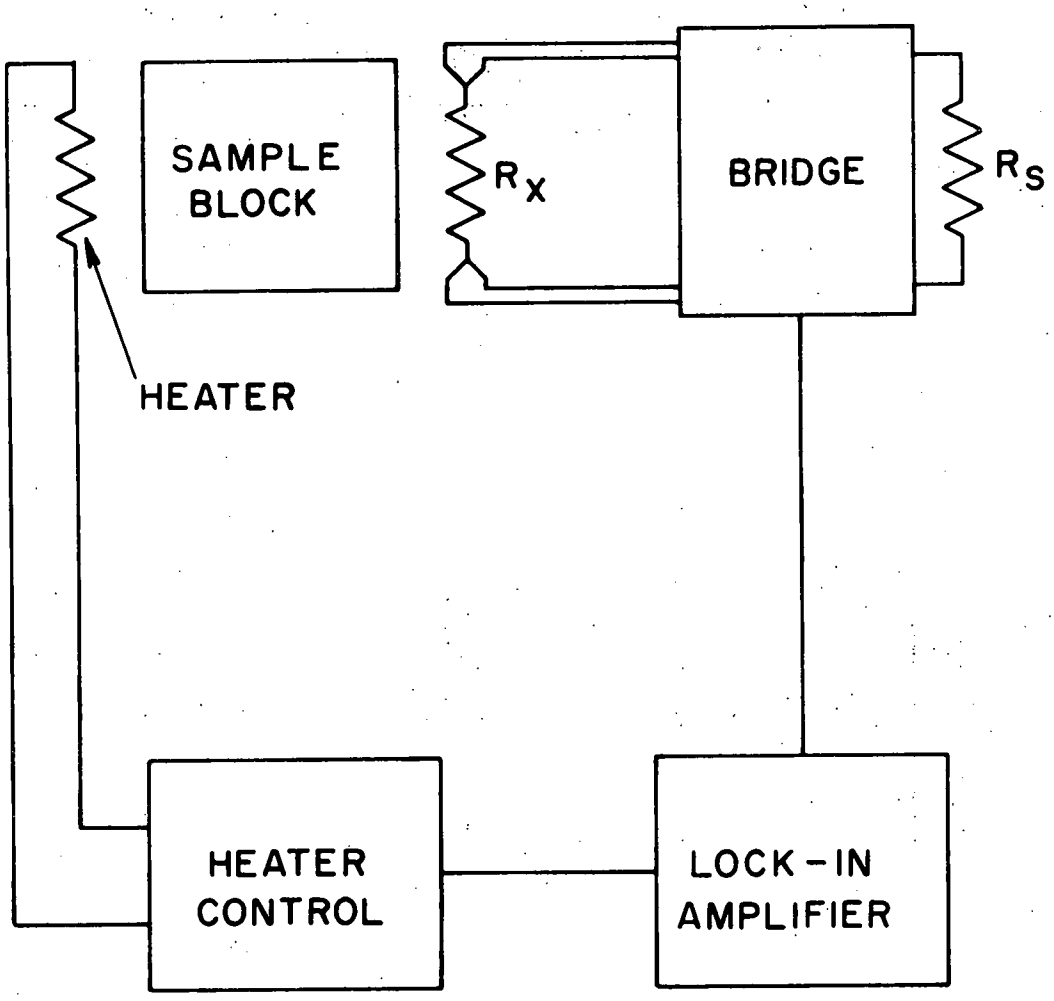

Fig. 4-4 Block diagram of the temperature control and measuring system.

response to a temperature error at the germanium resistor resulted in a temperature stability at the sample about a factor of 10 better than the bath stability. This was quite sufficient for the purposes of the experiment.

IV.4 Electronics and Data Acquisition

4.1 Shielding

One of the primary problems in doing the experiments described here is that of shielding the junction from electromagnetic interference. As discussed in Chapter II, a Josephson junction is inherently an rf sensitive device. Further, the effects sought result from thermal fluctuations whose average energy is on the order of $k_B T$, which for $T \sim 3$ K is about 4×10^{-23} J. Thus the amount of energy from outside sources necessary to substantially affect the current-voltage characteristics is small.

To eliminate most of the interference problem, the complete experimental apparatus was contained in a 10' x 10' x 8' shielded room.[125] Shielding from 10 kHz to 10 GHz was better than 120 db. All ac power entering the room was shielded to a comparable degree. Since any electromagnetic interference from instrumentation contained in the room would defeat the effectiveness of the shielding, electromagnetically noisy instruments such as oscilloscopes and digital voltmeters were not used in the room while data was being taken. Though lock-in amplifiers, of which two were used, have switching circuits in them, there was no apparent interference from them. As evidence that these precautions were required, current-voltage characteristics taken with the door of the shielded room open were not reproducible and often

showed no sign of a critical current when the expected critical current was on the order of 10μA or smaller. A second source of shielding is the cryostat itself which, though the signal leads into it were unfiltered, totally encloses the sample and acts as a Faraday shield when grounded.

Magnetic shielding is provided by a Mumetal shield enclosing the lower part of the cryostat external to the dewars. The measured magnetic field at the site of the sample was less than 3×10^{-3} Oe.

4.2 Current-Voltage Characteristics

The basic data for both experiments is the current-voltage characteristic of the junction. Since the experimentally interesting features in the current-voltage characteristic occur at voltages on the order of 1μV, an ac technique was used, eliminating any problem associated with thermocouple voltages. The basic system for acquiring the current-voltage characteristic is shown in Fig. 4-5.

The operation of this system is quite simple. When triggered, the ramp generator produces, starting from zero, a slow, linearly increasing voltage which is chopped at 400 Hz. The chopping rate is large compared to the ramp rate, which is typically 0.1 volts/sec, so that the output of the chopper appears as a square wave of slowly increasing amplitude. Advantage is taken of the low impedance of the junction by using a resistor to convert the chopped voltage to a chopped current. A square waveform is used because at its maximum value in a given cycle, the current dwells

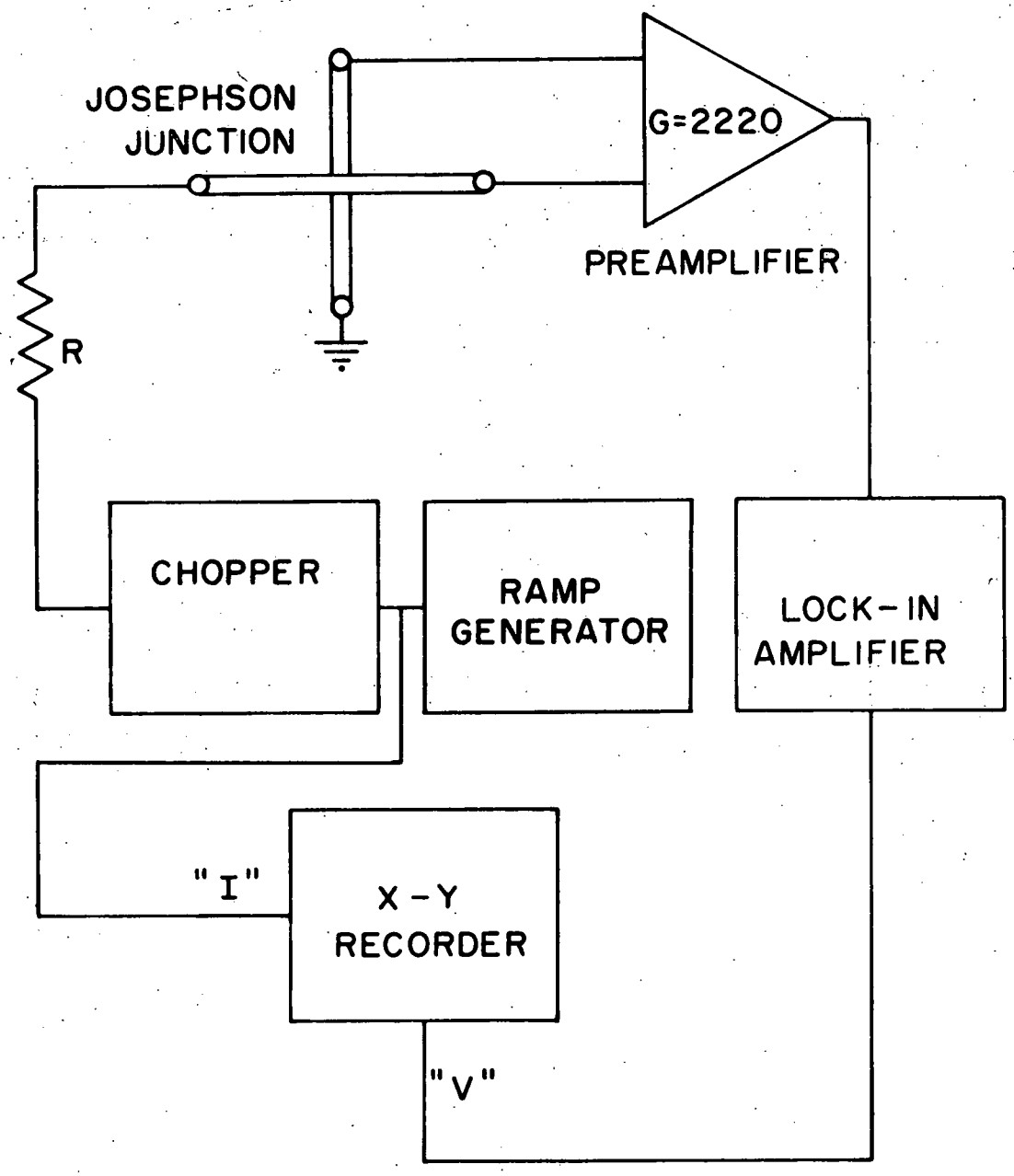

Fig. 4-5 Block diagram of current-voltage characteristic acquisition system.

at a specific location on the current-voltage characteristic. The output voltage of the junction is also a square wave, and the peak to peak voltage is the same as the dc voltage which would have appeared across the junction had it been driven with a dc current whose value was equal to that of the peak to peak ac current used. The lock-in amplifier detects the first harmonic of the junction voltage and records it, and the value, along with that of the current, on an X-Y recorder. Had any other waveform been used, the harmonic content of the junction voltage would vary depending on the location on the current-voltage characteristic, and the first harmonic would not be proportional to the junction voltage measured with dc current. The advantage of starting the ramp from zero is that there is no ambiguity in the position of the true zero whereas an ac current symmetrical about zero would average over any asymmetry in the current-voltage characteristic. The current and voltage scales are accurate to 2%.

Because of difficulties encountered in using electrical connectors at the top of the cryostat, and difficulties in properly grounding a remote preamplifier which amplified the voltage across the junction, a preamplifier was built, the circuit of which is given in Appendix B, which mounted at the top of the cryostat. The leads from the sample to the top of the cryostat were soldered directly to the input of the preamplifier. Designed with a gain of 2.22×10^3, the preamplifier has the correct gain to convert the measured rms first harmonic of the junction voltage to the true peak to peak square wave

amplitude across the junction. The noise equivalent input resistance of the preamplifier at 300 K is about 4 kΩ, and the input impedance is greater than 100 kΩ. Though it is possible to amplify the junction voltage with a preamplifier having a lower input noise resistance, by impedance matching, this was not done because it was desired to keep all circuit impedances connected at the junction fairly high to reduce the coupling of extraneous noise sources through the circuitry to the junction.

The estimated noise current in the junction from external sources is less than 10^{-8} A.

When it was found that the Exact 404 oscillator, which had been used to generate the ramp, emitted a spurious 4 MHz signal, it was replaced by a simple integrating circuit, given in Appendix C, which when supplied from a voltage source, would generate the required ramp.

4.3 Excess Current Measurement

To obtain the excess current for the pair susceptibility determination, it is necessary to subtract from the total junction current the current flowing in quasiparticle channels. These currents are of two types, quasiparticle tunneling current and ordinary conduction current through the barrier and through the bismuth oxide masking. The predominant quasiparticle contribution is from tunneling with ordinary conduction contributing at most 10%.

The subtraction of the conduction current is straightforward since it obeys Ohm's law. Generally, the quasiparticle current

is not linear, but as discussed in II.2, near T_c the quasiparticle conductance is approximately linear in the vicinity of the origin. We will assume that it is strictly linear because experimentally, deviations from linearity of greater than 1 part in 10^3 were not observed out to 40 μV on the current-voltage characteristic when the T was as close as 40 mK above the lowest temperature at which the excess current was observed.

The subtraction was accomplished in either of two ways. On sample PS-1, it was done graphically making the linear extrapolation for the quasiparticle current from the origin to a point at 12 μV on the current-voltage characteristic. On PS-2, subtraction was performed electronically, to a greater accuracy than could be achieved graphically, as part of the data-taking process thus providing a direct readout of the excess current. A block diagram for this process is shown in Fig. 4-6. The subtractor subtracts from the current scale an amount linearly dependent on the junction voltage, the proportion being determined by the quasiparticle conductivity. After subtraction, the scale can be further expanded for greater resolution by the gain of the X-Y recorder. Excess currents smaller than 1/10th the total current can be conveniently observed, the limitation being that for a greater scale expansion, there must be a corresponding decrease in the amount of noise on the voltage axis. Since that noise is controlled by the lock-in bandwidth, reduction of the noise is accompanied by a correspondingly increased time constant, and the rate at which the excess current curve can be recorded becomes impractically long for the small signal levels

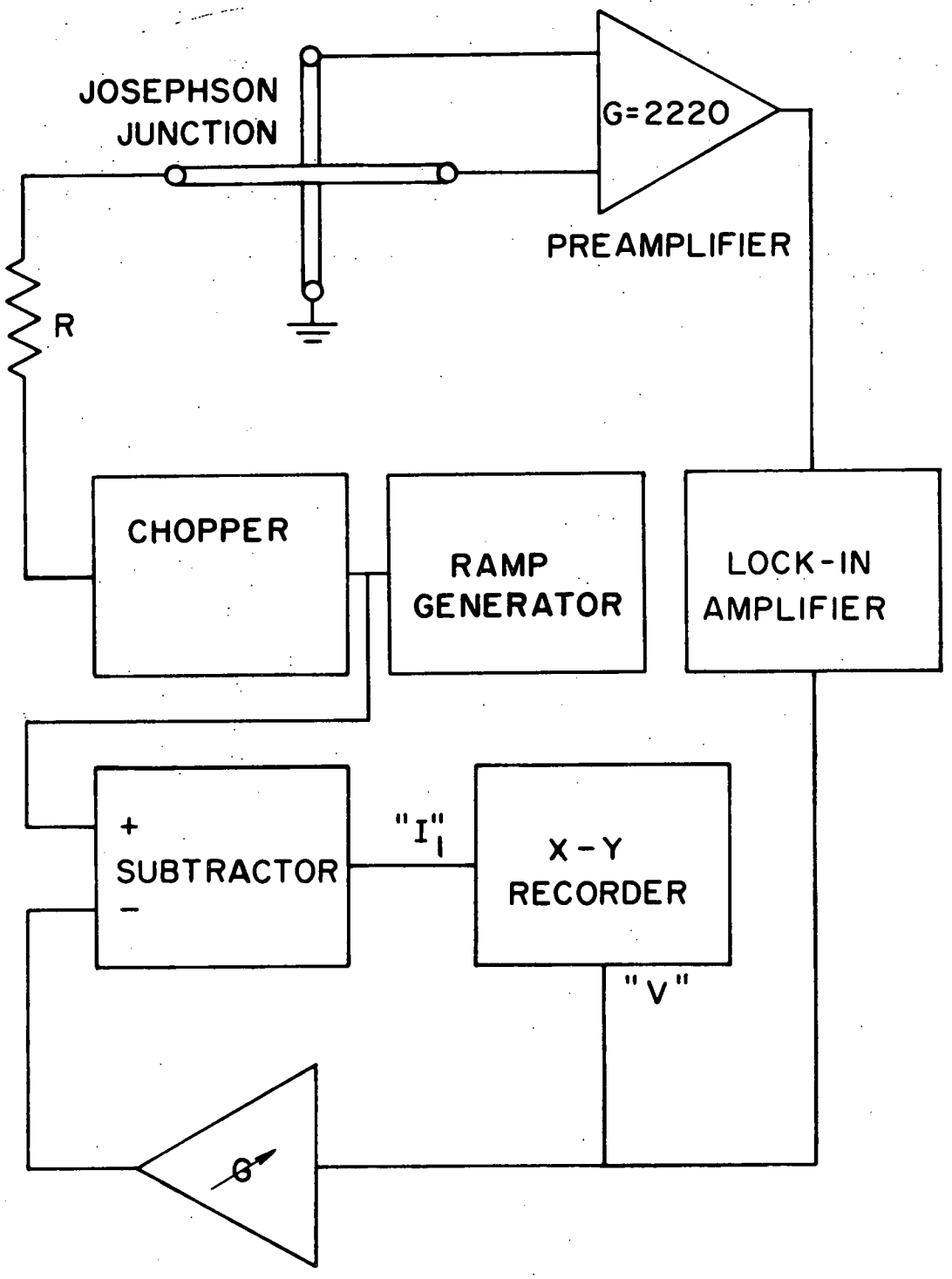

Fig. 4-6 Block diagram of the excess current measurement system.

at which the excess current is observed.

4.4 Miscellaneous

In some cases, it is of interest to determine the resistive transition of the tin films. This was done by passing current from (A) to (E) of Fig. 4-3 and measuring the voltage across either (B) and (H), or (H) and (F) with a lock-in amplifier. The maximum current density was less than 20 A/cm^2. For the films used here, the current was 1μA. Since the films have graded edges, it would provide no useful information to attempt to fit the transitions to the theory of Aslamasov and Larkin,[8] and no fit was attempted.

The magnetic field which was used to determine the current-field characteristic and to produce Fiske steps as part of the junction capacitance measurement was provided by a Helmholtz pair located outside the dewars, and centered on the sample. The field at the sample was 0.42 Oe/mA.

The magnetic field dependence of the Josephson current was found with the servo tracker shown in Fig. 4-7. As long as the current supplied to the junction is less than $I_1(T)$, no voltage appears across the junction. In this case, the signal controlling the current is the output of the adder which in the absence of any junction voltage supplies its maximum output. Normally, if $I_1(T)$ is exceeded, a voltage equal to the sum of the energy gaps appears across the junction. This is a discontinuous error signal and unsuitable for feedback. A .1-100 Ω resistor, where the lowest resistance is used with junctions having

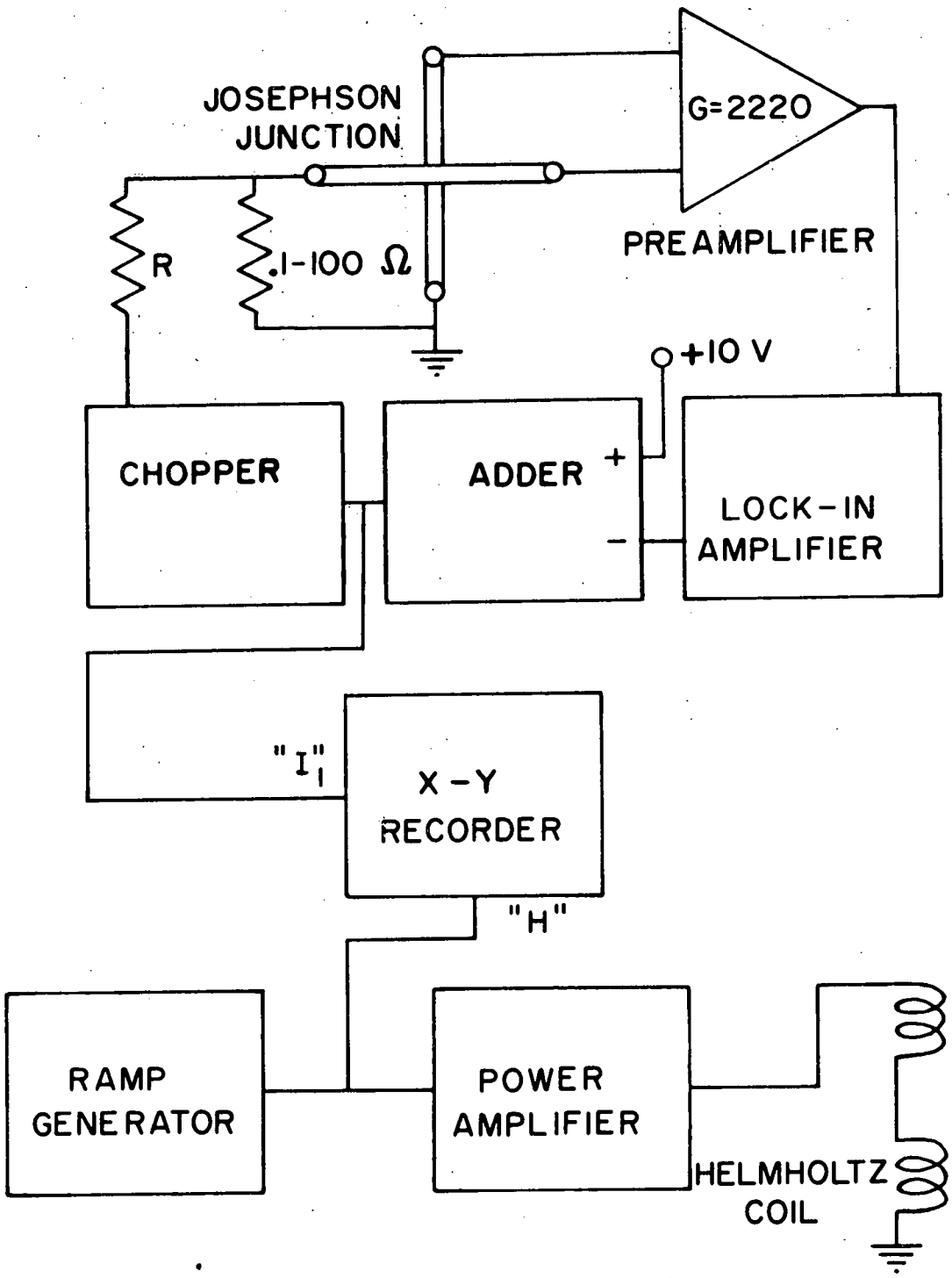

Fig. 4-7 Block diagram of the servo-system used to obtain current-field characteristics.

the greatest $I_1(T)$, was placed in parallel with the junction. Currents in excess of $I_1(T)$ then provide an output voltage approximately proportional to the amount the $I_1(T)$ is exceeded. Integration in the lock-in amplifier provides smoothing of the signal. The error signal was then used to control the output of the adder. It is estimated that $I_1(H)$ curves obtained this way have an error less than 10%.

IV.5 Junction Documentation

On cooling to less than T_c, several qualitative tests were performed on the junctions to determine their quality. The magnetic field dependence was examined for quasiperiodicity. If the junction coupling were completely uniform, then the expected field dependence would follow Eq. 2-47 (assuming that the junction is rectangular). Any random variation in the coupling strength tends to reduce the secondary maxima from that which would be expected according to Eq. 2-47, though quasiperiodicity usually is retained. In certain junctions, the field dependence was observed to be discontinuous, and it was assumed that this meant that the junction contained strongly inhomogeneous regions between which flux could be trapped in a ring-like fashion. The junction dimensions were much less than the Josephson penetration depth so the vortex structure of large junctions could not be responsible for the discontinuities. Another test was that the temperature dependence of the critical current be approximately correct. It was considered acceptable if the temperature dependence was qualitatively similar to Fig. 2-7. That is, for symmetrical junctions,

the slope near T_c should be approximately given by Eq. 2-34, for asymmetrical junctions the slope should approach infinity at T_{c_1}, and for both types, the slope near T=0 should approach zero.

In the junctions used in the pair susceptibility experiment, primary concern was that the junctions be free of filamentary shorts exhibiting supercurrents above T_{c_1} which appear to be pair tunneling currents. A strong short is easily detected by the absence of an energy gap, insensitivity to weak magnetic fields, and at currents near the critical current of the short, hysteresis in the current-voltage characteristic due to local heating in the shorted region. A short with a critical current less than that of the Josephson current is evident by the rapid disappearance of the Josephson portion of the current in a magnetic field with the remaining short current relatively insensitive to the field. A test for weak shorts is the presence of zero field steps in the current-voltage characteristic which Matisoo[127] has shown can result from metallic whiskers 1μ in diameter. Normally, steps appear in homogeneous junctions only in the presence of a magnetic or electromagnetic field. None of the junctions for which data is given had zero field steps.

Since both experiments are conducted near T_c, at least one and possibly both the metal films may be resistive. If the resistance of either film is on the order of the junction resistance, then the current-voltage characteristic will be distorted[128] by the non-uniform current flow across the films and the junction. This problem does not exist if the junction resistance is large compared to the resistance of the films

adjacent to the junction. The ratio of the junction resistance to the film resistance was greater than 20 for the junctions used in these experiments.

CHAPTER V. DATA AND ANALYSIS

V.1 Phase Fluctuations

1.1 Introduction

Having discussed the theory and experimental techniques, we are now in a position to present the data and its analysis. We have chosen to analyse the data in terms of the theory of Ambegoakar and Halperin (AH) which provides an integral equation for the current-voltage characteristics at all values of γ. The comparison of experiment to theory is qualitative as the theory describes a situation in which $\Omega = 0$ and the data was obtained from junctions in which $\Omega > 0$.

The data for the experiment comes from two junctions with quite different properties which are summarized in Table 5-1. One junction, PF-1, has a low critical current, moderate resistance and capacitance, and the other, PF-2, a very high critical current, very low resistance, and relatively large capacitance.[129] In PF-1, the phase fluctuations were studied with the coupling energy reduced to the order of $k_B T$ by working near T_c. The coupling energy of PF-2 was reduced by a combination of an applied magnetic field according to Eq. 2-47 and proximity to T_c. It was not possible to work as close to T_c with PF-2 as with PF-1 because the junction resistance of PF-2 was low compared to the film resistance in the normal state, and in the vicinity of T_c, the films appeared partially resistive with a consequent distortion of the current-voltage characteristic.

Table 5-1. Junction Properties of PF-1 and PF-2

	PF-1	PF-2	Units
Width	1.4×10^{-2}	5×10^{-3}	cm
Length	1.4×10^{-2}	1.5×10^{-2}	cm
R_N	1.3	0.02	ohms
$I_1(0)$	0.683	28	mA
T_c	3.89	3.72	K
Fiske Step spacing	179	90	μV
C	0.245	2.85	nF

1.2 Data

Shown in Fig. 5-1 are a set of current-voltage characteristics for PF-1 taken near T_c. These characteristics illustrate the increasing effect that phase fluctuations have as the critical current is lowered. If one plots the current-voltage characteristic at a temperature far from T_c, fluctuations are important only at currents just below $I_1(T)$ where the wells in coupling energy as a function of phase are shallow. Since k_BT at 4 K corresponds to about 0.2 μA, one would not expect to see fluctuation effects until the critical current was the order of several microamperes. Well below T_c, $I_1(T)$ might be several milliamperes so that the fluctuation sensitive portion of the current-voltage characteristic would be obscured by effects due to temperature fluctuations and self generated magnetic fields. It is clear that the easiest way to observe the effects of fluctuations is to reduce the coupling energy to a level such that the current-voltage characteristic below $I_1(T)$ is sharply affected by fluctuations.

The data shown in Fig. 5-2 illustrate the effects of a magnetic field on the shape of the current-voltage characteristic in the fluctuation sensitive region. The only qualitative difference between this situation and that in the vicinity of T_c is that the reduction in the coupling by a magnetic field is quasiperiodic whereas the effect of temperature is monotonic.

Ideally, one would like to compare experiment to the AH theory without the use of fitted parameters. That is, one would like to use parameters which can be directly measured such as

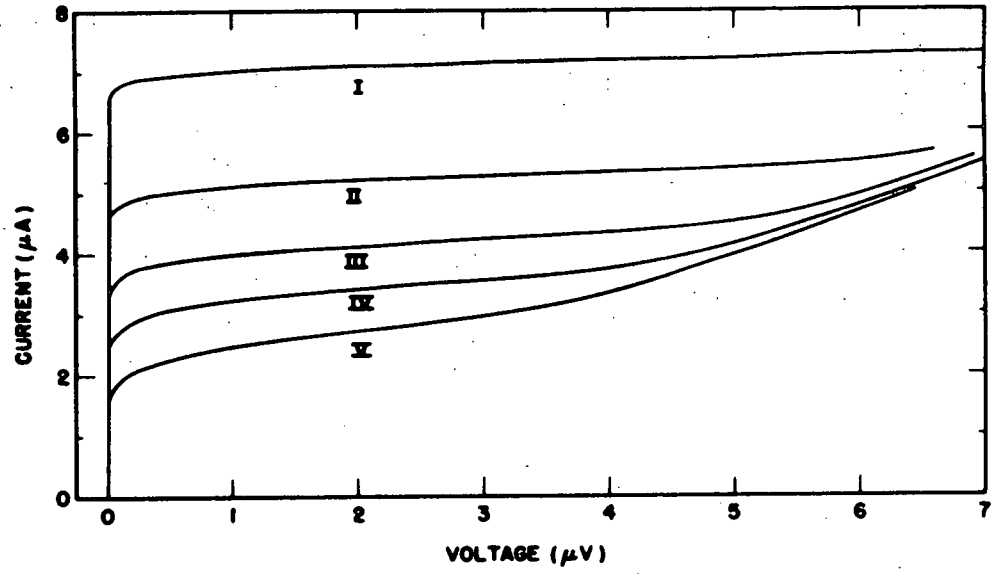

Fig. 5-1. Current-voltage characteristics for PF-1 taken near T_c. The temperatures for each of the curves are: (I) 3.839 K; (II) 3.845 K; (III) 3.849 K; (IV) 3.851 K; (V) 3.853 K.

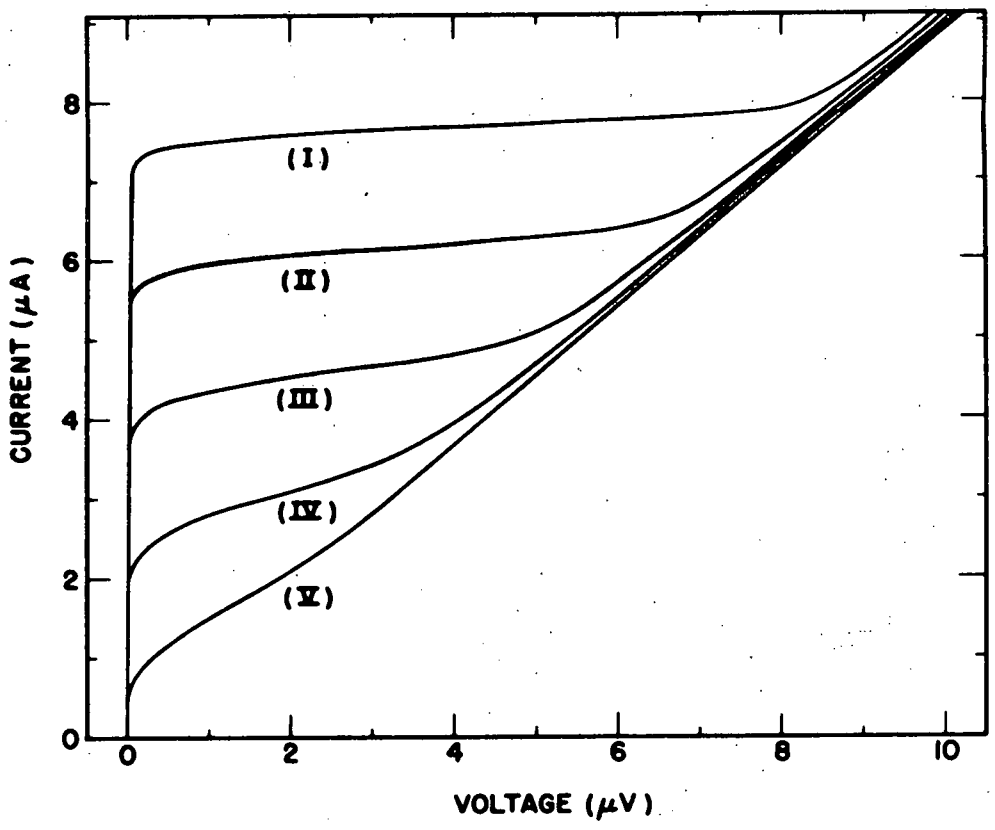

Fig. 5-2. Current-voltage characteristics for PF-2 taken in the presence of a magnetic field. The temperature is 3.796 K. The applied fields for each of the curves are: (I) 1.16 Oe; (II) 1.27 Oe; (III) 1.38 Oe; (IV) 1.49 Oe; (V) 1.66 Oe.

junction resistance, temperature, and magnetic field. Unfortunately, this was not possible with the samples we have produced. The major difficulty was in providing the correct value of zero voltage current. One should be able to use Eq. 2-34 and 2-47 in combination to predict, from the low temperature junction properties, the value of $I_1(T,H)$. There were several reasons why this was not possible. In the vicinity of T_c, the critical current may not be linearly dependent on T because of the grading of the transition temperatures in various regions of the tin films, in particular the edges. Though this effect is small, it produces an upward extension in temperature of the critical current in the same temperature range that fluctuations are important. Any prediciton of the critical current is smaller than the observed critical current. The effect is similar to, but smaller in magnitude than, that illustrated by Fig. 4-2. When the coupling is reduced by applying a magnetic field, the precise functional form of the critical current-magnetic field characteristic is needed in order to parameterize the current-voltage characteristic. It is thus necessary that the junction be homogeneous and rectangular. These conditions are difficult to meet. Furthermore, because of small residual magnetic fields not aligned with the Helmholtz coils, the current often does not go completely to zero at the minima. Fig. 5-3 amply illustrates the difficulty in attempting to predict $I_1(H)$.

For the reasons stated above, it was necessary to use the zero voltage current as a fitted parameter. In addition, it was necessary to treat the temperature as a second fitted parameter.

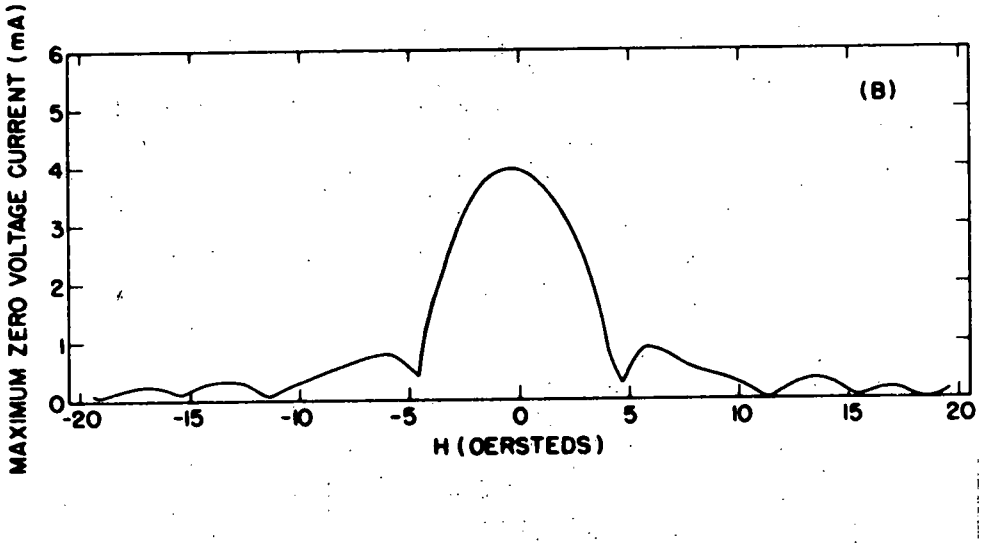

Fig. 5-3 Magnetic field dependence of the maximum zero-voltage current of PF-2 at T = 3.47 K .

This is tantamount to introducing an effective noise temperature. Ideally the noise temperature should equal the ambient temperature since the theory of AH assumes that the source of the noise is the quasiparticle resistance of the junction. Additional noise from other sources, such as noise on the electrical leads, would cause an increase in the apparent temperature. Other possibilities will be discussed later.

In the AH theory, it is assumed that the resistance is independent of voltage. Near T_c in a symmetrical junction, this is true and in addition, R is the normal state junction resistance since the energy gap is very small. Below T_c, the energy gap introduces structure into the current-voltage characteristic so that the choice of the correct resistance is not that of the junction in the normal state but is instead the effective quasiparticle resistance which is independent of voltage over the range of voltages of interest. The use of this R in the AH theory can be justified on the grounds that the noise is determined by the actual value of the resistance at a particular voltage.

Before comparing the data to the theory, we show in Table 2 V_m, the maximum voltage, and I_m, the maximum critical current, for which the AH theory is applicable. The condition $\Omega = 1$ determines I_m. It is desirable to have $\Omega \ll 1$ to effect quantitative comparison of experiment to theory. By reducing either the resistance or the capacitance, Ω can be reduced. The capacitance by itself imposes only the upper limit on the voltage, V_m. Other conditions on the applicability of the theory require that

RC and $RC^{1/2}$ be small. Thus if the capacitance is large, its effects can be compensated by a sufficiently small R. This is particularly true for the condition $\Omega < 1$ in which Ω depends on $RC^{1/2}$, and a reduction of R is much more effective than a reduction of C. The most suitable junctions will be those with thin insulating barriers since the capacitance varies inversely as the barrier thickness whereas the resistance decreases exponentially.

Table 5-2

Sample	V_m(μV)	I_m(μA)
PF-1	0.46	0.79
PF-2	0.13	680

Fig. 5-4 contains the pertinent data for PF-1, along with the curves fitted using Eq. 3-44. The fit was made to the data obtained over the first 100 nV of each curve and then extrapolated over the remainder of the range. The only curve for which $\Omega < 1$ is (v), all others having $\Omega > 1$. As can be seen, the fit is only successful for (v). It was not possible under any variation of I_1 and T, the two fitted parameters, to fit curves (i-iv). This might be expected as the hysteresis associated with the condition $\Omega > 1$ should be significant. The anticipated consequence of having $\Omega > 0$ in the experiment and zero in the theory is for the theory to underestimate the voltage at a given value of I/I_1. This is amply illustrated by curves (i-iv). The fit continues to be successful for (v) past V_m. In part,

this may be due to limited resolution in the data.

Shown in Fig. 5-5 A, B, and C are the magnetic field data for PF-2. Though the critical currents for the three curves shown are much larger than those of Fig. 5-4, the largest value of Ω is less than 0.1 as a result of the very low junction resistance. A good fit, within the limits of instrument noise, is possible with two fitted parameters. Again, however, a temperature much higher than ambient is required. Curves showing the fit using the critical current as the only fitted parameter are presented for comparison.

A correction to Eq. 3-44 for $\Omega > 0$ suggested by Halperin, Eq. 3-52, was tried in an attempt to improve the fit. No significant improvement was found, probably because of the high noise temperature.

The high noise temperature is a complication in the comparison of experiment to theory. Either a large Ω or an elevated noise temperature can produce a greater voltage for a given I/I_1 than would be predicted by theory on the basis of $\Omega = 0$ and the ambient temperature. Thus the higher high apparent temperature may be a consequence of the fact that $\Omega > 1$. However this suggestion is not born out by experiment since it implies that the larger Ω, the higher the noise temperature. Curves (i-iv) are monotonically decreasing in Ω yet the noise temperature remains constant. Furthermore, in the data of Fig. 5-5, Ω is less than 1 but the noise temperature remains high and decreases with increasing Ω. For PF-2, it is possible that some additional mode of phase fluctuations is present as

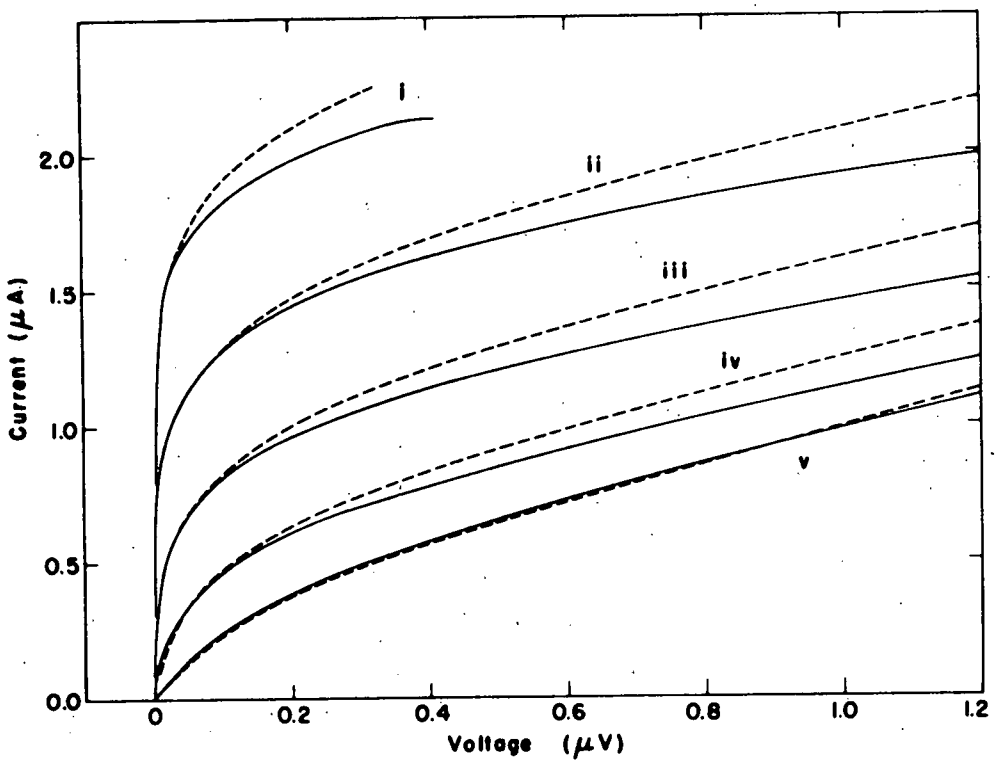

Fig. 5-4 Current-voltage characteristics of PF-1 at several temperatures near T_c. The solid lines are data, and the dashed lines are two parameter fits to the theory of Ambegaokar and Halperin with an effective noise temperature of 10 K for each curve. The relevant parameters for the curves are:

	T(K)	γ	$I_1(\mu A)$
(i)	3.855	14.7	3.1
(ii)	3.857	11.0	2.3
(iii)	3.859	8.0	1.7
(iv)	3.861	5.6	1.2
(v)	3.863	3.6	0.75

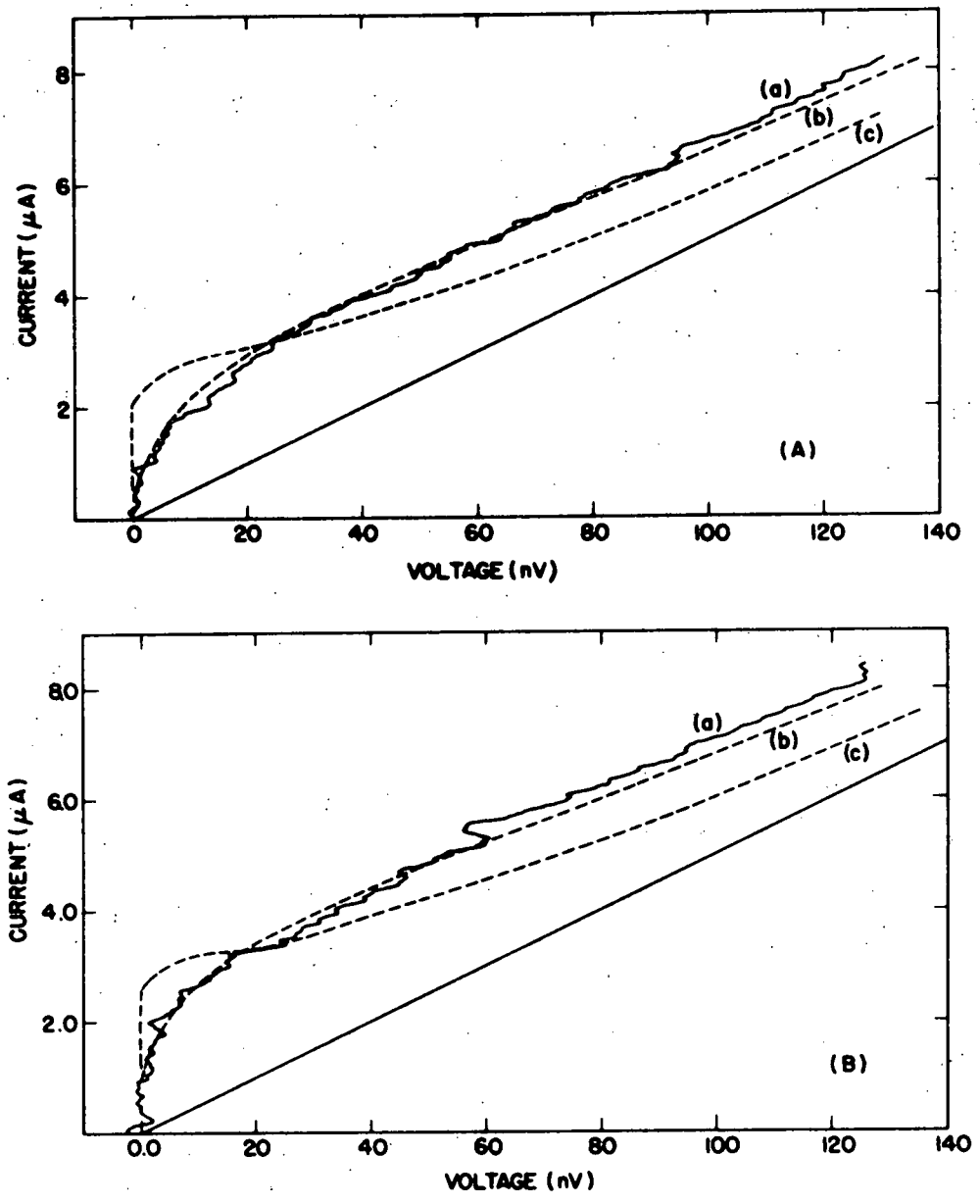

Fig. 5-5 Current-voltage characteristics of PF-2 in a magnetic field. In (A), (B), and (C) [following page], the actual temperature was 3.67 K. In all cases, (a) is the data, (b) the best fit to T and I_1, (c) the best fit to I_1 alone, and the solid straight line represents the assumed quasi-particle current. For (A), taken in a magnetic field or 21.4 Oe, a two parameter fit gives I_1 = 4.6 μA and T = 44 K, and a single parameter fit gives I_1 = 3.0 μA. For (B), taken in a magnetic field of 20.8 Oe, a two parameter fit gives I_1 = 4.9 μA and T = 35 K, and a one parameter fit gives I_1 = 3.4 μA .

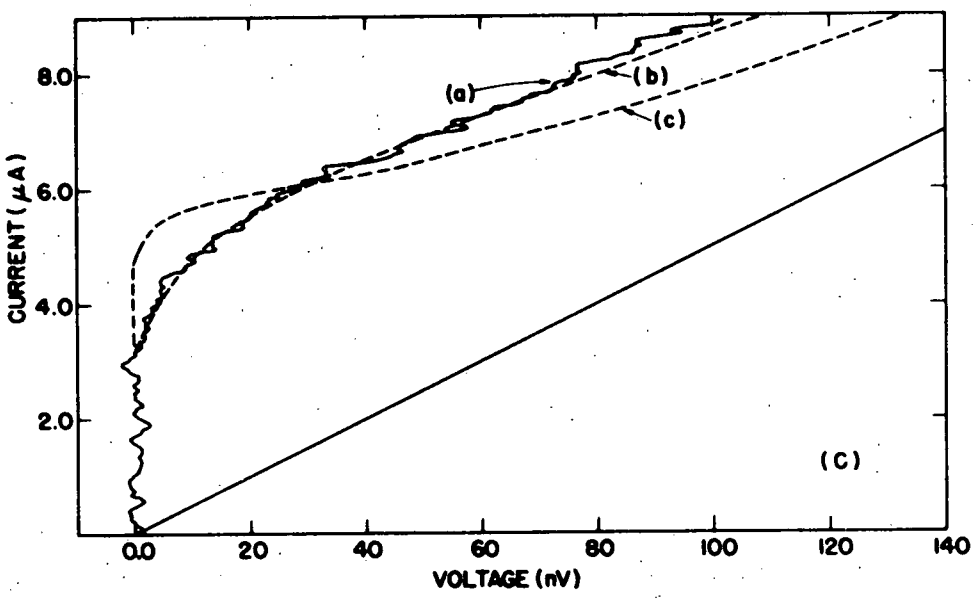

Fig. 5-5C For (C), taken in a magnetic field of 20.2 Oe, a two parameter fit gives I_1 = 7.6 μA and T = 34 K, and a one parameter fit gives I_1 = 6.1 μA .

the measurements were made in a magnetic field.

A second possible source of a high apparent noise temperature is that a junction has broken into several small sections which are not phase coherent. Each section would exhibit rounding appropriate to its individual coupling strength but the total junction current would be the sum of the currents from each section. Thus the rounding would be out of proportion to that expected on the basis of the total current. We have evidence from the current-field characteristic for PF-1 that the junction does begin to break up, perhaps because the edges remain superconducting above the bulk transition temperature. In PF-2, there is similar evidence that the junction geometry changes in the regime where phase fluctuations were observed. Furthermore, although the data on PF-2 was obtained 50 mK below T_c, the fields applied to reduce the coupling were sufficiently strong so that $T_c(H)$ was comparable to T and it is probable that PF-2 was also breaking up.

Finally, one can not eliminate the possibility that some external noise is reaching the sample despite the precautions taken. For example, it was discovered after the experiment was completed that the Exact 404 oscillator produced a weak, incoherent signal of approximately 4 MHz. The signal could not be detected on an oscilloscope, but was later detected by a junction used in the pair susceptibility experiment.

1.3 Critique

The major criticism of this experiment stems from the use

of fitted parameters. Though it is reasonable to fit $I_1(T,H)$ in lieu of an a priori method of obtaining it, fitting the noise temperature can be misleading. There is no guarantee that the noise is white since the source is not known. Defects in the junction structure can produce the observed effect, and without knowledge of the details of these defects, one can not anticipate how the current-voltage characteristic will be affected. The noise spectrum is relatively important since Kanter and Vernon[53] have shown that for low γ, low frequency noise produces qualitatively the same effect on the current-voltage characteristic as does wideband noise. Though the high noise temperature problem could be due to low frequency noise, we feel that the precautions taken to shield the sample are adequate and that the difficulties are more likely a consequence of the deterioration of the sample as it undergoes the transition to the normal state. Junction defects other than those noted are probably not present due to the care with which the junctions were selected.

Using the bismuth oxide masking technique developed for the pair susceptibility experiment, junctions can be produced which will be free from the graded transition temperature introduced by film edges. By forming the junction from a small area in the middle of a tin strip, a sharp transition will be obtained, and the critical current will follow closely the linear dependence of Eq. 2-33. Masking the edges will thus make possible the prediction of the critical current from low temperature properties of the junction.

V.2 Pair Susceptibility

2.1 Introduction

The data from the pair susceptibility experiment was analysed using the theory of Scalapino. All parameters of the theory were obtained from the physical properties of the samples and the superconductors used to prepare them.

The data for the experiment[130] was obtained from two junctions with similar properties which are given in Table 3. In both junctions, edge effects were eliminated by masking films with bismuth oxide. The junction resistances were large compared to the normal state resistances of the tin films so that there was no distortion of the current-voltage characteristics. Since the tin films are not manifestly superconducting in the temperature range of interest, this is an important consideration. Current-voltage characteristics were checked for evidence of filimentary shorts as described in IV.5.

2.2 Data

Shown in Fig. 5-6 are typical current-voltage characteristics obtained above T_{c1} of PS-1. A comparison of this figure with Fig. 5-1 obtained below T_c illustrates certain qualitative differences between the phase fluctuation rounded current-voltage characteristics and the characteristic resulting from the excess current. The prominent qualitative difference is that in the regime in which the pair susceptibility is determined, the current-voltage characteristic exhibits a linear portion, the slope of which varies regularly with temperature, whereas in the

Table 5-3. Junction Properties of PS-1 and PS-2

	PS-1	PS-2	Units
Area	3.1×10^{-4}	1.04×10^{-4}	cm^2
R_N	5	2.1	Ω
R_G	70.5	11.4	Ω
$I_1(0)$	1.7×10^{-4}	3.4×10^{-4}	A
T_c	3.712	3.886	K
d	1.5×10^{-5}	1.5×10^{-5}	cm

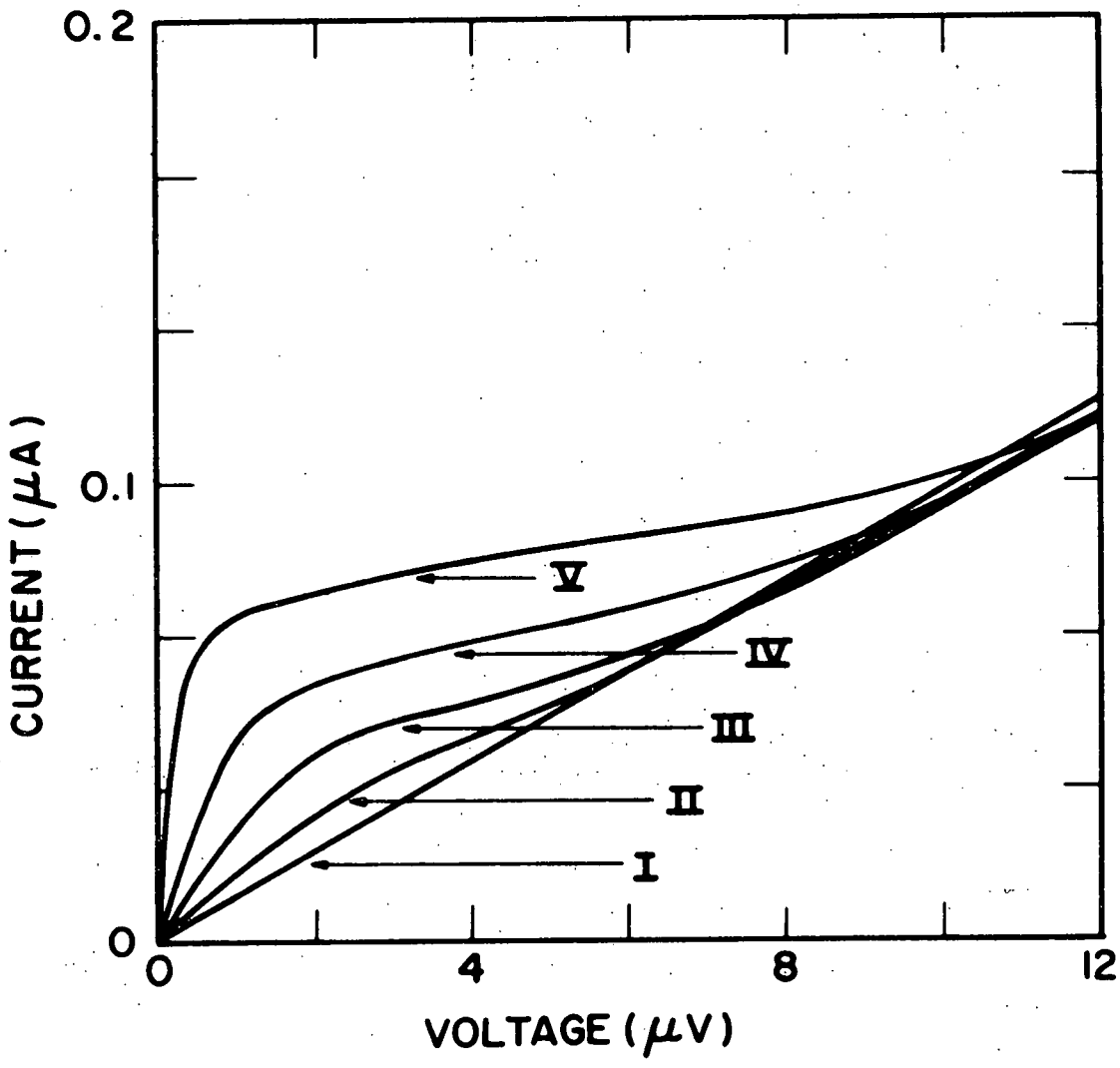

Fig. 5-6 Current-voltage characteristics of PS-1 above T_{c_1}. The reduced temperatures of each of the curves are: (I) $\epsilon = 7.8 \times 10^{-3}$; (II) $\epsilon = 3.91 \times 10^{-3}$; (III) $\epsilon = 2.94 \times 10^{-3}$; (IV) $\epsilon = 2.21 \times 10^{-3}$; (V) $\epsilon = 1.48 \times 10^{-3}$.

regime in which phase fluctuations are important, the characteristic exhibits a continuous curvature. We emphasize that this is a qualitative difference and not a test to distinguish the two types of behavior. The curve labeled (I) of Fig. 5-6 was obtained at a sufficiently high temperature that the pair current is not detectable, and is presented to demonstrate the linear quasiparticle current which must be subtracted from the current-voltage characteristic to find the excess current. After subtraction of the quasiparticle current, curves of excess current as a function of voltage and temperature are obtained. Fig. 5-7 shows typical excess current curves. From these may be read directly the peak current and voltage.

Several different methods were used to determine T_{c_1}, only one of which was used in the analysis of the data. Since the ordinary Josephson current disappears at T_{c_1}, one method is to extrapolate $I_1(T)$ to zero. As discussed in II.3.2, the Josephson current of an asymmetrical junction approaches zero with infinite slope at T_{c_1} so that in prinicpal one has an accurate method of determining T_{c_1}. In practice, the slope was sufficiently steep to find T_{c_1} within 0.5 mK. T_{c_1} may also be found from the resistive transition of the tin, though not as accurately as from the extrapolation of the critical current. The width of the transition and the inability to precisely locate the onset of superconductivity in the film limit the accuracy of this method. T_{c_1} obtained from the resistive transition was usually about 10 mK above that found from the critical current extrapolation. Film edges, which are excluded from the junction by

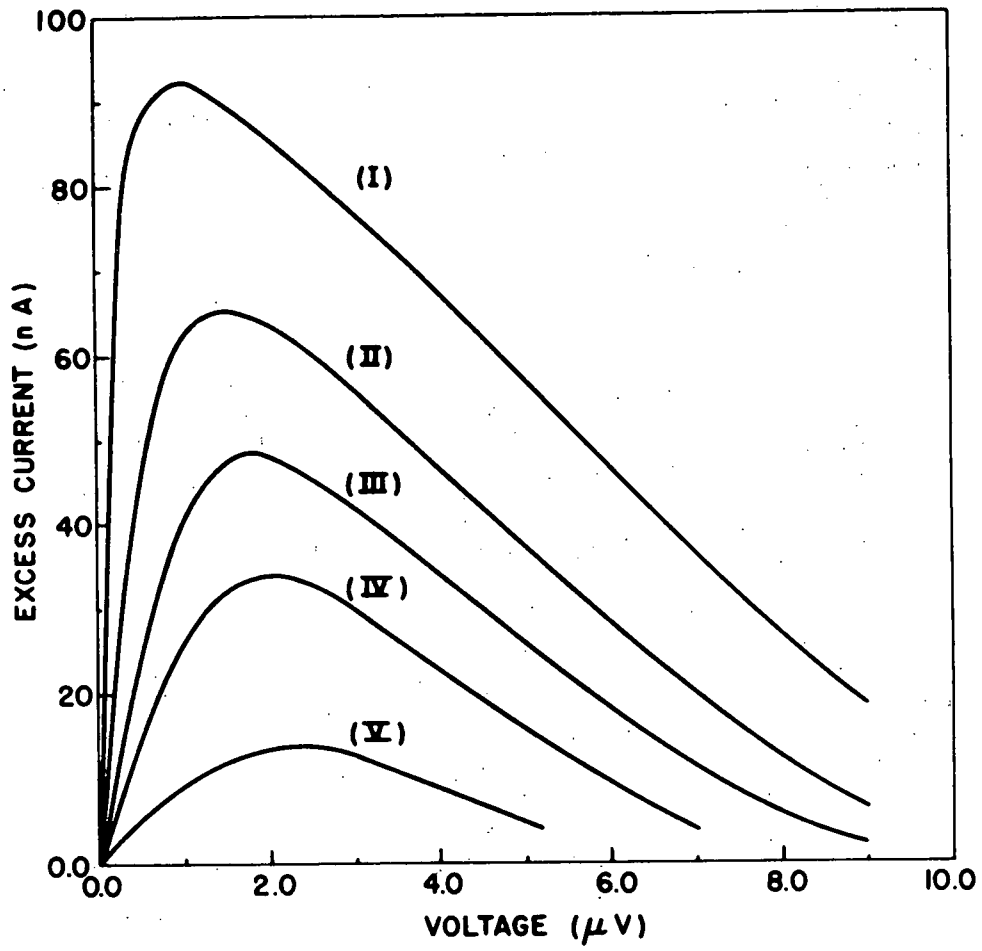

Fig. 5-7 Excess current-voltage characteristics of PS-1 at several temperatures. The reduced temperatures of each of the curves are: (I) $\epsilon = 1.48 \times 10^{-3}$; (II) $\epsilon = 1.97 \times 10^{-3}$; (III) $\epsilon = 2.45 \times 10^{-3}$; (IV) $\epsilon = 2.94 \times 10^{-3}$; (V) $\epsilon = 3.91 \times 10^{-3}$.

masking, are responsible for the observed shifting and broadening of the resistive transition. The transition temperature obtained this way does not represent T_{c_1} of the junction. The third method of finding T_{c_1} is to extrapolate V_p to zero. By Eq. 3-137, V_p decreases linearly with T to T_{c_1} so that $V_p = 0$ when $T = T_{c_1}$. T_{c_1} found in this manner was within 2 mK of that found from $I_1(T)$. The transition temperature used in the analysis of the data was that obtained using the V_p extrapolation since it represents the transition temperature governing the underlying physical processes. The difference between this transition temperature and that found from the critical current extrapolation represents the experimental error.

The qualitative behavior of the current-voltage characteristic is different above T_{c_1} from below T_{c_1}. Below T_{c_1}, the junction carries the usual Josephson current which is quasi-periodic in magnetic field. Above T_{c_1}, the Josephson current is replaced by the excess tunneling current, which for a given temperature and voltage, is monotonically decreasing with increasing magnetic field. It is emphasized that no evidence of periodicity is observed above T_{c_1}.

Shown in Fig. 5-8 is the dependence of V_p on ε for PS-1 and PS-2. Drawn with the data is the theoretical curve calculated from Eq. 3-137 and 3-138 using the bulk transition temperature of tin to estimate the pair relaxation frequency. Although the actual transition temperatures vary somewhat, the variations are not significant. The measured slope is 6.1×10^{-4} V which implies that the experimental relaxation rate is about 50% greater than

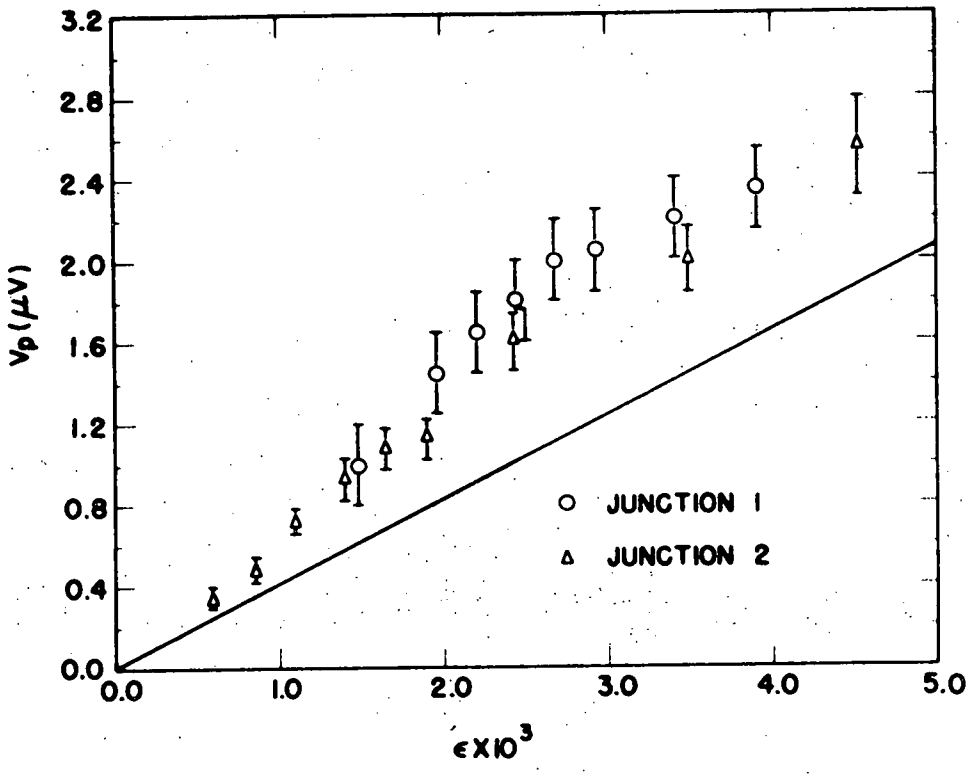

Fig. 5-8 V_p versus ϵ for PS-1 and PS-2.

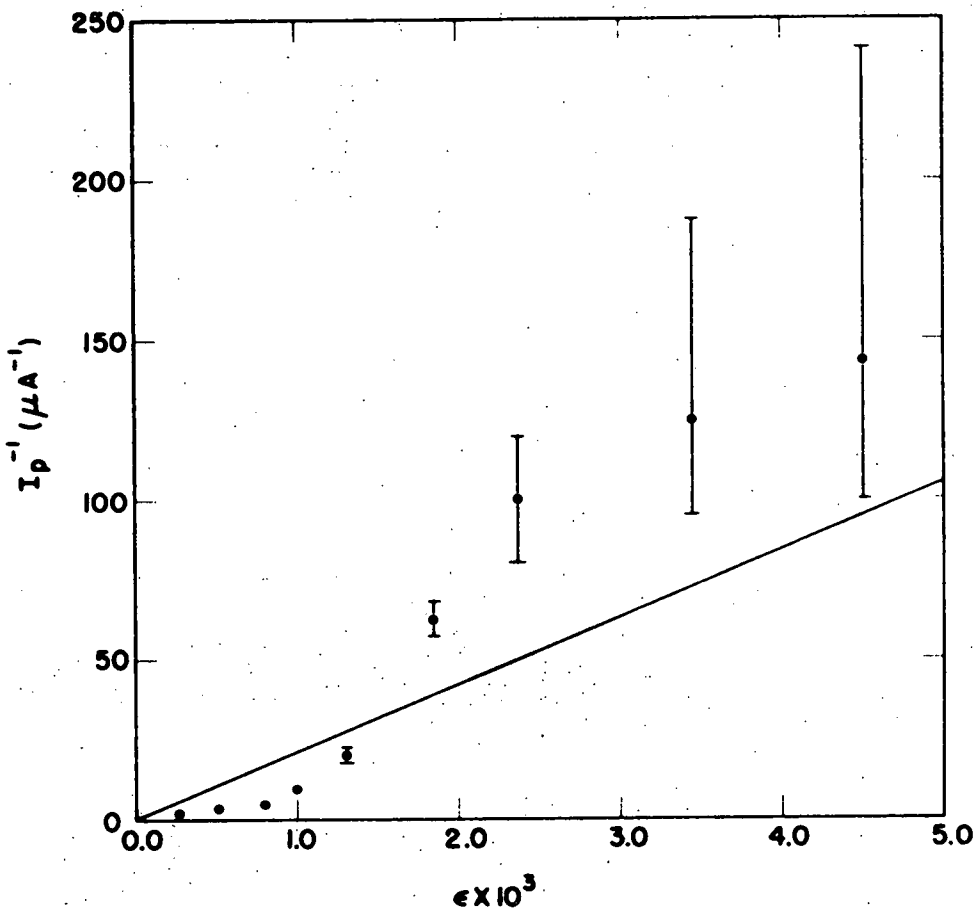

Fig. 5-9 I_p^{-1} versus ϵ for PS-1.

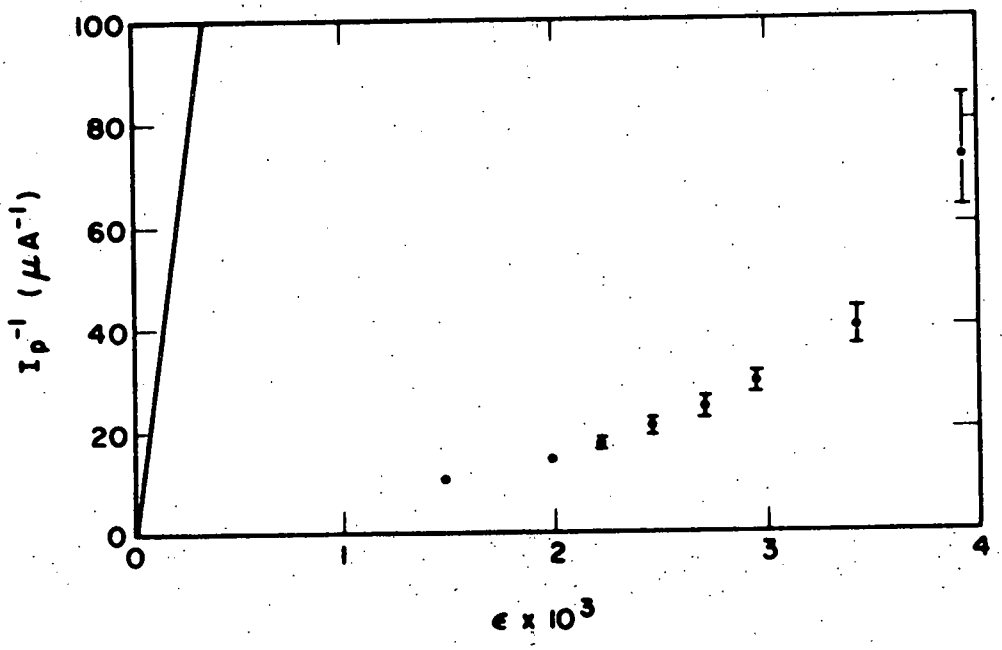

Fig. 5-10 I_p^{-1} versus ϵ for PS-2.

the theoretical value. It is not known if the knee at $\epsilon = 2.5 \times 10^{-3}$ is significant or an experimental artifact. With increasing ϵ, the excess current decreases, becoming a small correction to the quasiparticle current. In this regime, it is difficult to choose the subtractor gain correctly. At high ϵ, V_p is very susceptible to errors in the subtractor gain.

By Eq. 3-143, the peak current varies at $1/\epsilon$. Shown in Fig. 5-9 and 5-10 are graphs of I_p^{-1} versus ϵ for PS-1 and PS-2. The experimental value of $\bar{V}$ was used in Eq. 3-143 to calculate the theoretical curve. The agreement is not good, with the magnitude qualitatively correct only for PS-2. It is suspected that the larger than expected excess current in PS-1 is due to locally thin regions in the insulating barrier. In the calculations of III.2, it was assumed that ψ and ψ^* were proportional to the strength of the pairing field. If the pairing field is strong enough, the proximity effect,[131] by which higher order contributions to ψ and ψ^* eventually result in full superconductivity in the tin above T_c, becomes important. The additional superelectron density does not affect the resonance condition for V_p since it depends on the relaxation rate. However, it does increase the amplitude of the excess current. Below T_{c_1}, the proximity effect is no longer important since the tin is then fully superconducting. It is likely that the temperature dependence of the higher order terms is different from that of the susceptibility and their presence might account for the departures from linearity of the curves in Fig. 5-9 and 5-10. An additional complication is that in the critical region very close to T_{c_1},

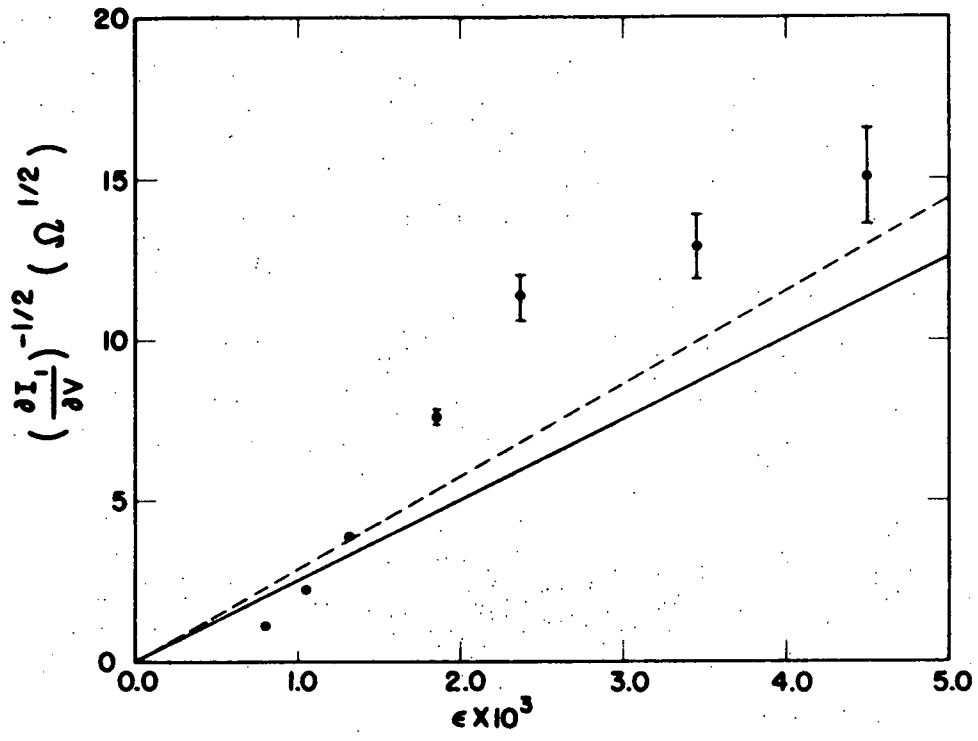

Fig. 5-11 $\sigma(0)^{-\frac{1}{2}}$ versus ϵ for PS-1. The solid line was calculated using Eq. 3-145. The dashed line is based on the work of Ref. 30 and was calculated using Eq. 3-153 and 154.

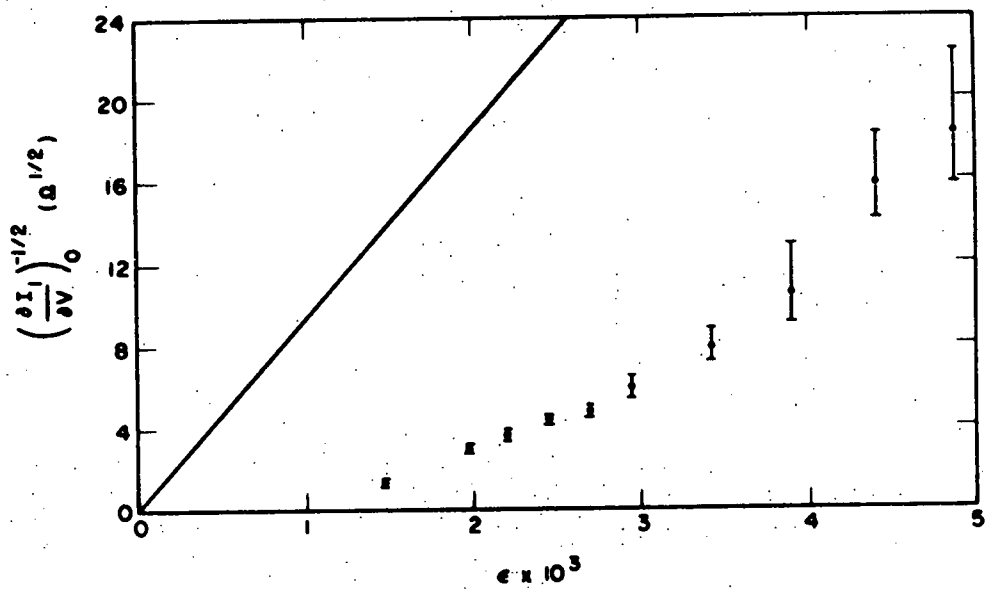

Fig. 5-12 $\sigma(0)^{-\frac{1}{2}}$ versus ϵ for PS-2. The solid line was calculated using Eq. 3-145.

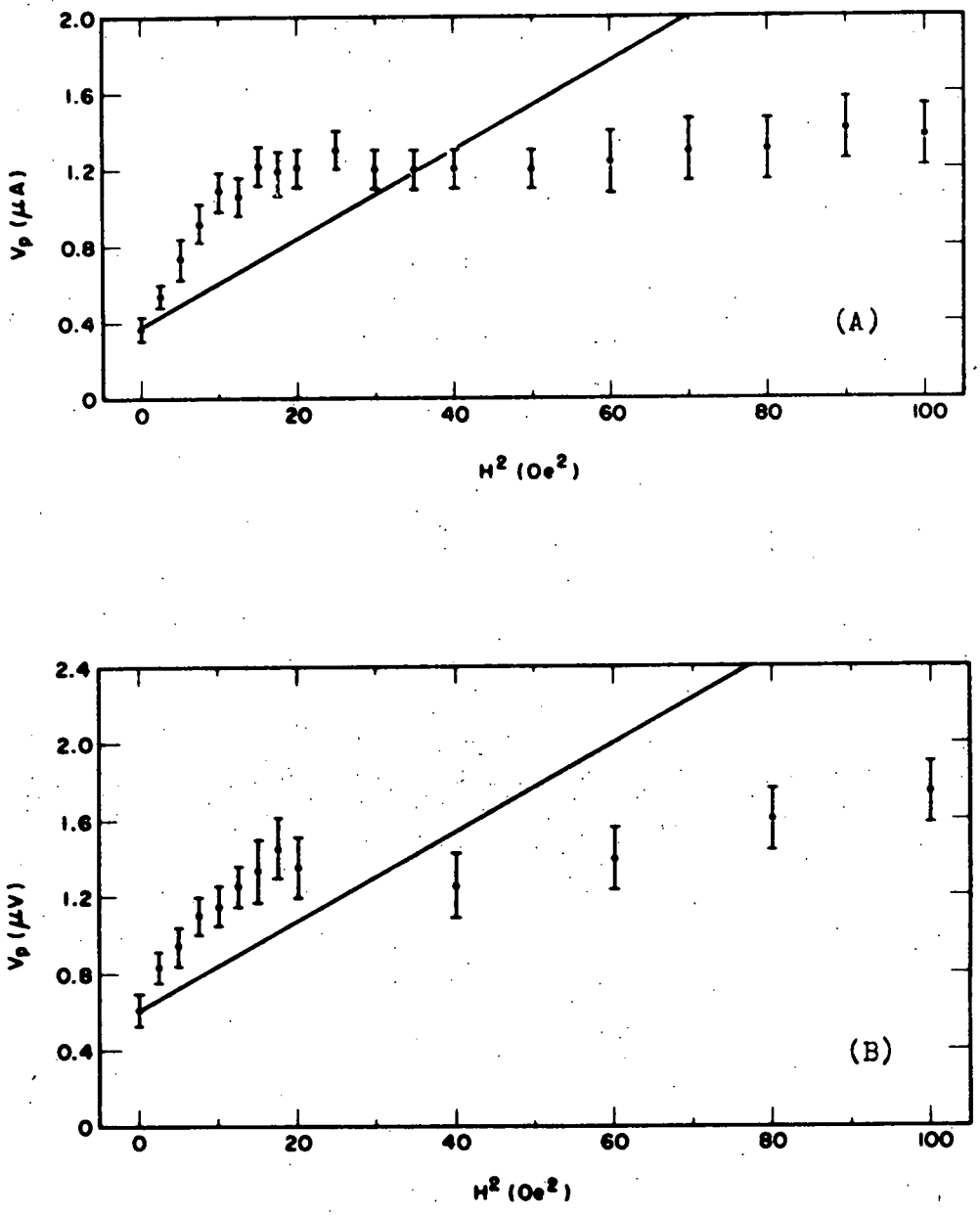

Fig. 5-13 V_p versus H^2 for PS-2 at several different temperatures. In (A) $\epsilon = 0.54 \times 10^{-3}$, and in (B) $\epsilon = 0.8 \times 10^{-3}$.

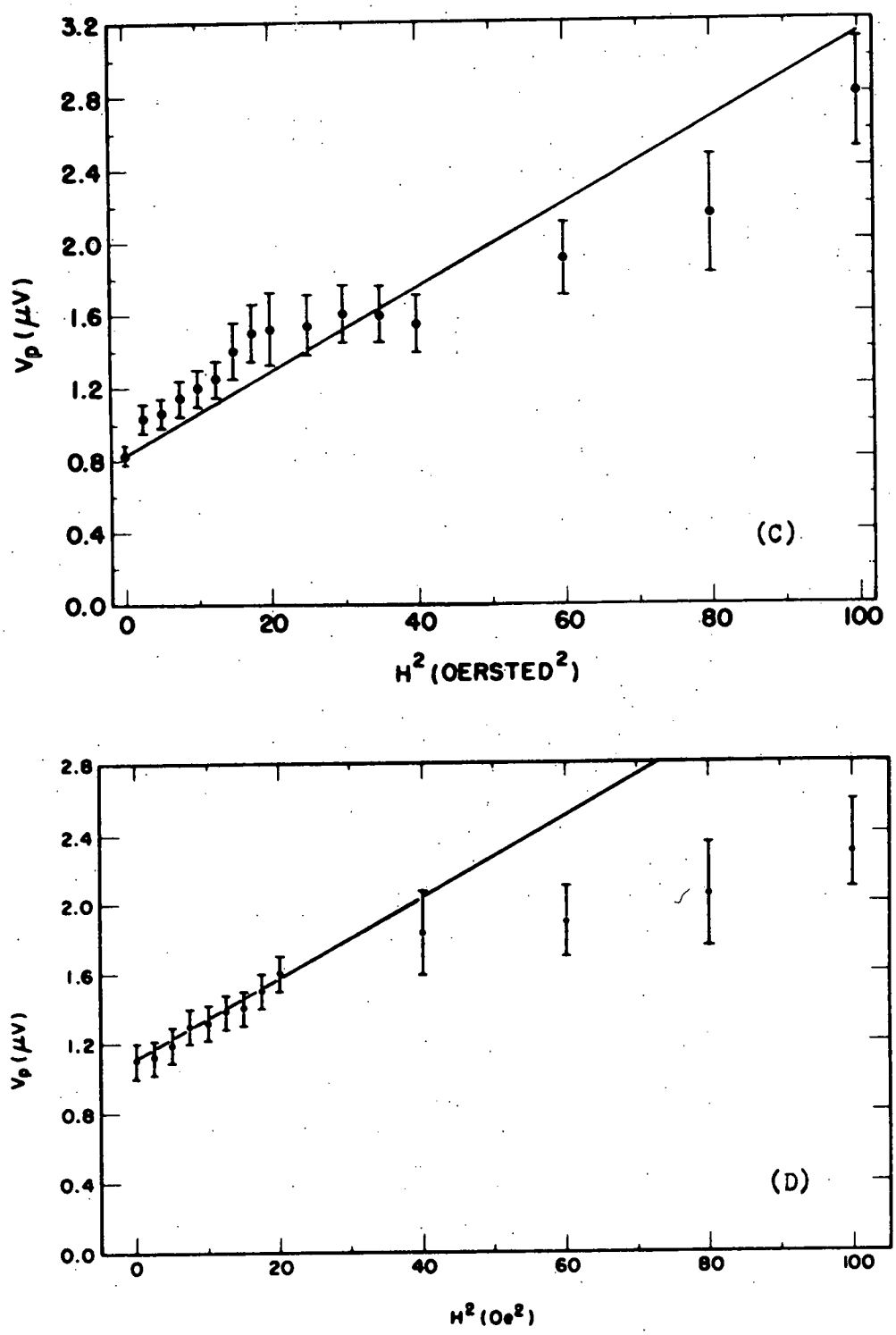

Fig. 5-13 (continued)
In (C) $\epsilon = 1.06 \times 10^{-3}$, and in (D) $\epsilon = 1.31 \times 10^{-3}$.

mean field theory, on which these calculations are based, no longer holds.

Figures 5-11 and 5-12 show the dependence of $\sigma(0)$ on ε. Since $\sigma(0)$ depends strongly on the pair amplitude, any deviation from theory of I_p is reflected in $\sigma(0)$.

The relaxation rate for finite q values can be determined from the dependence of V_p on H^2 since by Eq. 3-140 and 3-141, V_p is proportional to H^2. Figures 5-13 A, B, C, and D show $V_p(H^2)$ for PS-2 at several different values of ε. The theoretical line in each case was calculated from Eq. 3-140 and 3-141 using the clean limit value of 2300 Å for ξ_0 and the experimental value of $\bar{V}$. Resistance measurements[132] place $\bar{\ell}$ at 2500 Å, which is between the clean and dirty limits. Ideally, the initial slope should be almost independent of temperature, the only temperature dependence entering through $\lambda_2(T)$. Also, the saturation of V_p should not occur according to theory. We believe that it may result from an overestimate of the contribution from high q or short wavelength fluctuations[133] to the susceptibility by mean field theory. This effect may be related to the pathological behavior at high q observed in the magnetic susceptibility experiments of Gollub, Beasley, and Tinkham.[134] This question and that of the temperature dependent initial slope are subjects for future investigation.

Finally, in Fig. 5-14 we present a comparison of the theoretical excess current as a function of voltage with that observed experimentally. Using V_p and I_p from the experimental curve, the theoretical curve was calculated from

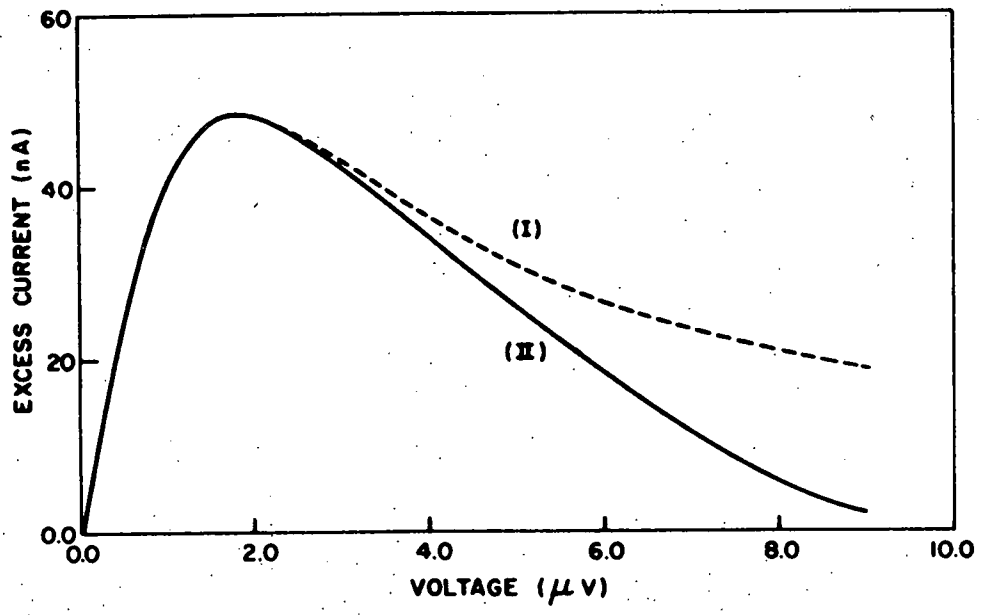

Fig. 5-14 Comparison of the experimental to the theoretical excess current-voltage characteristic. The solid line is the data and was obtained from PS-1 when $\epsilon = 2.45 \times 10^{-3}$.

$$I = 2I_p \frac{(V/V_p)}{1 + (V/V_p)^2} \qquad (1)$$

Though the experimental curve was obtained in zero magnetic field, it is representative of curves obtained in non-zero fields and at other values of ε. All show the more rapid decay of the excess current with voltage than predicted by Eq. 3-138.

2.3 Critique

Experimentally, the greatest difficulty with the pair susceptibility experiment is in establishing V_p far above the transition temperature (ε greater than a few tenths of a percent). There are two reasons for this: 1) only in very strongly coupled junctions is the excess current large enough to be seen against the quasiparticle background at large ε; 2) the amount of quasiparticle current subtracted from the total junction current becomes very critical at large ε due to the small amount of excess current. A small error in the subtractor gain can result in a substantial apparent shift in V_p. It would be expected that at higher values of ε, the contributions of the higher order terms to the excess current would be insignificant. Thus with increasing temperature, I_p should approach its theoretical value. The small range of ε in these experiments does not permit the testing of this hypothesis.

If the data for the peak current is to be considered representative, then some method must be found to establish the uniformity of junctions. Having done this, one would be able to determine whether the intrinsic data behaves as shown in Fig. 5-9

and 5-10.

No corrections have been made to account for phase fluctuation effects on the current-voltage characteristic. These effects should be unimportant when the quasiparticle current is small. It is still an open question as to whether such corrections are needed in the regime of the present experiment. A complete calculation of the excess current in asymmetrical junctions would require corrections. Kulik[115] has carried out a calculation of the excess current in symmetrical NN junctions where quasiparticle effects are important.

VI. CONCLUSIONS AND SUGGESTIONS FOR FUTURE WORK

VI.1 Phase Fluctuations

Within the small Ω limitation, the data is qualitatively consistent with the theory of Ambegaokar and Halperin. No fit was possible with $\Omega > 1$, but for PF-2, which had small Ω over a wide current range, it was possible to fit the data to theory with two parameters. It was necessary to fit the parameters not because of the theory, but because of experimental considerations.

The major difficulty in the data reported here was that the junctions were not uniform and did not possess low values for Ω at critical currents of interest. Edge effects, which are the primary source of nonuniformity, can be eliminated by the bismuth oxide masking technique developed for the pair susceptibility experiment. This would ensure uniform junction structures in the vicinity of T_c. The problem of reducing Ω can be solved by making junctions of low resistance. Additional efforts to toward locating and eliminating undesirable sources of noise should be made.

A further generalization of the theory to include the case of non-zero capacitance is necessary before definitive comparison to experiment can be made. The effort of Ambegaokar and Kurkijärvi with the Monte Carlo techniques is useful, but either a series correction formula or a numerical solution to the Fokker-Planck equation would be more satisfactory.

VI.2 Pair Susceptibility

The observed current-voltage characteristics exhibit an excess current which has the resonant behavior of the pair fluctuation current. The experimental dependence of the peak voltage on temperature and magnetic field is consistent with theory. The magnitude of the excess current, a quantity highly dependent on the junction structure, has the correct order of magnitude. Thus we believe the experiments to be a determination of the imaginary part of the pair susceptibility of a superconductor.

The most obvious extension of the pair susceptibility experiment is to make measurements on other superconductors. To do this, it would be extremely useful to develop standardized procedures. In the present experimental configuration, the tin film is the film on which the insulating barrier is grown. It is unlikely that tin will be used in conjunction with the investigation of other superconductors as it does not have a very high transition temperature. Thus it would be better in the future to produce the insulating barrier on the reference metal, which in this case was lead.

A second experimental improvement should be in the general technology of producing thin uniform junctions. A thin barrier allows the excess current to be seen at much higher values of than used here. A thin barrier is almost absolutely essential to the investigation of superconductors with very low transition temperatures. In those cases, $\bar{V}$ will be considerably smaller than for tin, and it will be necessary to track V_p over a wide temperature range to establish a value for $\bar{V}$. The importance

of the uniformity of the barrier has already been discussed in relation to the determination of the pair tunneling amplitude. Further procedures to document the uniformity of the barrier would be useful.

A better method of retrieving the data than the simple ac technique described in IV.4.3 would improve the accuracy and resolution over that presented here. Some type of signal averaging combined with an accurately controlled electronic subtraction of a linear current, followed by digitizing, is suggested. The original data could later be resynthesized by computer and a refined subtraction of the quasiparticle current, more carefully determined by experiment and theory, made. The improvement is not in the replacement of the linear approximation, since the quasiparticle current is linear within the resolution of the apparatus, but in the substitution of a procedure that provides a consistent means of determining the amount of current to be subtracted. It is hoped that such a procedure will determine whether the apparent break in the V_p versus ε curve is real or an experimental artifact.

Theoretical work should concentrate on improving the H^2 dependence of the peak voltage, and the effects of phase fluctuations on the measurements. There are reasons to believe that the classical theory overestimates the contributions of short wavelength fluctuations. In addition, some attention should be given to the role of the proximity effect in determining the magnitude of the excess current.

APPENDIX A. BRIDGE CIRCUIT

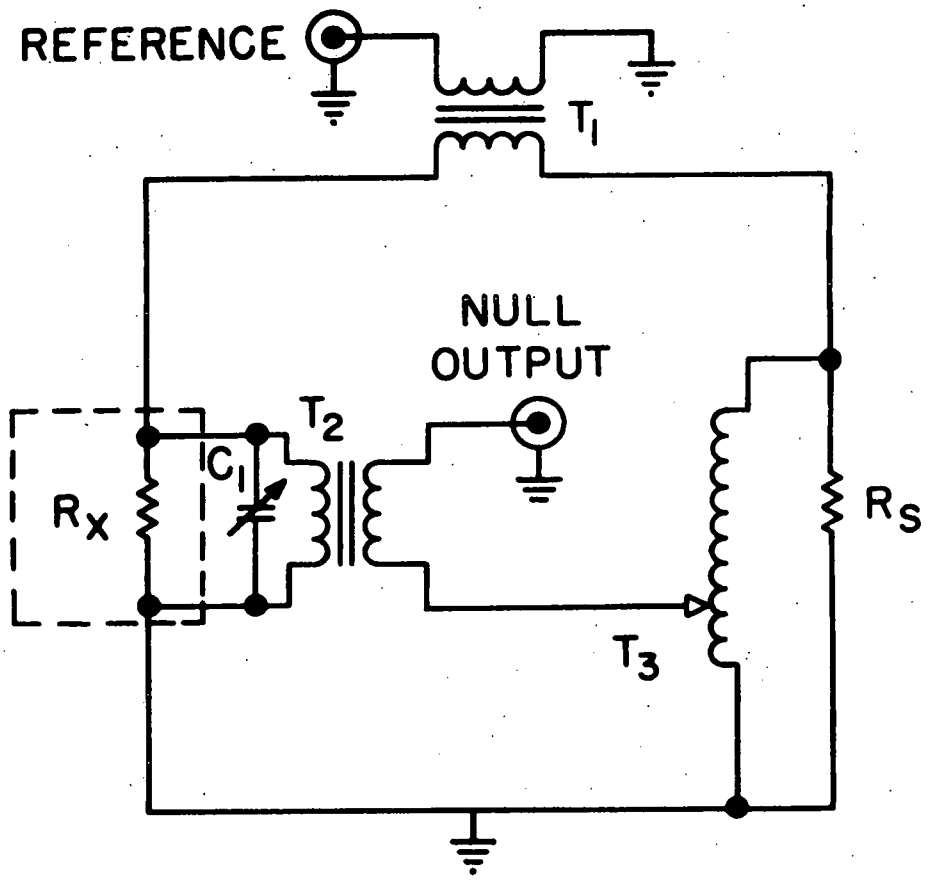

Fig. A-1. The bridge circuit. The description of the components is as follows: T_1 is 1:6 turns ratio chopper transformer with the low impedance (~ 1000Ω) winding connected to the reference; T_2 is a North Atlantic Industries T-300 1:1 phase reversal transformer with an input impedance ~ 10^5Ω; T_3 is an Electra Scientific Industries "Dekatron" ratio transformer with a resolution of 1 part in 10^7; R_s is the standard resistor which has an accuracy and a temperature stability of better than 50 ppm; R_x is the germanium resistor; C_1 is a decade capacitor for reactive balancing of the bridge. The dashed lines indicate the helium bath. At 4 K, typical values of R_s, R_x, and C_1 are 10 kΩ, 1kΩ, and 0.02 μF respectively.

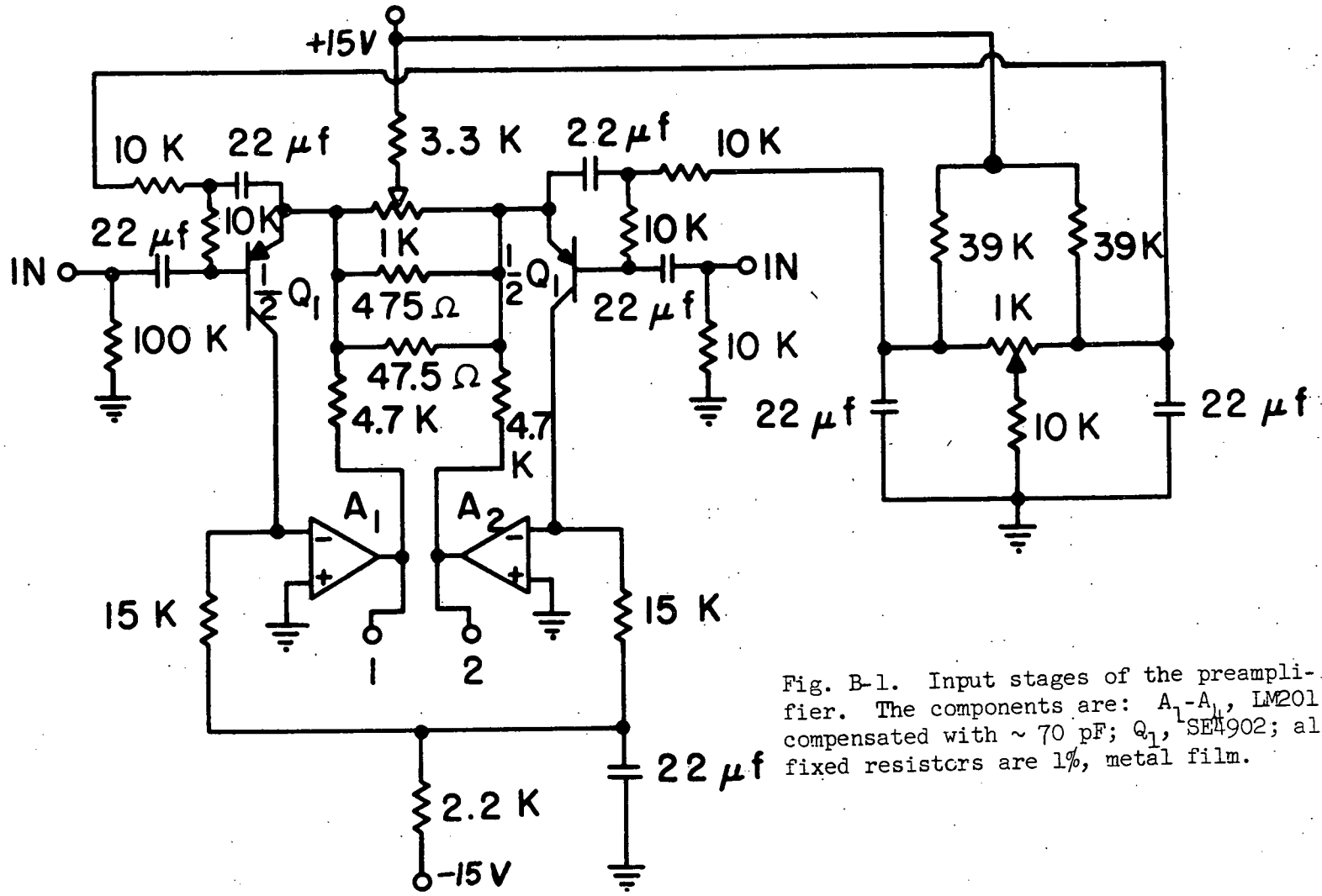

Fig. B-1. Input stages of the preamplifier. The components are: A_1-A_4, LM201 compensated with ~ 70 pF; Q_1, SE4902; all fixed resistors are 1%, metal film.

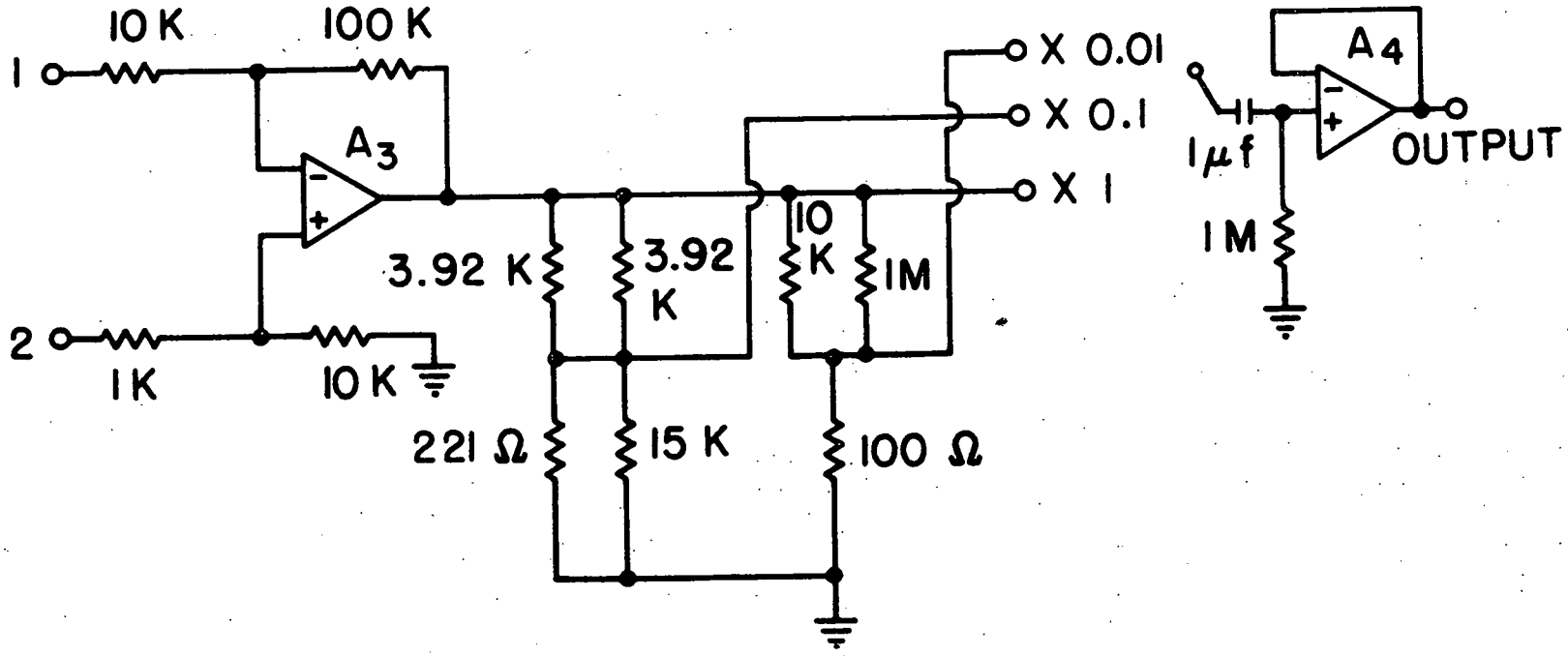

Fig. B-2. Output stages of the preamplifier. The notes of Fig. B-1 apply. (1) and (2) are connected to (1) and (2) of Fig. B-1. A_1-A_4 of all stages of the preamplifier are powered with ± 15 V.

APPENDIX C. RAMP GENERATOR CIRCUIT

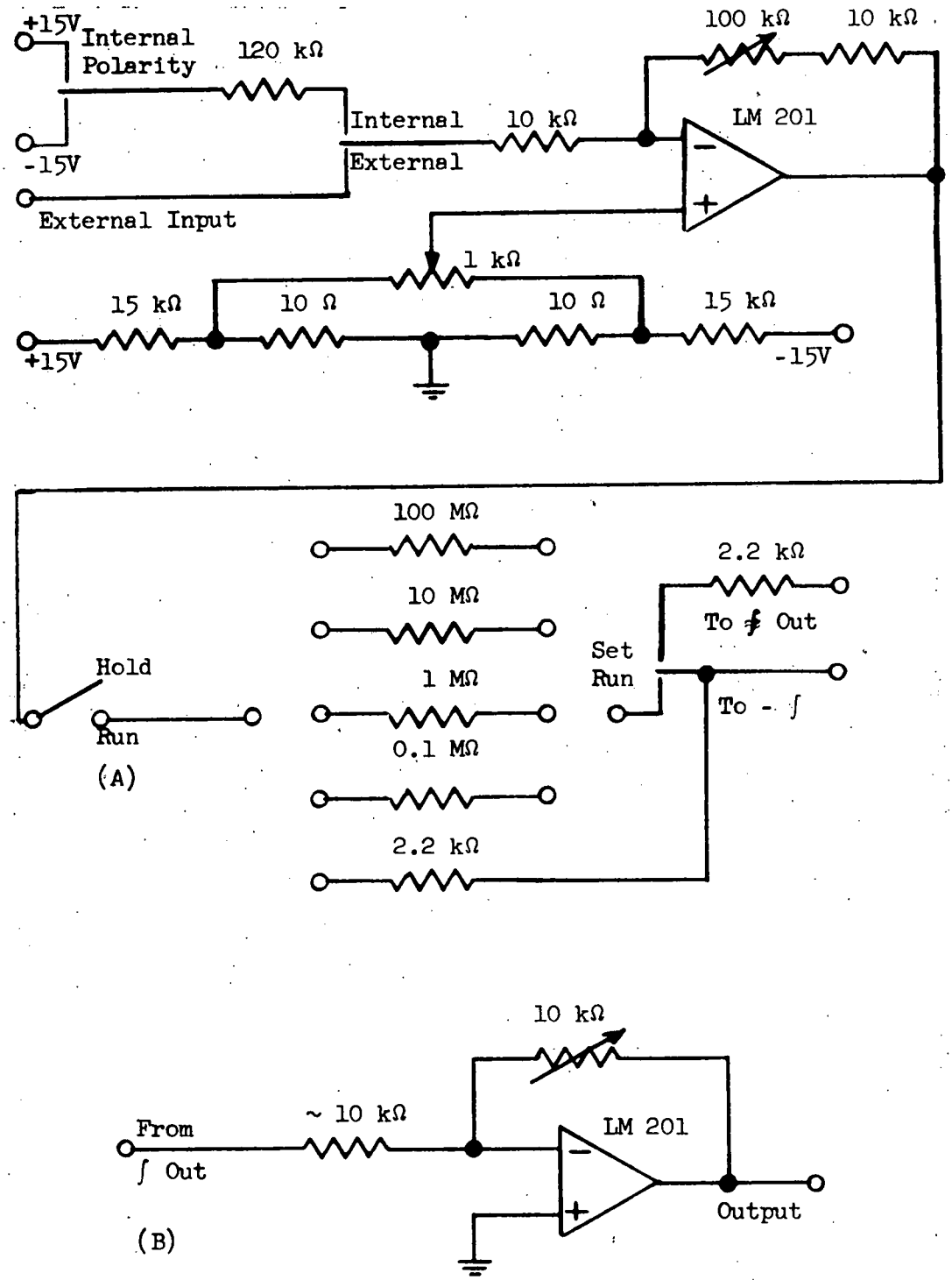

Fig. C-1. Rate control and output stage for the ramp generator. The rate control is shown in (A), and the output stage in (B). All LM201 in this figure and in Fig. C-2 are compensated with ~ 70 pF and powered with ± 15 v.

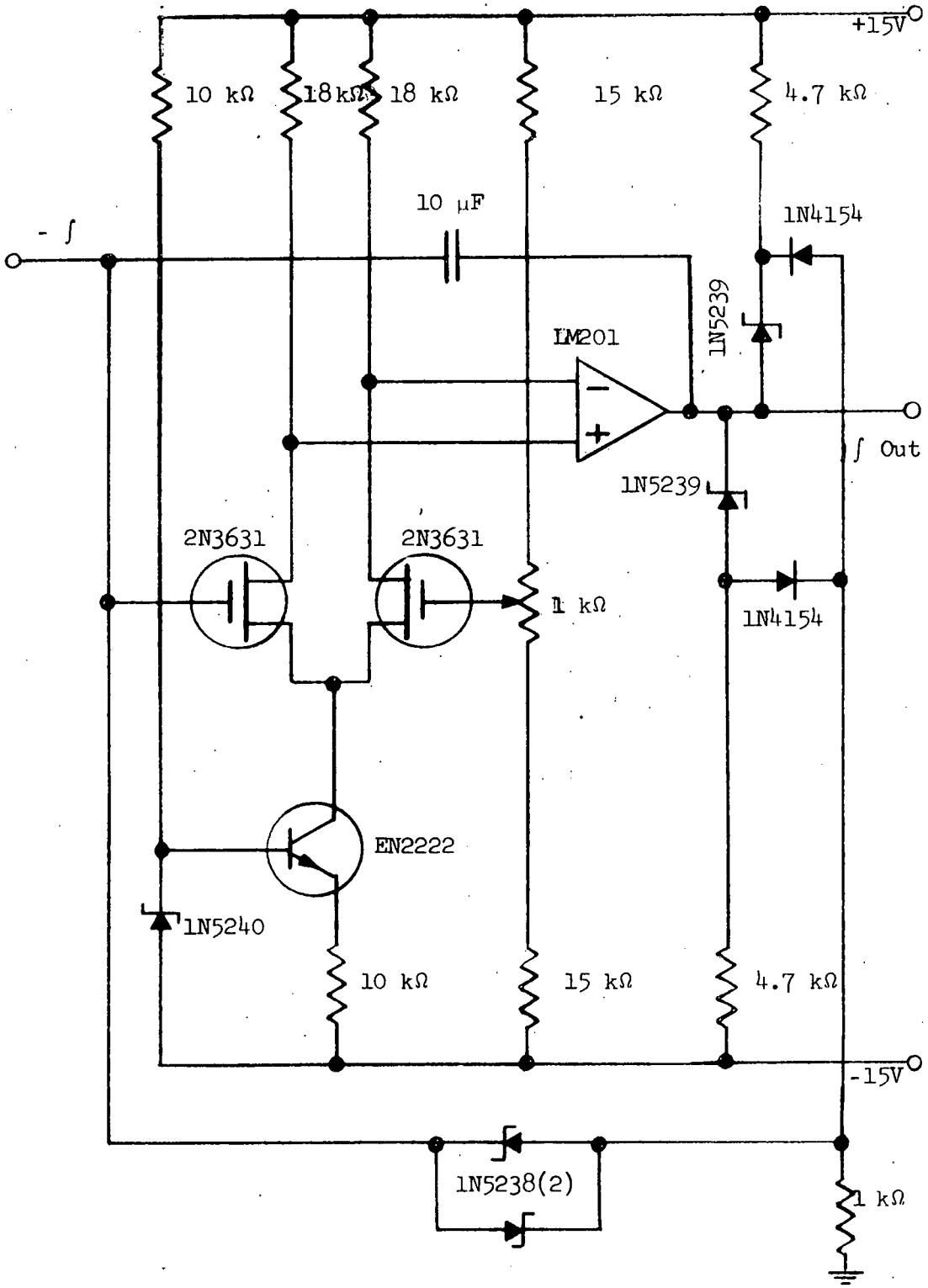

Fig. C-2. Integrator for ramp generator. The 10 μF capacitor must have a low leakage dielectric such as mylar.

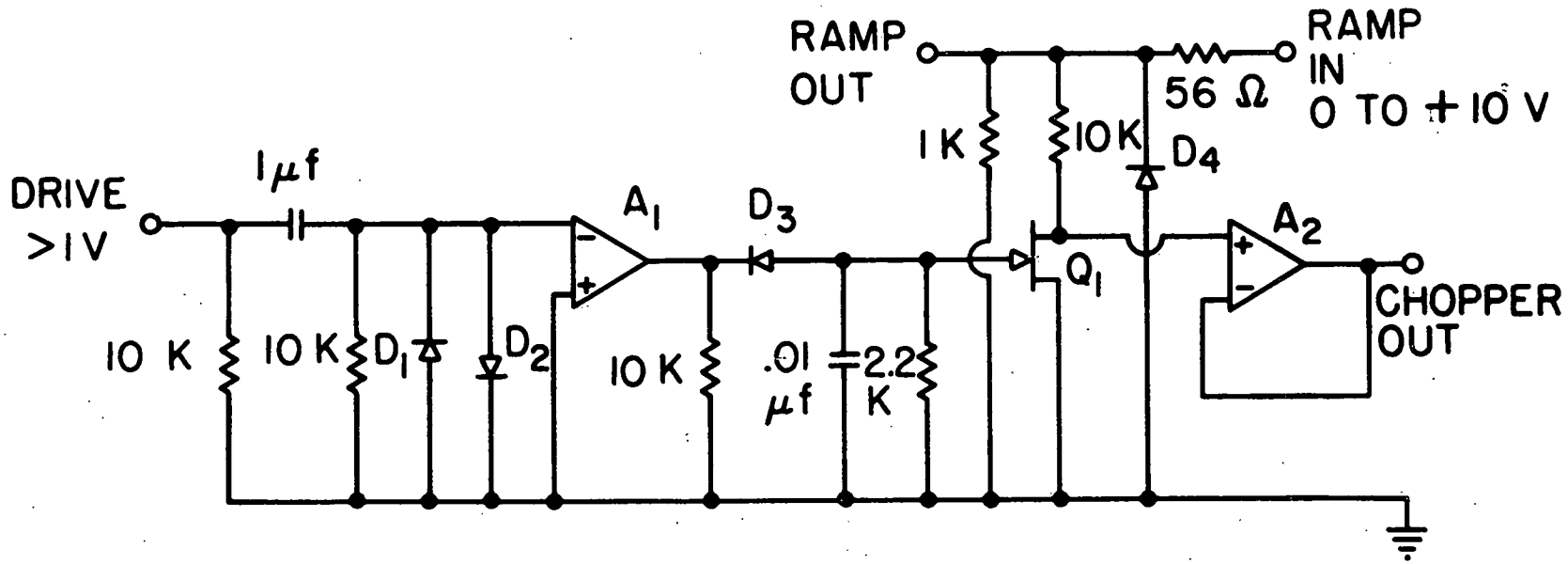

Fig. D-1. Chopper circuit. The components are: A_1-A_2, LM201 compensated with ~ 70 pF; Q_1, VCR-2N; D_1-D_3, 1N4154; D_4, 0.25 watt 10 v zener diode.

APPENDIX E. ADDER/SUBTRACTOR CIRCUIT

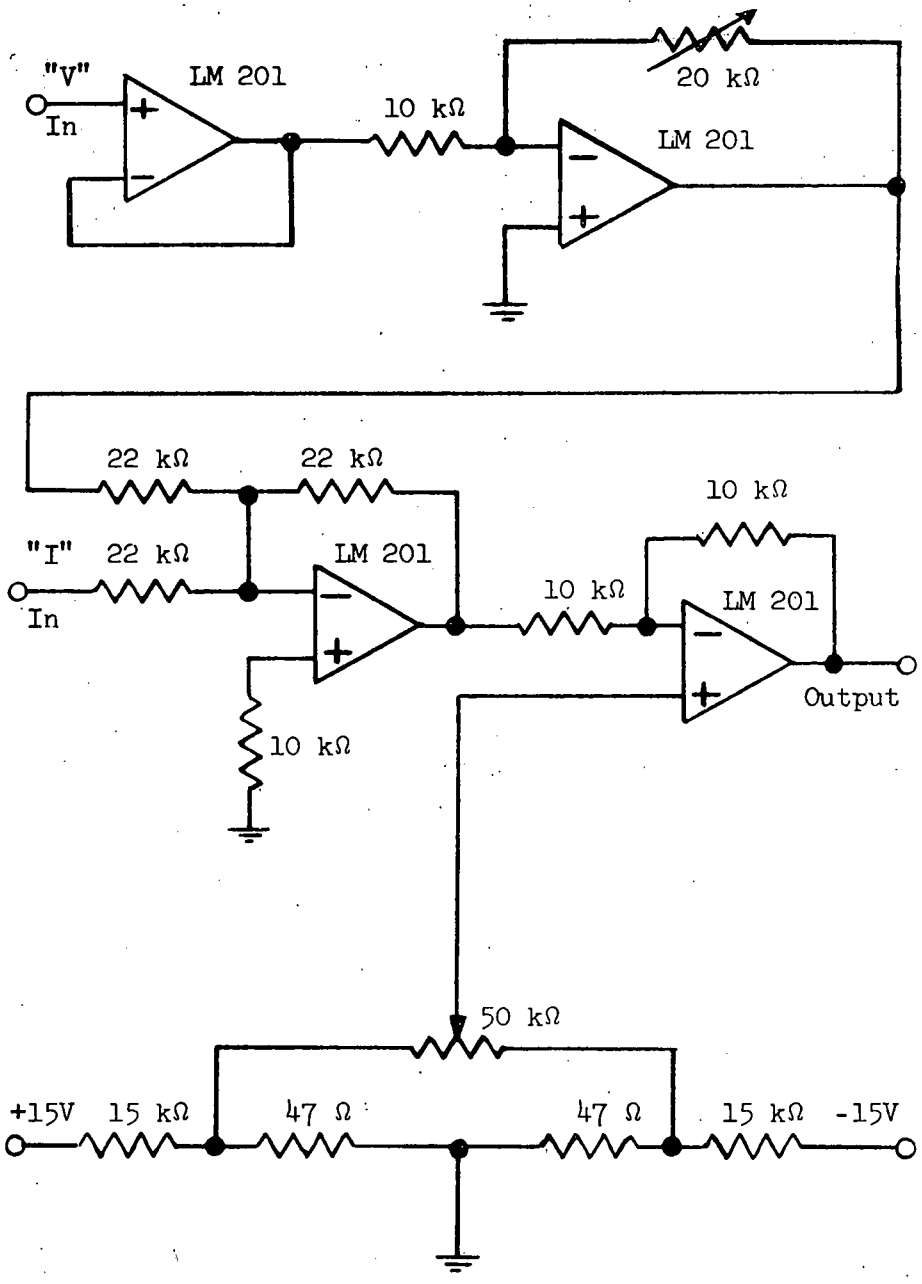

Fig. E-1. Adder/subtractor circuit. All LM201 are compensated with ~ 70 pF and powered with ± 15 v.

REFERENCES

1. For a recent review of fluctuations in superconductors, see: R. D. Parks, Proceedings of the XIIth International Conference on Low Temperature Physics, Kyoto, Japan (1970, to be published).

2. Proceedings of the Conference on Fluctuations in Superconductors, Pacific Grove, Calif., W. F. Goree and F. Chilton, eds. (Stanford Research Institute, 1968).

3. The basis for the early pessimism on the observability of fluctuations in superconductors is discussed in: P. C. Hohenberg, Proceedings of the XIIth International Conference on Low Temperature Physics, Kyoto, Japan (1970, to be published).

4. J. S. Langer and V. Ambegaokar, Phys. Rev. 164, 498 (1967).

5. R. D. Parks and R. P. Groff, Phys. Rev. Letters 18, 342 (1967).

6. R. J. Warburton and W. W. Webb, Proceedings of the International Conference on the Science of Superconductivity, Palo Alto, Calif. (1969, to be published in Physica).

7. R. E. Glover, III, Phys. Letters 25A, 542 (1967).

8. L. G. Aslamazov and A. I. Larkin, Fiz. Tverd. Tela 10, 1104 (1968) [translation: Sov. Phys.-Solid State 10, 875 (1968)].

9. E. Abrahams and J. W. F. Woo, Phys. Letters 27A, 117 (1968).

10. A. Schmid, Z. Physik 215, 210 (1968).

11. H. Schmid, Z. Physik 216, 336 (1

12. W. A. Little, Proceedings of the Symposium on Superconducting Devices, Charlottesville, Va. (University of Virginia, 1967).

13. John M. Pierce, Bull. Am. Phys. Soc. 15, 1353 (1970).

14. J. E. Lukens, R. J. Warburton, and W. W. Webb, Proceedings of the XIIth International Conference on Low Temperature Physics, Kyoto, Japan (1970, to be published).

15. A. Schmid, Phys. Kondens. Materie 5, 302 (1966).

16. A. Schmid, Phys. Rev. 180, 527 (1969).

17. J. P. Gollub, M. R. Beasley, and M. Tinkham, Proceedings of the XIIth International Conference on Low Temperature Physics, Kyoto, Japan (1970, to be published).

18. R. E. Prange, Phys. Rev. B 1, 2349 (1970).

19. L. L. Vant-Hull and J. E. Mercereau, Proceedings of the International Conference on the Science of Superconductivity, Palo Alto, Calif. (1969, to be published in Physica).

20. H. Takayama, Prog. Theor. Phys. 43, 1445 (1970).

21. R. W. Cohen, B. Abeles, and C. R. Fuselier, Phys. Rev. Letters 23, 377 (1969).

22. B. D. Josephson, Phys. Letters 1, 251 (1962).

23. P. W. Anderson, Lectures on the Many Body Problem, edited by E. R. Caianiello (Academic Press, New York, 1964).

24. P. W. Anderson, Progress in Low Temperature Physics, Vol. V, C. J. Gorter, editor (North Holland, Amsterdam, 1967), Chapter 1.

25. B. D. Josephson, Adv. Phys. 14, 419 (1965).

26. G. F. Zharkov, Usp. Fiz. Nauk 88, 419 (1966) [translation: Sov. Phys.-Usp. 9, 198 (1966)].

27. J. E. Mercereau, Tunneling Phenomena in Solids, E. Burstein and S. Lundqvist, editors (Plenum Press, New York, 1969), Chapter 31.

28. D. J. Scalapino, Tunneling Phenomena in Solids, E. Burstein and S. Lundqvist, editors (Plenum Press, New York, 1969), Chapter 33.

29. D. N. Langenberg, Tunneling Phenomena in Solids, E. Burstein and S. Lundqvist, editors (Plenum Press, New York, 1969), Chapter 33.

30. R. A. Ferrel, Low Temp. Phys. 1, 423 (1969).

31. I. O. Kulik, ZhETF Pis. Red. 10, 488 (1969) [translation: JETP Lett. 10 313 (1969)].

32. D. J. Scalapino, Phys. Rev. Letters 24, 1052 (1970).

33. J. T. Anderson and A. M. Goldman, Phys. Rev. Letters 25, 743 (1970); Erratum, Phys. Rev. Letters 26, 534 (1971).

34. H. Takayama, Proceedings of the XIIth International Conference on Low Temperature Physics, Kyoto, Japan (1970, to be published).

35. K. Yoshihiro and K. Kajimura, Phys. Letters 32A, 71 (1970).

36. S. G. Lipson, C. G. Kuper, Amiram Ron, Proceedings of the International Conference on the Science of Superconducitivity, Palo Alto, Calif. (1969, to be published in Physica).

37. M. J. Stephen, Phys. Rev. 182, 531 (1969).

38. Yu. M. Ivanchenko and L. A. Zil'berman, Zh. Eksp. Teor. Fiz. 58, 211 (1970) [translation: Sov. Phys.-JETP 31 117 (1970)].

39. W. H. Parker, D. N. Langenberg, A. Denenstein, and B. N. Taylor, Phys. Rev. 177, 639 (1969).

40. T. Shige, I. Saji, S. Nakaya, K. Uchino, and T. Aso, J. Phys. Soc. Japan 20, 1276 (1965).

41. An investigation of a system in which the zero-voltage current was completely suppressed by fluctuations, but in which the existence of coherence at finite voltages was demonstrated, has been carried out by: L. L. Vant-Hull and J. E. Mercereau, Phys. Rev. Letters 17, 629 (1966).

42. Yu. M. Ivanchenko and L. A. Zil'berman, ZhETF Pis. Red. 8, 189 (1968) [translation: JETP Letters 8, 113 (1968)].

43. A. A. Galkin, B. U. Borodai, V. M. Svistunov, and V. N. Tarasenko, ZhETF Pis. Red. 8, 521 (1968) [translation: JETP Letters 8, 318 (1968)].

44. Yu. M. Ivanchenko and L. A. Zil'berman, Zh. Eksp. Teor. Fiz. 55, 2395 (1968) [translation: Sov. Phys.-JETP 28, 1272 (1969)].

45. V. Ambegaokar and B. I. Halpern, Phys. Rev. Letters 22, 1364 (1969).

46. J. T. Anderson and A. M. Goldman, Phys. Rev. Letters 23, 128 (1969).

47. J. T. Anderson and A. M. Goldman, Proceedings of the International Conference on the Science of Superconductivity, Palo Alto, Calif. (1969, to be published in Physica).

48. A. C. Biswas and Sudhanshu S. Jha, Phys. Rev. B 2, 2543 (1970).

49. J. Kurkijärvi and V. Ambegaokar, Phys. Letters 31A, 314 (1970).

50. M. Simmonds and W. H. Parker, Phys. Rev. Letters 24, 876 (1970).

51. H. Kanter and F. L. Vernon, Phys. Letters 32A, 155 (1970).

52. S. A. Buckner, J. T. Chen, and D. N. Langenberg, Phys. Rev. Letters 25, 738 (1970).

53. An experiment in which low frequency noise currents were used to produce rounding of the dc current-voltage characteristic was reported by: H. Kanter and F. L. Vernon, Jr., Phys. Rev. B 2, 4694 (1970).

54. J. Ziman, Electrons and Phonons (Clarendon Press, Oxford, (1960).

55. A survey of applications of tunneling to solid state physics is contained in: Tunneling Phenomena in Solids, E. Burstein and S. Lundqvist, editors (Plenum Press, New York, 1969).

56. J. Bardeen, L. N. Cooper, and J. R. Schrieffer, Phys. Rev. 108, 1175 (1957).

57. P. Anderson and J. Rowell, Phys. Rev. Letters 10, 230 (1963).

58. S. Shapiro, Phys. Rev. Letters 11, 80 (1963).

59. I. Yanson, V. Svistunov, and I. Dmitrenko, Zh. Eksp. Teor. Fiz. 48, 976 (1965) [translation: Sov. Phys.-JETP 21, 650 (1965)].

60. D. N. Langenberg, D. J. Scalapino, B. N. Taylor, and R. E. Eck, Phys. Rev. Letters 15, 294 (1965); Erratum, Phys. Rev. Letters 15, 842 (1965).

61. J. J. Sakurai, Advanced Quantum Mechanics (Addison-Wesley, Reading, Mass., 1967), p. 16.

62. J. E. Zimmerman and A. H. Silver, Phys. Letters 10, 47 (1964).

63. J. E. Zimmerman and A. H. Silver, Phys. Rev. 141, 367 (1966).

64. J. Clarke, Proc. Roy. Soc. A (GB) 308, 447 (1969).

65. P. W. Anderson and A. H. Dayem, Phys. Rev. Letters 13, 195 (1964).

66. D. H. Douglass and L. M. Falicov, Progress in Low Temperature Physics, Vol. IV, C. J. Gorter, editor (North Holland, Amsterdam, 1964), p. 97.

67. W. A. Harrison, Phys. Rev. 123, 85 (1961).

68. I. Giaever, Tunneling Phenomena in Solids, E. Burstein and S. Lundqvist, editors (Plenum Press, New York, 1969), p. 267.

69. J. M. Rowell, Tunneling Phenomena in Solids, E. Burstein and S. Lundqvist, editors (Plenum Press, New York, 1969), Chapter 27.

70. A. I. Larkin and Yu. N. Ovchinnikov, Zh. Eksp. Teor. Fiz. 51, 1535 (1966) [translation: Sov. Phys.-JETP 24, 1035 (1967)].

71. V. Ginzburg and L. Landau, Zh. Eksp. Teor. Fiz. 20, 1065 (1950) [translation: D. ter Haar, Men of Physics: L. D. Landau I (Pergamon, New York, 1965)].

72. Richard P. Feynman, Robert B. Leighton, and Matthew Sands, The Feynman Lectures on Physics, Vol. III (Addison-Wesley, Reading, Mass., 1965), Chapter 21, p. 14.

73. P. G. DeGennes, Superconductivity of Metals and Alloys (W. A. Benjamin, New York, 1966), p. 107.

74. M. Cohen. L. Falicov, and J. Phillips, Phys. Rev. Letters 8, 316 (1962).

75. J. Bardeen, Phys. Rev. Letters 6, 57 (1961).

76. J. Bardeen, Phys. Rev. Letters 9, 147 (1962).

77. L. P. Gorkov, Zh. Eksp. Teor. Fiz. 36, 1918 (1959) [translation: Sov. Phys.-JETP 9, 1364 (1959)].

78. V. E. Riedel, Z. Naturforsch. 19A, 1634 (1964).

79. D. J. Scalapino and T. M. Wu, Phys. Rev. Letters 17, 315 (1966).

80. V. Ambegaokar and A. Baratoff, Phys. Rev. Letters 10, 486 (1963); Erratum Phys. Rev. Letters 11, 104 (1963).

81. R. A. Ferrell and R. E. Prange, Phys. Rev. Letters 10, 479 (1963).

82. C. S. Owen and D. J. Scalapino, Phys. Rev. 164, 538 (1967).

83. R. Jaklevic, J. Lambe, A. Silver, and J. Mercereau, Phys. Rev. Letters 12, 159 (1964).

84. R. Jaklevic, J. Lambe, A. Silver, and J. Mercereau, Phys. Rev. Letters 12, 274 (1964).

85. R. C. Jaklevic, J. Lambe, J. E. Mercereau, and A. H. Silver, Phys. Rev. 140, A1628 (1965).

86. J. E. Zimmerman and J. E. Mercereau, Phys. Rev. Letters 14, 887 (1965).

87. J. C. Swihart, J. Appl. Phys. 32, 461 (1961).

88. R. E. Eck, D. J. Scalapino, and B. N. Taylor, Phys. Rev. Letters 13, 15 (1963).

89. D. D. Coon and M. D. Fiske, Phys. Rev. 138, A744 (1965).

90. This method of determining the junction capacitance was suggested to us by D. J. Scalapino.

91. The theory of stochastic equations is contained in: D. Middleton, Introduction to Statistical Communication Theory (McGraw-Hill, New York, 1960).

92. A number of papers on stochastic processes are contained in: Selected Papers on Noise and Stochastic Processes, Nelson Wax, editor (Dover Publications, New York, 1954).

93. D. J. Scalapino, University of Virginia Report No. AD 661848 (1967, unpublished).

94. T. D. Clark and D. R. Tilley, Phys. Letters 28A, 62 (1968).

95. A. I. Larkin and Yu. N. Ovchinnikov, Zh. Eksp. Teor. Fiz. 53, 2159 (1967) [translation: Sov. Phys.-JETP 26, 1219 (1968)].

96. D. E. McCumber, J. Appl. Phys. 39, 3113 (1968).

97. Ming Chen Wang and G. E. Uhlenbeck, Rev. Mod. Phys. 17, 323 (1945). This paper is included in Ref. 92.

98. S. Chandrasekhar, Rev. Mod. Phys. 15, 1 (1943). This paper is included in Ref. 92.

99. H. A. Kramers, Physica 7, 284 (1940).

100. The formal criterion for a Markoff process is given by "Doob's Theorem." See either Ref. 91, Ref. 97, or: J. L. Doob, Ann. Am. Stat. 15, 229 (1944).

101. B. I. Halperin, private communication (1969).

102. V. I. Tikhonov, Avtomatica: Telemekhanika 20, 1188 (1959) [translation: P. I. Kuznetsov, R. L. Stratonovich, and V. I. Tikhonov, Non-Linear Transformation of Stochastic Processes (Pergamon Press, New York, 1965)].

103. T. A. Fulton and R. C. Dynes, Phys. Rev. Letters 25, 794 (1970).

104. Herbert B. Callen and Theodore A. Welton, Phys. Rev. 83, 34 (1951).

105. P. G. DeGennes, Superconductivity of Metals and Alloys (W. A. Benjamin, New York, 1966), Chapter 6.

106. L. D. Landau, Phys. Z. Sowiet Un. 11, 545 (1937) [translation: D. ter Haar, Men of Physics: L. D. Landau II (Pergamon, New York, 1969)].

107. Albert Schmid, Phys. kondens. Materie 5, 302 (1966).

108. E. Abrahams and T. Tsuneto, Phys. Rev. 152, 416 (1966).

109. R. Kubo, J. Phys. Soc. Japan 12, 570 (1957).

110. R. Kubo, Lectures in Theoretical Physics, Vol. 1 (Interscience, New York, 1959), Chapter 4.

111. The calculation of thermal averages in this manner is identical to that given in Ref. 11.

112. The expression for $\frac{dE}{dt}$ in a Josephson junction was contributed by A. M. Goldman.

113. R. V. D'Aiello and S. J. Freedman, Phys. Rev. Letters 22, 515 (1969).

114. S. L. (A.) Lehoczky and C. V. Briscoe, Phys, Rev. Letters 23, 695 (1969).

115. I. O. Kulik, Zh. Eksp. Teor. Fiz. 59, 937 (1970).

116. A comprehensive bibliography on the preparation of the barriers used in Josephson junctions can be found in: Walter Schroen, J. Appl. Phys. 39, 2671 (1968).

117. For a listing of proper sources, melting and evaporation temperatures, consult the "Vacuum Evaporation Sources Catalog," R. D. Mathis Company, 2840 Gundry Avenue, Long Beach, Calif. 90806.

118. The original suggestion of masking Josephson junctions with bismuth oxide is due to Milan D. Fiske of the General Electric Laboratories.

119. Freon Precision Cleaning Agent, trademark of the E. I. DuPont Co.

120. W. Zernik, British J. Appl. Phys. 8, 117 (1957).

121. Liquid Alloy Solder, Viking-LS232, Elmat Corp. 1271 Terra Bella Avenue, Mountain View, Calif. 74041.

122. Cryocal, Inc., 1371 Avenue "E", Riviera Beach, Florida 33404

123. F. G. Brickwedde, H. van Dijk, M. Durieux, J. R. Clement, and J. R. Logan, The 1958 He^4 Scale of Temperatures, National Bureau of Standards Monograph No. 10 (U.S. Government Printing Office, Washington, D.C., 1960).

124. J. S. Blakemore, J. Winstel, and R. V. Edwards, Rev. Sci. Instr. 41, 835 (1970).

125. The circuit for the resistance bridge used was suggested by Francis M. Gasparini and is based on a bridge used by Kierstead: H. A. Kierstead, Phys. Rev. 153, 258 (1967).

126. Ace Engineering and Machine Company, Inc., Huntington Valley, Pa.

127. J. Matisoo, Phys. Letters 29A, 473 (1969). 10, 29 (1967).

128. R. J. Pedersen and F. L. Vernon, Jr., Appl. Phys. Letters 10, 29, (1967).

129. The data for PF-1 was originally published in Ref. 46, and the data for PF-2 in Ref. 47.

130. The data for the pair susceptibility experiment was originally published in Ref. 33.

131. G. Deutscher and P. G. DeGennes, Superconductivity, Vol. 2, R. D. Parks, editor (Marcel Dekker, New York, 1969), Chapter 17.

132. The mean free path for tin was calculated from $\bar{\ell}\rho = 2 \times 10^{-11}$ Ω-cm^2 given in: J. L. Olsen, Electron Transport in Metals (Interscience, New York, 1962), p. 84.

133. B. R. Patton, V. Ambegaokar, and J. W. Wilkins, Solid State Commun. 7, 1287 (1969).

134. J. P. Gollub, M. R. Beasley, and M. Tinkham, Phys. Rev. Letters 25, 1646 (1970).